SANDIA REPORT

SAND2015-0889
Unlimited Release
Printed February 2015

Thermal Diffusivity and Specific Heat Measurements of Titanium Potassium Perchlorate, Titanium Subhydride Potassium Perchlorate, 9013 Glass, 7052 Glass, SB-14 Glass, and C-4000 Muscovite Mica Using the Flash Technique

Paul E. Specht and Marcia A. Cooper

Prepared by
Sandia National Laboratories
Albuquerque, New Mexico 87185 and Livermore, California 94550

Sandia National Laboratories is a multi-program laboratory managed and operated by Sandia Corporation, a wholly owned subsidiary of Lockheed Martin Corporation, for the U.S. Department of Energy's National Nuclear Security Administration under contract DE-AC04-94AL85000.

Issued by Sandia National Laboratories, operated for the United States Department of Energy by Sandia Corporation.

Available to DOE and DOE contractors from
U.S. Department of Energy
Office of Scientific and Technical Information
P.O. Box 62
Oak Ridge, TN 37831

Telephone: (865) 576-8401
Facsimile: (865) 576-5728
E-Mail: reports@adonis.osti.gov
Online ordering: http://www.osti.gov/bridge

Available to the public from
U.S. Department of Commerce
National Technical Information Service
5285 Port Royal Rd
Springfield, VA 22161

Telephone: (800) 553-6847
Facsimile: (703) 605-6900
E-Mail: orders@ntis.fedworld.gov
Online ordering: http://www.ntis.gov/help/ordermethods.asp?loc=7-4-0#online

SAND2015-0889
Unlimited Release
Printed February 2015

Thermal Diffusivity and Specific Heat Measurements of Titanium Potassium Perchlorate, Titanium Subhydride Potassium Perchlorate, 9013 Glass, 7052 Glass, SB-14 Glass, and C-4000 Muscovite Mica Using the Flash Technique

Paul E. Specht and Marcia A. Cooper
Explosives Components Facility
Sandia National Laboratories
P.O. Box 5800
Albuquerque, NM 87185-1454
pespech@sandia.gov

Abstract

The flash technique was used to measure the thermal diffusivity and specific heat of titanium potassium perchlorate (TKP) ignition powder (33wt% Ti - 67wt% KP) with Ventron supplied titanium particles, TKP ignition powder (33wt% Ti - 67wt% KP) with ATK supplied titanium particles, TKP output powder (41wt% Ti - 59wt% KP), and titanium subhydride potassium perchlorate (THKP) (33wt% $TiH_{1.65}$ - 67wt% KP) at 25 °C. The influence of density and temperature on the thermal diffusivity and specific heat of TKP with Ventron supplied titanium particles was also investigated. Lastly, the thermal diffusivity and specific heats of 9013 glass, 7052 glass, SB-14 glass, and C-4000 Muscovite mica are presented as a function of temperature up to 300 °C.

Acknowledgment

Funding for this work has been provided by multiple sources: Research challenge LDRD "Revisiting the Applied Mechanics Paradigm: Mulit-scale Modeling of Transport Processes ion Complex Materials" (PI Jermey Lechman - Org. 1516) and the B61 LEP R&D (PRT leads Tracy Zullo and Nathan Glenn - Org. 2552). The authors would also like to thank, Duane Richardson (Org. 2554) for TKP and THKP sample preparation, Ryan Haggarty (Org. 2718) for 9013, 7052, and SB-14 glass sample preparation, Heather Finkner (Org. 2557) and Jerome Norris (Org. 2552) for helping to locate material for the SB glass samples, Will Wente (Org. 2552) for training and providing the 9013 and 7052 glass samples, and Robert Patton (Org. 2556) for ESD training and use of his laboratory.

The authors would also like to acknowledge the help of Gregg Radtke (Org. 2552) and Will Wente (Org. 2552) for reviewing this manuscript.

Contents

Appendix

List of Figures

List of Tables

This page intentionally left blank.

Chapter 1

Introduction

The flash method can be used to determine the thermal diffusivity and specific heat of a material following ASTM Standard E1461-13 [1]. The method involves exposing one side of a sample to a high intensity, short duration pulse of light. The temperature rise on the opposite side of the sample is measured with a thermocouple or infrared detector. The measured back surface response is used to determine the thermal diffusivity and, through comparisons to a known reference, the specific heat. A commercial Netzsch NanoFlash® LFA 447 machine is available for thermal diffusivity and specific heat measurements on energetic materials in the Explosives Components Facility. The NanoFlash® machine comes with software for the execution of the experiment and data analysis. The numerics of the Proteus® LFA analysis program [17] are not available for scrutiny. To provide more confidence in the measured results and corresponding uncertainties, a MATLAB® [14] program was developed for analyzing the raw voltage data.

The thermal diffusivities and specific heats of the following materials are reported.

- Titanium potassium perchlorate (TKP)
  - TKP ignition powder (33wt% Ti - 67wt% KP) with Ventron titanium particles (Ventron TKP-IP) per specification SS2A7929
    - At densities ranging from 2.0 to 2.3 g/cm^3 at 25 °C
    - At a density of 2.1 g/cm^3 and temperatures ranging from 25 to 250 °C
  - TKP ignition powder (33wt% Ti - 67wt% KP) with ATK titanium particles (ATK TKP-IP) at a density of 2.1 g/cm^3 at 25 °C per specification SS2A7929
  - TKP output powder (41wt% Ti - 59wt% KP) (TKP-OP) at a density of 2.5 g/cm^3 at 25 °C per specification SS2A7930
- Titanium subhydride potassium perchlorate (33wt% $TiH_{1.65}$ - 67wt% KP) (THKP) at a density of 2.3 g/cm^3 at 25 °C per specification SS2A7931
- 9013 glass at temperatures ranging from 25 to 300 °C
- 7052 glass at temperatures ranging from 25 to 300 °C

- SB-14 glass at temperatures ranging from 25 to 300 °C
- C-4000 Muscovite mica powder pressed to a density of 1.9 g/cm^3 at temperatures ranging from 25 to 300 °C

The specific heats are reported using both pocographite and Pyroceram® as the reference material. Determining the specific heat with the flash technique is prone to errors. Its accuracy relies on identical experimental parameters (*i.e.* temperature, flash voltage, flash duration, filter, masks, and coatings) and thermal properties between the sample and reference. To enable appropriate judgment of the specific heats reported, the physical and thermal properties of the pocographite and Pyroceram® reference samples are presented.

Chapter 2

Analysis Program

The MATLAB® analysis program works on the assumption that the recorded back surface voltage is directly proportional to the temperature. Additionally, each individual flash, or shot, is assumed to be essentially identical given the same NanoFlash® machine parameters. The analysis code loads in the NanoFlash® data files and calculates the thermal diffusivity using either the Parker [18] or Cowan [7, 8] model. Data for a reference material can then be loaded for the determination of the material's specific heat. Below is a description of the thermal diffusivity and specific heat calculations along with the associated error approximations.

2.1 Thermal Diffusivity Calculations

2.1.1 Parker Model

A simple adiabatic model for determining a material's thermal diffusivity was proposed by Parker *et al.* [18]. The Parker model assumes that the normalized temperature, V, can be represented by the following equations.

$$V = 1 + 2\sum_{n=1}^{\infty}(-1)^n \exp(-n^2\omega) \tag{2.1}$$

$$\omega = \frac{\pi^2 \alpha t}{L} \tag{2.2}$$

Here, α is the thermal diffusivity, t is time, and L is the sample thickness. At the half rise time, $t_{0.5}$, $V = 0.5$ and ω is equal to 1.38785. The thermal diffusivity directly follows.

$$\alpha = \frac{1.38785 L^2}{\pi^2 t_{0.5}} \tag{2.3}$$

The MATLAB® code implements the Parker model by first determining the zero time of the voltage record. The NanoFlash® machine has an inherent delay between the start of

voltage recording and the flash of the Xenon lamp. This delay is related to the parameters of the experiment and is extracted from the NanoFlash® data file. The voltage record before the zero time is fit to a linear polynomial in time. This linear fit is applied to the entire voltage record to compensate for possible sensor drift during the measurement. After this correction, the voltage record is normalized. Like all raw data, the recorded signal has inherent noise. This is seen in the raw data obtained from a Ventron TKP-IP pressed pellet shown in Figure 2.1. To estimate the maximum voltage, the MATLAB® code smooths the raw data and locates the beginning of the voltage rise. The initiation of the rise was chosen as 5% of the maximum value for easy identification in signals with high noise. To avoid anomalies caused by bleed through of the flash, the first 1 ms after the zero time is excluded when locating the voltage rise. Flash bleed through can be an issue for porous and transparent samples.

After locating the rise point, the raw data after the rise point is fit to a double exponential equation. This fitting was done in MATLAB® with the default algorithm for the *fit* command [13], which is the Levenberg-Marquardt method [11, 12]. This is the algorithm used to determine the coefficients and associated error for all curve fitting in this program.

$$T = C_1 \exp(C_2 t) + C_3 \exp(C_4 t) \tag{2.4}$$

The double exponential function was chosen since it provides an excellent fit to the raw data as seen in Figure 2.2. The time and amplitude of the maximum value of this curve fit is then determined.

$$t_{max} = \frac{1}{C_4 - C_2} \ln\left(\frac{-C_1 C_2}{C_3 C_4}\right) \tag{2.5}$$

$$T_{max} = C_1 \exp(C_2 t_{max}) + C_3 \exp(C_4 t_{max}) \tag{2.6}$$

The raw data is normalized by T_{max} and fit to Equation 2.1 with the number of terms in the series specified by the user. From the value of ω obtained, α is calculated from Equation 2.3.

An example of the Parker model fit to the Ventron TKP-IP pellet using 10 terms is shown in Figure 2.3. The Parker model poorly matches the peak and late time voltages, due to the adiabatic nature of the model. Without incorporating heat losses, the late time voltages are bound to a single value and can not decrease like the measured response.

2.1.1.1 Uncertainty Analysis

Since the raw data was normalized with an analytical fit, there is an inherent uncertainty in each of the coefficients. This uncertainty will propagate through the calculation effecting the certainty to which α is known. This error is determined through the use of the standard error equation for $Y = f(x_i)$ [3].

$$\delta Y = \sqrt{\sum_i \left(\frac{\partial Y}{\partial x_i} \delta x_i\right)^2} \tag{2.7}$$

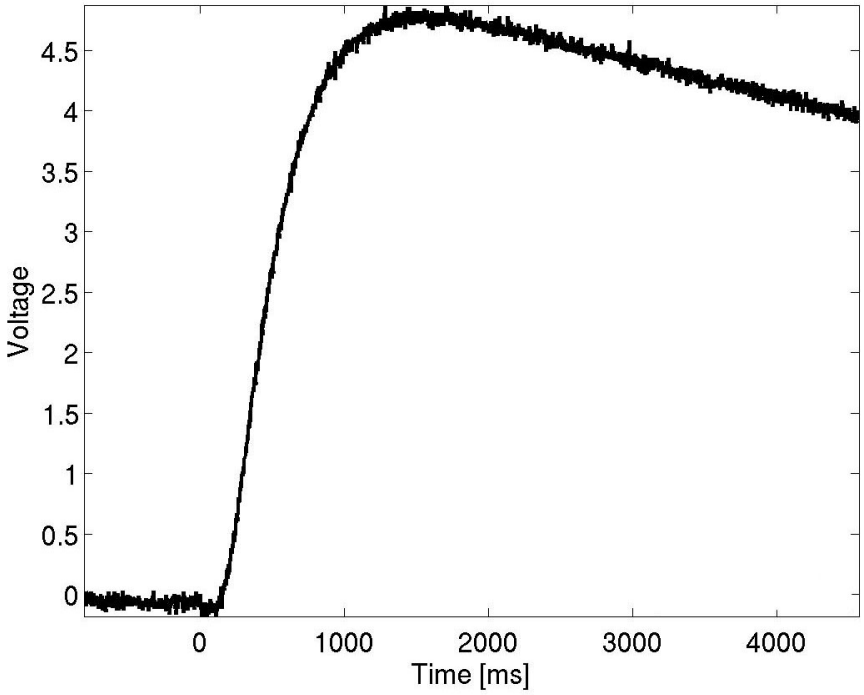

Figure 2.1: Raw data from a Ventron TKP-IP pellet.

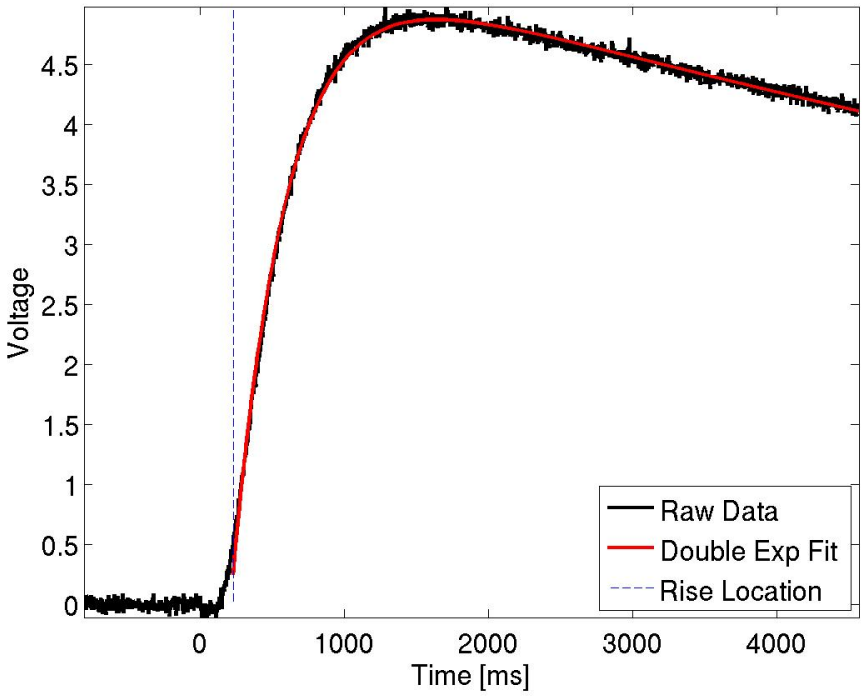

Figure 2.2: Double exponential fit to the Ventron TKP-IP pellet raw data.

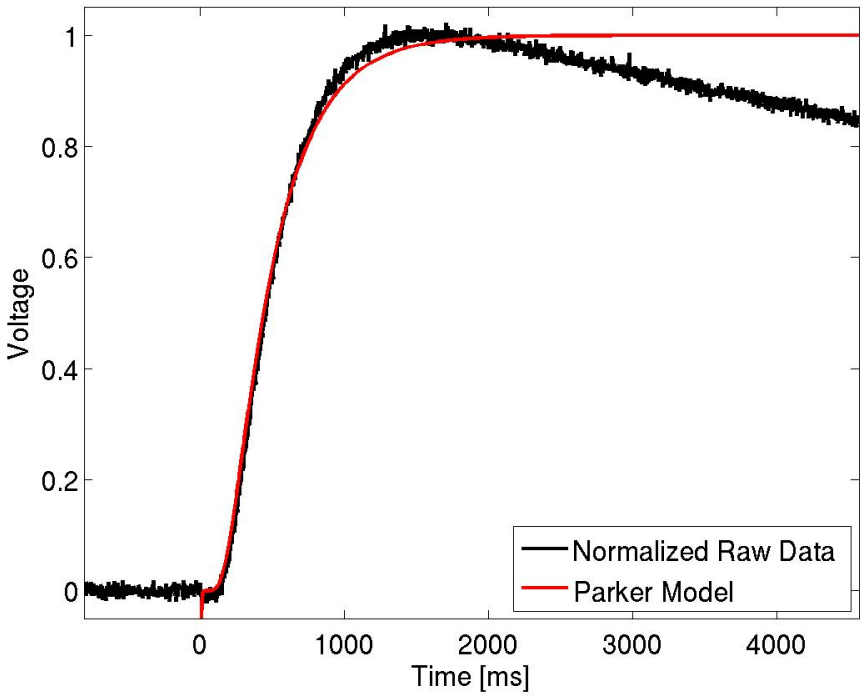

Figure 2.3: Parker model fit to the Ventron TKP-IP pellet raw data using 10 terms.

Using the double exponential fit for the raw voltage (Equation 2.4), the following partial derivatives are determined for T_{max}.

$$\frac{\partial T_{max}}{\partial C_1} = \exp(C_2 t_{max}) \tag{2.8}$$

$$\frac{\partial T_{max}}{\partial C_2} = C_1 t_{max} \exp(C_2 t_{max}) \tag{2.9}$$

$$\frac{\partial T_{max}}{\partial C_3} = \exp(C_4 t_{max}) \tag{2.10}$$

$$\frac{\partial T_{max}}{\partial C_4} = C_3 t_{max} \exp(C_4 t_{max}) \tag{2.11}$$

$$\frac{\partial T_{max}}{\partial t_{max}} = C_1 C_2 \exp(C_2 t_{max}) + C_3 C_4 \exp(C_4 t_{max}) \tag{2.12}$$

$$\tag{2.13}$$

The uncertainties in C_1 through C_4 (*i.e.* δC_i) are obtained from the MATLAB® fit. The uncertainty in t_{max} is found using the partial derivatives of Equation 2.5.

$$\frac{\partial t_{max}}{\partial C_1} = \frac{1}{C_1(C_4 - C_2)} \tag{2.14}$$

$$\frac{\partial t_{max}}{\partial C_2} = \frac{1}{C_2(C_4 - C_2)} + \frac{1}{(C_4 - C_2)^2} \ln\left(\frac{-C_1 C_2}{C_3 C_4}\right) \tag{2.15}$$

$$\frac{\partial t_{max}}{\partial C_3} = \frac{-1}{C_3(C_4 - C_2)} \tag{2.16}$$

$$\frac{\partial t_{max}}{\partial C_4} = \frac{-1}{C_4(C_4 - C_2)} - \frac{1}{(C_4 - C_2)^2} \ln\left(\frac{-C_1 C_2}{C_3 C_4}\right) \tag{2.17}$$

$$\tag{2.18}$$

Using these partial derivatives and the uncertainties in each quantity, δT_{max} is calculated using Equation 2.7. The error in the normalized voltage, δV, as a percentage is the following.

$$\frac{\delta V}{V} = \frac{\delta T_{max}}{T_{max}} \tag{2.19}$$

The fit of the Parker model to the normalized voltage leads to an uncertainty in ω. Using the uncertainty in V and ω, a 3×3 matrix is developed of potential half rise times, $\delta t_{0.5}$. This consists of every iteration using the upper, lower, and median values of ω and V. Half the difference between the maximum and minimum half rise time in the matrix is used to define the associated uncertainty, since it is a more conservative error estimation than the standard deviation. The uncertainty in α, $\delta\alpha$, is found using the partial derivatives of Equation 2.3 and the error associated with each quantity.

$$\frac{\partial \alpha}{\partial t_{0.5}} = \frac{-1.38785 L^2}{\pi^2 t_{0.5}^2} \tag{2.20}$$

$$\frac{\partial \alpha}{\partial L} = \frac{2.7757 L}{\pi^2 t_{0.5}} \tag{2.21}$$

$$\tag{2.22}$$

In these calculations, the uncertainties represent the standard deviation. The 95% confidence interval is obtained by multiplying the standard deviation by 1.96.

2.1.2 Cowan Model

The model proposed by Cowan [7, 8] to determine the thermal diffusivity with the flash technique accounts for radiation and convective losses at the sample surfaces. These loses lead to the decrease in voltage seen in the raw data of Figure 2.1 at later times. This

correction makes the Cowan model more appropriate for determining the thermal diffusivity of most samples.

If the front of a sample is exposed to a high-intensity, short duration pulse of energy, the temperature response, $\Theta(0,t)$, at the back of the sample can be described with the following relation.

$$\frac{Lc_p\rho\Theta(0,t)}{Q} = 2\sum_{n=0}^{\infty}\frac{y_n^2}{D_n\exp\left(\frac{\alpha y_n^2 t}{L^2}\right)} \tag{2.23}$$

Here, L is the sample thickness, c_p is the specific heat, ρ is the density, Q is the total energy deposited per unit area, and α is the thermal diffusivity. The terms y_n are the solution of the following equation over the interval $n\pi < y < (n+1)\pi$.

$$\cot y = \frac{y}{a} - \frac{b}{ay} \tag{2.24}$$

In this equation, the terms a and b relate to the energy lost at the irradiated, c_L, and back surfaces, c_0.

$$a = L(c_0 + c_L) = Lc_0(1+r) \tag{2.25}$$

$$b = \frac{ra^2}{(1+r)^2} \tag{2.26}$$

$$r = \frac{c_L}{c_0} \tag{2.27}$$

The term D_n is then defined as the following.

$$D_n = y_n\sin(y_n)\left(1 + a - \frac{2b}{a} + \frac{y_n^2}{a} + \frac{b}{y_n^2} + \frac{b^2}{ay_n^2}\right) \tag{2.28}$$

This set of equations can be solved to a high degree of accuracy with a rough knowledge of r by taking two ratios of the temperature response at different times [8]. This results from the thermal diffusivity being relatively insensitive to r for a values below 5 as seen in Figure 2.4. Typically, the following ratios are chosen.

$$R_5 = \frac{\Theta(0,5t_{0.5})}{\Theta(0,t_{0.5})} \tag{2.29}$$

$$R_{10} = \frac{\Theta(0,10t_{0.5})}{\Theta(0,t_{0.5})} \tag{2.30}$$

$$\tag{2.31}$$

Since samples in the flash method usually have similar graphite coatings and masks on the irradiated and back surfaces, r is assumed to be unity. Variations in r (*i.e.* from 0 to 100) were found to alter the calculated thermal diffusivity in a Ventron TKP-IP pellet by less than

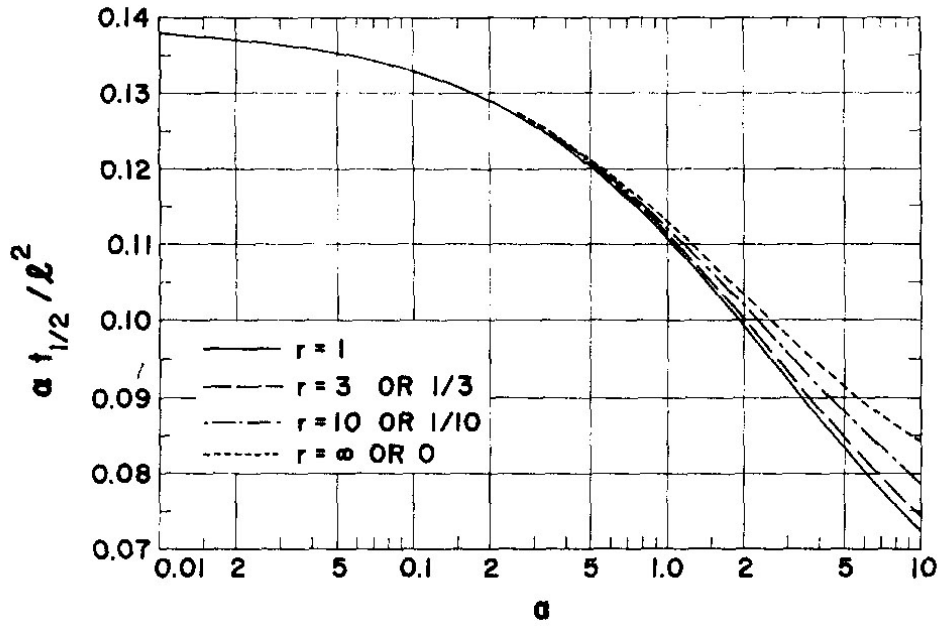

Figure 2.4: Variation of the thermal diffusivity as a changes for various r values [8]. For a values up to 5, the thermal diffusivity is relatively insensitive to changes in r.

0.2%. Errors corresponding to uncertainties in the value of r are assumed to be included in the conservative error estimations described in Section 2.1.2.1.

Calculating the thermal diffusivity using the Cowan model begins with fitting the raw data to a double exponential function (Equation 2.4) and normalizing the curve by the maximum voltage identical to that done for the Parker model (Section 2.1.1). This double exponential fit is used to find V at 1, 5, and 10 half times. The value determined at 1 half time is used to get a rough estimate of the thermal diffusivity using the Parker model (Equation 2.3). This rough approximation of α is used as an initial guess to expedite fitting the Cowan model to the data.

Cowan suggests that an adequate approximation of a can be determined by assuming the energy is deposited as a step function [7]. This effectively leads to analyzing the drop in normalized voltage due to heat loss. Taking the natural logarithm of the normalized voltage, V, for all time after the peak, a curve is generated that asymptotically approaches a straight line. This curve is shown in Figure 2.5. The second half of this curve is fit to a linear equation, $F(0,t)$. The value of this linear fit at t_{max} provides an estimation of a.

$$F(0,t_{max}) \cong 1 + \frac{a}{6} \tag{2.32}$$

This crude approximation is only valid if the first term in Equation 2.23 at t_{max}, $V_0(0,t_{max})$, differs from unity by around 0.08 [7].

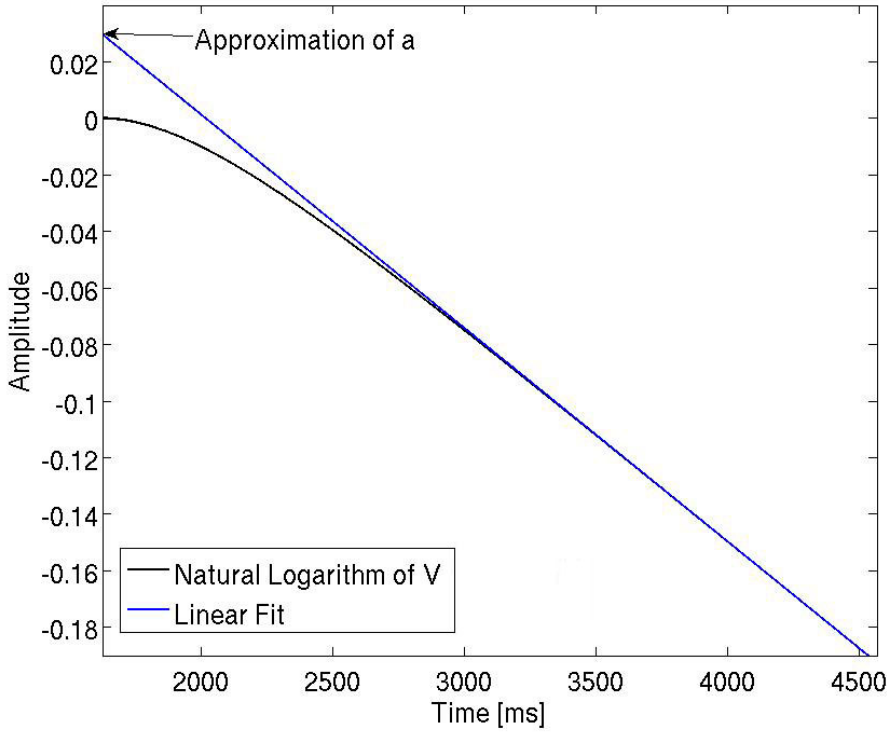

Figure 2.5: Plot of the natural logarithm of the normalized voltage, V. The second half of $ln(V)$ is fit to a linear polynomial, the value of which at t_{max} provides a rough approximation of a.

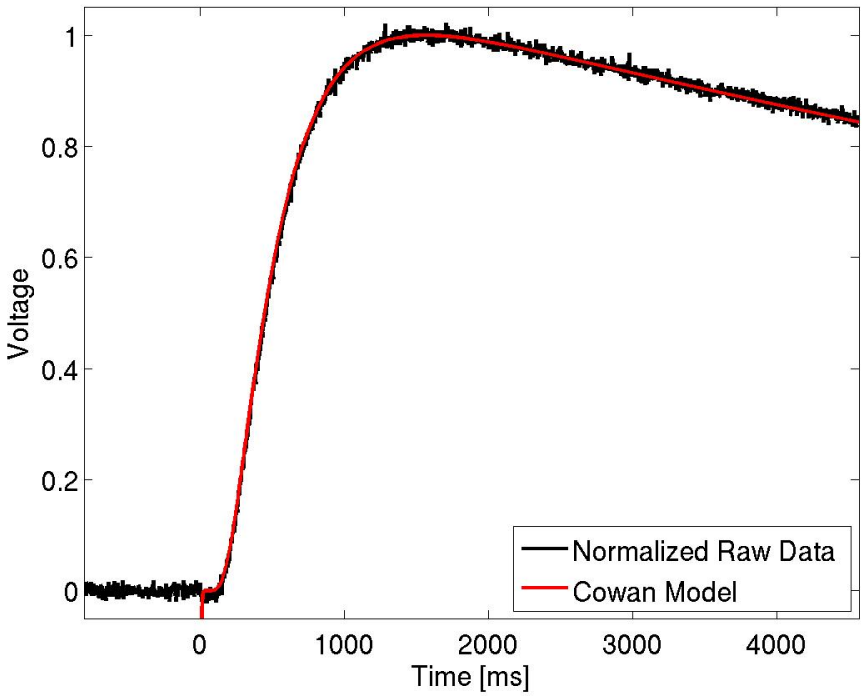

Figure 2.6: Cowan model fit to the raw data for a shot on a Ventron TKP-IP pellet using 10 terms. The Cowan model is seen to fit the experimental data much better than the Parker model due to its incorporation of heat losses.

With this approximation of a, the values of y_n and D_n are found. Equation 2.23 is then used to find the thermal diffusivity, α that matches the temperature ratios at R_5 and R_{10}. The α given by both ratios should match. However, given the crude nature in which a was approximated, this is not the case. The MATLAB® code iterates to obtain an α that satisfies both ratios. Figure 2.4 shows that, as a increases, α decreases. A refined α value is then defined as the average of the values obtained from R_5 and R_{10} and it is compared to the previous approximation. If the new value of α is lower than the previous one, a is increased. If the new value is higher, a is decreased. This new a value is then used to recalculate α. The process repeats until α converges to a desired tolerance. The MATLAB® code changes the a value by 1% for each iteration. There is no strong reason for this magnitude of change other than it seemed to give a convergence of α to within a tolerance of 0.1% in under 50 iterations. If the values don't converge to the desired tolerance after 60 iterations, the code resets to the initial approximation of a and iterates until the best agreement possible is reached. This is typically within 5% and is common for high-noise signals. A Cowan model fit with 10 terms to the Ventron TKP-IP pellet is shown in Figure 2.6. The Cowan model fits the raw data very well, providing a much better estimation of the thermal diffusivity than the Parker model.

2.1.2.1 Uncertainty Analysis

Since the raw data was normalized in the same method as the Parker model, the error in V_{max} is accounted for in the same way as in Section 2.1.1.1. This same proceedure is extended to find the errors in V, at 1, 5, and 10 half times, which provide the errors in R_5 and R_{10}. Equation 2.23 also relies on the pellet thickness, which also has a measured error. Using the errors in R_5, R_{10}, and L, a 6×3 matrix is developed. The first 3×3 section corresponds to α calculated using $R_5 \pm \delta R_5$ and $L \pm \delta L$, while the second corresponds to that using $R_{10} \pm \delta R_{10}$ and $L \pm \delta L$ (*i.e.* all iterations of the maximum, minimum, and median values of each parameter). Once again, the error recorded in α is half the difference between the maximum and minimum values obtained in this 6×3 matrix.

2.2 Specific Heat Calculations

The specific heat of a sample can be determined with the flash method through comparison to a known reference sample. The heat applied to a sample can be expressed with the following.

$$Q = mc_p\Delta T \tag{2.33}$$

If the reference and sample undergo the same flash exposure and have the same absorption coefficient, the heat imparted to them can be set equal. The specific heat of the sample can then be related to the specific heat of the reference.

$$c_{p_{sample}} = \frac{m_{ref}}{m_{sample}} \frac{\Delta T_{ref}}{\Delta T_{sample}} c_{p_{ref}} \tag{2.34}$$

If the sample and reference have the same flash parameters (*i.e.* temperature, flash voltage, flash duration, filter, masks, and coatings), Equation 2.34 can be rewritten as the following.

$$c_{p_{sample}} = \frac{T_{adb_{ref}}}{T_{adb_{sample}}} \frac{A_{sample}}{A_{ref}} \frac{\rho_{ref}}{\rho_{sample}} \frac{L_{ref}}{L_{sample}} c_{p_{ref}} \tag{2.35}$$

Here, T_{adb} is the adiabatic temperature rise, which corresponds to the maximum temperature of the reference and sample assuming no heat losses. To ensure a proper comparison, this ratio is multiplied by the ratio of the electronic gain factors used in the measurement of each, A_{sample} and A_{ref}. If identical masks are used, the area of the sample and reference are the same and the mass term reduces to ρL.

To use Equation 2.35, the adiabatic temperature rise must be determined. This is done in the MATLAB® routine using both the Cowan and Parker models. For both the sample and the reference, the half rise time, $t_{0.5}$, and thermal diffusivity, α, are calculated using the Cowan model, since it accounts for heat loses. These half rise times are used to calculate

the normalized voltage, $V_{Ct_{0.5}}$, from the double exponential fit to the data. This normalized voltage, $V_{Ct_{0.5}}$, will be below the 0.5 expected under adiabatic conditions. The ratio of 0.5 to $V_{Ct_{0.5}}$ provides an estimate of the fraction of heat dissipated in the first half of the rise. The fraction of heat lost in the first half of the rise is assumed to be identical to that lost in the second half of the rise. The recorded voltage at the half rise time is multiplied by this ratio and doubled to provide an estimate of the expected maximum voltage rise given adiabatic conditions, T_{adb}. From this approximation, c_p is calculated from Equation 2.35.

2.2.1 Uncertainty Analysis

The error associated with the adiabatic temperature rise follows from the error method used for finding the maximum voltage and half rise time outlined previously in Section 2.1.1.1. Error in t_{max} is found with the Cowan model, as described in Section 2.1.2.1. The error in $V_{Ct_{0.5}}$ found with the exponential fit follows that for V_{max} outlined in Section 2.1.1.1. The error of c_p for the sample is then a simple application of the standard error equation for all variables in Equation 2.35.

It should be noted that specific heats found with the flash method are prone to errors and should be used with caution. Errors in the specific heat of the reference will inherently cause errors in the specific heat of the sample. Identical experimental parameters (*i.e.* temperature, flash voltage, flash duration, filter, masks, and coatings) and similar thermal properties between the sample and reference are also necessary. Care must be taken when using such data.

This page intentionally left blank.

Chapter 3

Measurements on Titanium Potassium Perchlorate and Titanium Subhydride Potassium Perchlorate Formulations

3.1 Material Properties

Various formulations of titanium and potassium perchlorate (KP) with differing hydride levels, Ti powders, and mixture ratios were measured using the flash technique.

- Titanium potassium perchlorate ignition powder (33wt% Ti - 67wt% KP) with Ventron Ti particles (Ventron TKP-IP)
- Titanium potassium perchlorate ignition powder (33wt% Ti - 67wt% KP) with ATK Ti particles (ATK TKP-IP)
- Titanium potassium perchlorate output powder (41wt% Ti - 59wt% KP) (TKP-OP)
- Titanium subhydride potassium perchlorate (33wt% $TiH_{1.65}$ - 67wt% KP) (THKP).

The various TKP and THKP formulations were pressed into pellets. The properties of which are given in Table 3.1. The uncertainty in the sample weights are taken as the uncertainty of the scale used. The uncertainty of the height are obtained from 4 independent measurements at different locations on the sample. The sample was made with a high precision die, so negligible error is assumed for the diameter. The uncertainty in the density was obtained from the standard error equation (Equation 2.7). All uncertainties listed in this report represent the 95% confidence interval.

The Ventron TKP-IP was pressed into pellets with roughly 68, 71, 76, and 79% theoretical maximum density (TMD) in order to study the change in thermal properties of TKP

with pellet density. The Ventron TKP-IP was chosen, since it was easier to handle once pressed than the ATK TKP-IP. The density range represents the highest TMD capable of the press and the lowest TMD thought to provide robust enough samples to measure. Two distinct pellet heights of the ATK TKP-IP were also pressed to ensure all measurements were representative of the bulk material. The ATK TKP-IP was brittle once pressed. As a result, only a single 1 mm tall ATK TKP-IP pellet survived for testing along with the three 3 mm pellets.

3.2 Experimental Arrangement

The thermal diffusivity of each TKP and THKP pellet was measured at least 5 times at 25 °C. In addition, Ventron TKP-IP pellets IP-V-1-71-1 and IP-V-1-71-2 were measured at 50, 100, 150, 200, and 250 °C to understand the change in thermal diffusivity and specific heat with temperature. Measurements were stopped at 250 °C for two reasons: the crystallographic phase transition in KP at around 300 °C [10], and loss of graphite coating adhesion at higher temperatures. The NanoFlash® machine allows for a 0.5 °C deviation from the specified temperature with a 0.1 °C accuracy of the reading. This is the source of the temperature error reported in the experimental results. The samples were coated with graphite ($\sim$ 5 microns) to ensure uniform and thorough absorption of the Xenon flash energy. The flash was run with 270 V for the 1 mm tall pellets and 292 V for the 3 mm tall pellets. The higher voltage for the 3 mm tall pellets was done to improve the signal-to-noise ratio. Every shot had no filter (NanoFlash® filter option 5). The temperature rise on the back side of each pellet was measured with a InSb IR sensor cooled with liquid nitrogen. In all tests, the flash duration ($\sim$ 250 μs - NanoFlash® pulse option "Medium" for the 1 mm tall pellets and $\sim$ 450 μs - NanoFlash® pulse option "Long" for the 3 mm tall pellets) is significantly less than the half rise time ($\sim$ 300 ms for 1 mm tall pellets and $\sim$ 5000 ms for 3 mm tall pellets), so no correction for the pulse duration is needed [2]. The NanoFlash® machine parameters are all listed in Table 3.2.

3.3 Experimental Results

3.3.1 Thermal Diffusivity

All shots on the TKP and THKP pellets were analyzed using the Cowan model [7, 8], since it accounts for radiative and conductive heat losses. The Cowan model can be implemented with any number of terms. Table 3.3 shows the computed thermal diffusivity for Ventron TKP-IP pellet IP-V-1-71-1 as the number of terms varies. Convergence occurs with only 3 terms. However, for all results presented in this report, 10 terms were used to ensure

convergence.

The thermal diffusivity and accompanying error for each shot on the TKP and THKP pellets are presented in Table 3.4. The average thermal diffusivity and accompanying error for each pellet at 25 °C along with the average thermal diffusivity for each TKP and THKP formulation (*i.e* the average of all pellets) are listed in Table 3.5. For most TKP and THKP formulations, the sample-to-sample variation is small ($< 5\%$). With such repeatability in the thermal diffusivity it is assumed that 1 mm is representative of the bulk material response. The exception is TKP-OP. Pellet OP-1-80-1 has a significantly lower thermal diffusivity than pellets OP-1-80-2 or OP-1-80-3. While the exact reason for this is unknown, it could be tied to the lower density of pellet OP-1-80-1. Further studies on the change in thermal diffusivity with density need to be performed on TKP-OP to verify this hypothesis.

A comparison of the TKP-IP pellets at around 71% TMD shows a large difference between the Ventron and ATK formulations ($\sim 18\%$). This difference may be tied to the different particle morphologies of the Ti or unique powder compressibility causing unique density gradients. Dependance of thermal diffusivity on thickness is also observed in ATK TKP-IP. The 1 mm ATK pellet has around a 14% higher thermal diffusivity than the 3 mm tall pellets. This is likely due to a change in density gradient of the thicker samples. Further studies are necessary to validate this assumption.

3.3.1.1 Effect of Density on Thermal Diffusivity

Table 3.5 shows an upward trend in thermal diffusivity with density in the Ventron TKP-IP at 25 °C. This trend is fit to a quadratic equation using the data from all four samples, and is shown in Figure 3.1. The data suggests that the thermal diffusivity remains relatively constant at lower densities before increasing dramatically. This trend could be tied to a critical connectivity between Ti particle, which could be investigated with stereological methods. Since the 2.0 g/cm^3 pellets proved to be sturdy, pellets at even lower densities could be pressed to further investigate the lower density regime. Use of a different press would also allow studies to higher densities.

3.3.1.2 Effect of Temperature on Thermal Diffusivity

Since the Ventron TKP-IP was measured at various temperatures, it is important to consider the effect of thermal expansion. With the coefficient of thermal expansion, CTE, the thickness and density of a material as a function of temperature can be described with the following.

$$t(T) = t_o(1 + (T - T_0))CTE \tag{3.1}$$

$$\rho(T) = \frac{m}{V_o(1 + 3(T - T_0)CTE)} \tag{3.2}$$

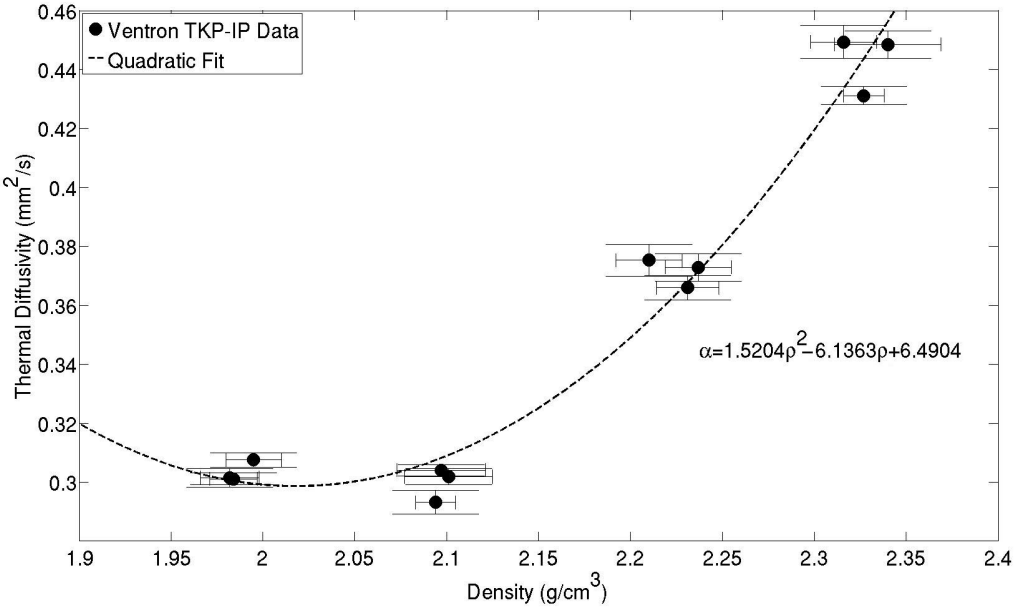

Figure 3.1: Thermal diffusivity as a function of density for the Ventron TKP-IP pellets at 25 °C. The data shows an upward trend in thermal diffusivity with increasing density, which is fit to a quadratic equation.

Here, t_o is the initial thickness, V_o is the initial volume, and $T - T_0$ is the temperature diference from reference measured in Celsius. Taking the CTE to be as high as 50×10^{-6} C^{-1} leads to a small change (*i.e.* $< 2.0\%$) in the measured thermal diffusivity and specific heat of the Ventron TKP at 250 °C. For this reason, the effects of thermal expansion are considered to be included in the conservative error estimations reported.

The flash method relies on exposing one side of the sample to a high intensity short duration pulse of light. KP undergoes a crystallographic phase transition at roughly 300 °C [10]. It is important to consider the amount of KP that has transformed during the measurement to ensure the results are representative of nascent TKP. The amount of KP transformed can be estimated by modeling the sample's temperature distribution assuming all the laser energy is immediately and uniformly absorbed into a thin layer of the material [18].

$$T(x,t) = \frac{Q}{Dc_pL}\left[1 + 2\sum_{n=1}^{\infty}\cos\left(\frac{n\pi x}{L}\right)\frac{\sin\left(\frac{n\pi g}{L}\right)}{\left(\frac{n\pi g}{L}\right)}\exp\left(\frac{-n^2\pi^2}{L^2}\alpha t\right)\right] + T_o \tag{3.3}$$

Here, Q is the radiant energy of the laser pulse in J/cm^2, D is the sample density in g/cm^3, c_p is the sample specific heat in J/gK, L is the sample thickness in cm, g is the absorption layer thickness in cm, α is the samples thermal diffusivity in cm^2/s, and T_o is the initial temperature of the sample.

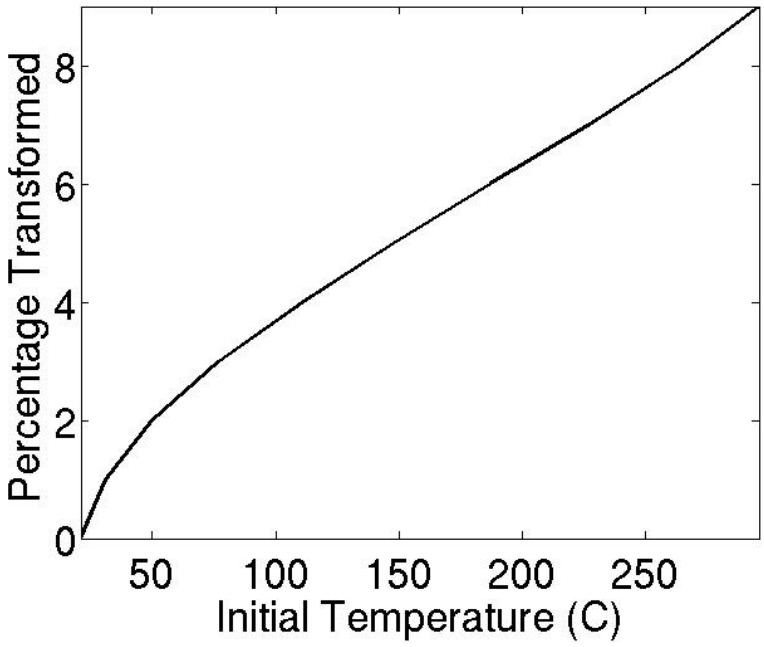

Figure 3.2: Fraction of KP transformed as a function of temperature. The results show that up to 290 °C less than 10% of the TKP-IP has transformed

As a rough approximation, all the energy is assumed to instantly and uniformly absorbed into a 5 micron graphite layer. Ideally, a two phase model should be used, since the above equation assumes a homogenous material. However, this simplification will suffice as a rough estimate. The NanoFlash® machine is reported to have a maximum energy deposition of 3 J/cm^2 [16]. Since the Ventron TKP was run with a 270 V flash and a duration of $\sim$ 250 μs, the radiant laser energy is assumed to be just 2 J/cm^2. The sample density, thickness, and thermal diffusivity are all taken from the measured values. A mass average value is taken for the specific heat, which is discussed in Section 3.3.2.3. Using these values and 10 terms in the summation, the fraction of the sample having transformed KP at each temperature measured can be calculated and is plotted in Figure 3.2. It can be seen that even up to 290 °C less than 10% of the TKP-IP has transformed. These results are the same order of magnitude as previous estimates using a radiant heat flux boundary condition [4]. Based on both of these approximations, it is assumed that the amount of KP transformed in the measurements can be neglected and that the results are representative of nascent TKP.

The average thermal diffusivity for Ventron TKP-IP at each temperature measured is listed in Table 3.6. For both IP-V-1-71-1 and IP-V-1-71-2, the thermal diffusivities show a similar downward trend in thermal diffusivity with temperature. This trend is fit to a quadratic equation using the data from both samples, and is shown in Figure 3.3.

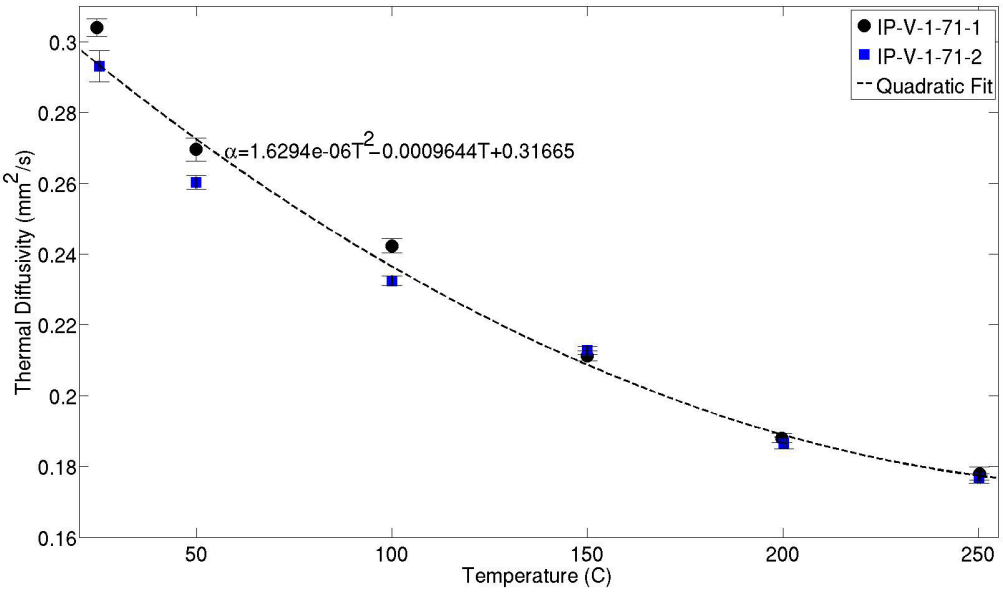

Figure 3.3: Thermal diffusivity as a function of temperature for both Ventron TKP-IP samples IP-V-1-71-1 and IP-V-1-71-2. The data shows a downward trend in thermal diffusivity with increasing temperature, which is fit to a quadratic equation.

3.3.2 Specific Heat

The specific heat of a sample can be found with the flash technique through comparisons to a reference material. The accuracy of this method relies on identical experimental parameters (*i.e.* temperature, flash voltage, flash duration, filter, masks, and coatings) and thermal properties between the sample and reference. ASTM Standard E1461-13 [1] also requires a short time lapse between the sample and reference measurements. Specific heats found using reference measurements with delays ranging from minutes to weeks of the sample gave essentially identical results (*i.e* the errors overlapped). This supports the reported repeatability in NanoFlash® Xenon flash[16]. As a result, no effort was made to have short delays between reference and sample measurement, with some being as much as weeks apart.

The NanoFlash® machine at Sandia has two reference materials: pocographite and Pyroceram®. The thermal properties of which are listed in Section 8. While the TKP and THKP formulations have identical NanoFlash® machine parameters to the reference materials, they do not have similar thermal properties. Care should be taken when using the specific heats reported here.

The specific heats measured for each shot on the TKP and THKP pellets using pocographite are given in Table 3.7, while those using Pyroceram® are given in Table 3.9. The average response at 25 °C for each TKP and THKP formulation using pocographite are listed in Table

3.8, while those found using Pyroceram® are in Table 3.10. To calculate the specific heat, each pellet was compared to the average of 5 shots on the reference materials at identical machine parameters and temperatures. There is an observed variability in specific heat with reference material. Specific heats found with pocgraphite have $\sim 15\%$ higher value when compared to those found with Pyroceram®. This result is related to the differing thermal properties of pocographite and Pyroceram®. This variability highlights the importance of similar parameters between the sample and reference. The differing thermal and physical properties between the reference and sample make measuring the specific heat of a sample to a high degree of accuracy difficult. These considerations must be kept in mind when using this data.

Table 3.1: Parameters of the TKP Pellets.

Pellet Label	Energetic Material	TMD (%)	Diameter (mm)	Weight (g)	Height (mm)	Density (g/cm^3)
IP-V-1-68-1	TKP-IP (Ventron)	68.0	12.725	0.257 ± 0.0005	1.013 ± 0.007	1.995 ± 0.015
IP-V-1-68-2	TKP-IP (Ventron)	67.6	12.725	0.252 ± 0.0005	0.999 ± 0.005	1.984 ± 0.013
IP-V-1-68-3	TKP-IP (Ventron)	67.5	12.725	0.252 ± 0.0005	1.000 ± 0.007	1.982 ± 0.016
IP-V-1-71-1	TKP-IP (Ventron)	71.4	12.725	0.272 ± 0.0005	1.020 ± 0.011	2.097 ± 0.024
IP-V-1-71-2	TKP-IP (Ventron)	71.3	12.725	0.271 ± 0.0005	1.018 ± 0.004	2.094 ± 0.011
IP-V-1-71-3	TKP-IP (Ventron)	71.4	12.725	0.269 ± 0.0005	1.007 ± 0.011	2.101 ± 0.024
IP-V-1-76-1	TKP-IP (Ventron)	75.3	12.725	0.290 ± 0.0005	1.032 ± 0.008	2.210 ± 0.018
IP-V-1-76-2	TKP-IP (Ventron)	76.2	12.725	0.293 ± 0.0005	1.030 ± 0.007	2.237 ± 0.018
IP-V-1-76-3	TKP-IP (Ventron)	76.0	12.725	0.293 ± 0.0005	1.033 ± 0.007	2.231 ± 0.017
IP-V-1-79-1	TKP-IP (Ventron)	79.3	12.725	0.349 ± 0.0005	1.179 ± 0.004	2.327 ± 0.011
IP-V-1-79-2	TKP-IP (Ventron)	78.9	12.725	0.341 ± 0.0005	1.158 ± 0.008	2.316 ± 0.018
IP-V-1-79-3	TKP-IP (Ventron)	79.7	12.725	0.344 ± 0.0005	1.156 ± 0.014	2.340 ± 0.029
IP-A-1-71-1	TKP-IP (ATK)	70.6	12.725	0.265 ± 0.0005	1.000 ± 0.009	2.084 ± 0.019
IP-A-3-71-1	TKP-IP (ATK)	71.0	12.725	0.852 ± 0.0005	3.195 ± 0.017	2.097 ± 0.011
IP-A-3-71-2	TKP-IP (ATK)	70.4	12.725	0.849 ± 0.0005	3.211 ± 0.006	2.079 ± 0.005
IP-A-3-71-3	TKP-IP (ATK)	71.1	12.725	0.852 ± 0.0005	3.190 ± 0.005	2.100 ± 0.004
OP-1-80-1	TKP-OP	79.5	12.725	0.322 ± 0.0005	1.034 ± 0.007	2.449 ± 0.019
OP-1-80-2	TKP-OP	81.0	12.725	0.326 ± 0.0005	1.028 ± 0.008	2.494 ± 0.021
OP-1-80-3	TKP-OP	80.6	12.725	0.325 ± 0.0005	1.030 ± 0.013	2.482 ± 0.033
THKP-1-80-1	THKP	80.8	12.725	0.303 ± 0.0005	1.038 ± 0.005	2.295 ± 0.013
THKP-1-80-2	THKP	80.0	12.725	0.303 ± 0.0005	1.047 ± 0.011	2.275 ± 0.025
THKP-1-80-3	THKP	80.4	12.725	0.306 ± 0.0005	1.053 ± 0.003	2.285 ± 0.010

Table 3.2: NanoFlash® Machine Parameters for Each TKP and THKP Pellet.

Pellet Label	Energetic Material	Temperature (C)	Shots	Volts (V)	Flash Duration (μs)	Preamp Gain	Main Gain	Recording Time (ms)
IP-V-1-68-1	TKP-IP (Ventron)	24.58 ± 0.26	5	270	250	10	2520	4920
IP-V-1-68-2	TKP-IP (Ventron)	25.16 ± 0.43	5	270	250	10	2520	4920
IP-V-1-68-3	TKP-IP (Ventron)	25.18 ± 0.36	5	270	250	10	2520	4920
IP-V-1-71-1	TKP-IP (Ventron)	24.56 ± 0.28	5	270	250	10	2520	5376
IP-V-1-71-1	TKP-IP (Ventron)	49.92 ± 0.18	5	270	250	10	1260	5966
IP-V-1-71-1	TKP-IP (Ventron)	100.02 ± 0.18	5	270	250	10	623	5966
IP-V-1-71-1	TKP-IP (Ventron)	150.02 ± 0.18	5	270	250	10	315	7248
IP-V-1-71-1	TKP-IP (Ventron)	199.74 ± 0.42	5	270	250	10	155	8130
IP-V-1-71-1	TKP-IP (Ventron)	250.24 ± 0.30	5	270	250	10	155	8130
IP-V-1-71-2	TKP-IP (Ventron)	25.18 ± 0.36	5	270	250	10	2520	5376
IP-V-1-71-2	TKP-IP (Ventron)	49.96 ± 0.21	5	270	250	10	1260	6424
IP-V-1-71-2	TKP-IP (Ventron)	100.02 ± 0.19	5	270	250	10	623	6424
IP-V-1-71-2	TKP-IP (Ventron)	150.02 ± 0.19	5	270	250	10	315	6424
IP-V-1-71-2	TKP-IP (Ventron)	200.26 ± 0.51	5	270	250	10	155	8130
IP-V-1-71-2	TKP-IP (Ventron)	250.14 ± 0.32	5	270	250	10	78.8	8130
IP-V-1-71-3	TKP-IP (Ventron)	25.20 ± 0.64	5	270	250	10	2520	5376
IP-V-1-76-1	TKP-IP (Ventron)	25.38 ± 0.19	5	270	250	10	2520	4452
IP-V-1-76-2	TKP-IP (Ventron)	24.82 ± 0.88	5	270	250	10	2520	4452
IP-V-1-76-3	TKP-IP (Ventron)	24.82 ± 0.69	5	270	250	10	2520	4452
IP-V-1-79-1	TKP-IP (Ventron)	25.04 ± 0.57	5	270	250	10	2520	5186
IP-V-1-79-2	TKP-IP (Ventron)	24.84 ± 0.80	5	270	250	10	2520	5186
IP-V-1-79-3	TKP-IP (Ventron)	25.26 ± 0.28	5	270	250	10	2520	4668
IP-A-1-71-1	TKP-IP (ATK)	24.76 ± 0.35	7	270	250	10	2520	6048
IP-A-3-71-1	TKP-IP (ATK)	24.90 ± 0.30	5	292	450	10	5002	55672
IP-A-3-71-2	TKP-IP (ATK)	25.12 ± 0.36	5	292	450	10	5002	55672
IP-A-3-71-3	TKP-IP (ATK)	25.08 ± 1.30	5	292	450	10	5002	55672
OP-1-80-1	TKP-OP	25.08 ± 0.48	5	270	250	10	2520	5376
OP-1-80-2	TKP-OP	25.38 ± 0.39	5	270	250	10	2520	5376
OP-1-80-3	TKP-OP	25.30 ± 0.41	5	270	250	10	2520	4892
THKP-1-80-1	THKP	24.88 ± 0.26	5	270	250	10	2520	5478
THKP-1-80-2	THKP	25.12 ± 1.37	5	270	250	10	2520	5478
THKP-1-80-3	THKP	25.14 ± 0.40	5	270	250	10	2520	5478

Table 3.3: Change in the Thermal Diffusivity with the Number of Terms Used in the Cowan Model.

Number of Terms	2	3	4	5	10
α (mm^2/s)	0.3108	0.3050	0.3050	0.3050	0.3050

Table 3.4: Measured Thermal Diffusivity in mm^2/s of the TKP and THKP Pellets.

Pellet Label	Temperature (C)	Shot #1	Shot #2	Shot #3	Shot #4	Shot #5	Shot #6	Shot #7
IP-V-1-68-1	24.58 ± 0.26	0.3085 ± 0.0015	0.3083 ± 0.0016	0.3060 ± 0.0015	0.3052 ± 0.0015	0.3101 ± 0.0017	-	-
IP-V-1-68-2	25.16 ± 0.43	0.3007 ± 0.0013	0.2997 ± 0.0014	0.3038 ± 0.0011	0.3009 ± 0.0014	0.3004 ± 0.0015	-	-
IP-V-1-68-3	25.18 ± 0.36	0.3058 ± 0.0016	0.3002 ± 0.0015	0.3024 ± 0.0016	0.3001 ± 0.0016	0.2989 ± 0.0015	-	-
IP-V-1-71-1	24.56 ± 0.28	0.3050 ± 0.0017	0.3043 ± 0.0018	0.3022 ± 0.0017	0.3036 ± 0.0017	0.3054 ± 0.0017	-	-
IP-V-1-71-1	49.92 ± 0.18	0.2653 ± 0.0013	0.2710 ± 0.0015	0.2692 ± 0.0014	0.2705 ± 0.0015	0.2719 ± 0.0015	-	-
IP-V-1-71-1	100.02 ± 0.18	0.2439 ± 0.0014	0.2419 ± 0.0014	0.2422 ± 0.0013	0.2409 ± 0.0013	0.2433 ± 0.0013	-	-
IP-V-1-71-1	150.02 ± 0.18	0.2121 ± 0.0011	0.2110 ± 0.0010	0.2113 ± 0.0011	0.2102 ± 0.0011	0.2113 ± 0.0011	-	-
IP-V-1-71-1	199.74 ± 0.42	0.1883 ± 0.0009	0.1886 ± 0.0009	0.1873 ± 0.0010	0.1884 ± 0.0008	0.1872 ± 0.0008	-	-
IP-V-1-71-1	250.24 ± 0.30	0.1775 ± 0.0009	0.1785 ± 0.0010	0.1796 ± 0.0009	0.1779 ± 0.0009	0.1762 ± 0.0009	-	-
IP-V-1-71-2	25.18 ± 0.36	0.2967 ± 0.0013	0.2890 ± 0.0012	0.2912 ± 0.0014	0.2912 ± 0.0014	0.2981 ± 0.0013	-	-
IP-V-1-71-2	49.96 ± 0.21	0.2610 ± 0.0010	0.2606 ± 0.0010	0.2582 ± 0.0010	0.2620 ± 0.0010	0.2594 ± 0.0011	-	-
IP-V-1-71-2	100.02 ± 0.19	0.2318 ± 0.0009	0.2331 ± 0.0010	0.2330 ± 0.0011	0.2323 ± 0.0011	0.2321 ± 0.0010	-	-
IP-V-1-71-2	150.02 ± 0.19	0.2127 ± 0.0007	0.2118 ± 0.0008	0.2132 ± 0.0008	0.2130 ± 0.0010	0.2133 ± 0.0008	-	-
IP-V-1-71-2	200.26 ± 0.51	0.1887 ± 0.0008	0.1859 ± 0.0007	0.1862 ± 0.0008	0.1855 ± 0.0008	0.1869 ± 0.0007	-	-
IP-V-1-71-2	250.14 ± 0.32	0.1761 ± 0.0007	0.1765 ± 0.0008	0.1771 ± 0.0008	0.1756 ± 0.0007	0.1778 ± 0.0007	-	-
IP-V-1-71-3	25.20 ± 0.64	0.3009 ± 0.0017	0.3029 ± 0.0017	0.3016 ± 0.0016	0.3051 ± 0.0018	0.2991 ± 0.0016	-	-
IP-V-1-76-1	25.38 ± 0.19	0.3675 ± 0.0017	0.3740 ± 0.0018	0.3801 ± 0.0019	0.3803 ± 0.0019	0.3748 ± 0.0019	-	-
IP-V-1-76-2	24.82 ± 0.88	0.3749 ± 0.0020	0.3795 ± 0.0020	0.3691 ± 0.0017	0.3688 ± 0.0018	0.3721 ± 0.0019	-	-
IP-V-1-76-3	24.82 ± 0.69	0.3625 ± 0.0017	0.3664 ± 0.0019	0.3679 ± 0.0018	0.3620 ± 0.0018	0.3714 ± 0.0019	-	-
IP-V-1-79-1	25.04 ± 0.57	0.4281 ± 0.0019	0.4304 ± 0.0019	0.4306 ± 0.0015	0.4351 ± 0.0020	0.4319 ± 0.0019	-	-
IP-V-1-79-2	24.84 ± 0.80	0.4426 ± 0.0020	0.4449 ± 0.0021	0.4523 ± 0.0021	0.4532 ± 0.0023	0.4541 ± 0.0021	-	-
IP-V-1-79-3	25.26 ± 0.28	0.4552 ± 0.0026	0.4443 ± 0.0024	0.4468 ± 0.0025	0.4480 ± 0.0027	0.4481 ± 0.0027	-	-
IP-A-1-71-1	24.76 ± 0.35	0.2430 ± 0.0013	0.2443 ± 0.0013	0.2466 ± 0.0012	0.2472 ± 0.0013	0.2459 ± 0.0014	0.2474 ± 0.0013	0.2457 ± 0.0013
IP-A-3-71-1	24.90 ± 0.30	0.2270 ± 0.0019	0.2233 ± 0.0018	0.2283 ± 0.0020	0.2188 ± 0.0019	0.2220 ± 0.0016	-	-
IP-A-3-71-2	25.12 ± 0.36	0.2178 ± 0.0021	0.2161 ± 0.0027	0.2044 ± 0.0021	0.2158 ± 0.0021	0.2215 ± 0.0019	-	-
IP-A-3-71-3	25.08 ± 1.30	0.1947 ± 0.0024	0.2055 ± 0.0019	0.2125 ± 0.0018	0.2129 ± 0.0017	0.2114 ± 0.0018	-	-
OP-1-80-1	25.08 ± 0.48	0.3032 ± 0.0014	0.3071 ± 0.0014	0.3062 ± 0.0015	0.3040 ± 0.0014	0.3044 ± 0.0015	-	-
OP-1-80-2	25.38 ± 0.39	0.3324 ± 0.0016	0.3332 ± 0.0015	0.3256 ± 0.0015	0.3233 ± 0.0016	0.3307 ± 0.0017	-	-
OP-1-80-3	25.30 ± 0.41	0.3340 ± 0.0018	0.3359 ± 0.0017	0.3413 ± 0.0020	0.3331 ± 0.0019	0.3401 ± 0.0019	-	-
THKP-1-80-1	24.88 ± 0.26	0.2980 ± 0.0013	0.3012 ± 0.0014	0.2919 ± 0.0012	0.2980 ± 0.0013	0.2927 ± 0.0012	-	-
THKP-1-80-2	25.12 ± 1.37	0.3014 ± 0.0016	0.3029 ± 0.0013	0.3034 ± 0.0016	0.3099 ± 0.0017	0.3065 ± 0.0017	-	-
THKP-1-80-3	25.14 ± 0.40	0.3156 ± 0.0014	0.3171 ± 0.0012	0.3158 ± 0.0013	0.3184 ± 0.0014	0.3125 ± 0.0013	-	-

Table 3.5: Average Thermal Diffusivity in mm^2/s for Each TKP and THKP Formulation.

Pellet Label	Temperature (C)	Average Thermal Diffusivity	Formulation Thermal Diffusivity
IP-V-1-68-1	24.58 ± 0.26	0.3076 ± 0.0024	
IP-V-1-68-2	25.16 ± 0.43	0.3011 ± 0.0020	0.3034 ± 0.0056
IP-V-1-68-3	25.18 ± 0.36	0.3015 ± 0.0031	
IP-V-1-71-1	24.56 ± 0.28	0.3041 ± 0.0024	
IP-V-1-71-2	25.18 ± 0.36	0.2932 ± 0.0040	0.2997 ± 0.0082
IP-V-1-71-3	25.20 ± 0.64	0.3019 ± 0.0027	
IP-V-1-76-1	25.38 ± 0.19	0.3753 ± 0.0054	
IP-V-1-76-2	24.82 ± 0.88	0.3729 ± 0.0047	0.3714 ± 0.0082
IP-V-1-76-3	24.82 ± 0.69	0.3660 ± 0.0042	
IP-V-1-79-1	25.04 ± 0.57	0.4312 ± 0.0031	
IP-V-1-79-2	24.84 ± 0.80	0.4494 ± 0.0056	0.4430 ± 0.0142
IP-V-1-79-3	25.26 ± 0.28	0.4485 ± 0.0047	
IP-A-1-71-1	24.76 ± 0.35	0.2457 ± 0.0019	0.2457 ± 0.0019
IP-A-3-71-1	24.90 ± 0.30	0.2239 ± 0.0042	
IP-A-3-71-2	25.12 ± 0.36	0.2151 ± 0.0066	0.2155 ± 0.0139
IP-A-3-71-3	25.08 ± 1.30	0.2074 ± 0.0113	
OP-1-80-1	25.08 ± 0.48	0.3050 ± 0.0021	
OP-1-80-2	25.38 ± 0.39	0.3290 ± 0.0045	0.3236 ± 0.0209
OP-1-80-3	25.30 ± 0.41	0.3369 ± 0.0040	
THKP-1-80-1	24.88 ± 0.26	0.2964 ± 0.0040	
THKP-1-80-2	25.12 ± 1.37	0.3048 ± 0.0037	0.3057 ± 0.0131
THKP-1-80-3	25.14 ± 0.40	0.3159 ± 0.0025	

Table 3.6: Average Thermal Diffusivity in mm^2/s for the Ventron TKP-IP at Temperature.

Pellet Label	Temperature (C)	Average Thermal Diffusivity
IP-V-1-71-1	24.56 ± 0.28	0.3041 ± 0.0024
IP-V-1-71-1	49.92 ± 0.18	0.2696 ± 0.0033
IP-V-1-71-1	100.02 ± 0.18	0.2424 ± 0.0020
IP-V-1-71-1	150.02 ± 0.18	0.2112 ± 0.0014
IP-V-1-71-1	199.74 ± 0.42	0.1880 ± 0.0013
IP-V-1-71-1	250.24 ± 0.30	0.1780 ± 0.0018
IP-V-1-71-2	25.18 ± 0.36	0.2932 ± 0.0044
IP-V-1-71-2	49.96 ± 0.21	0.2603 ± 0.0020
IP-V-1-71-2	100.02 ± 0.19	0.2325 ± 0.0013
IP-V-1-71-2	150.02 ± 0.19	0.2128 ± 0.0011
IP-V-1-71-2	200.26 ± 0.51	0.1866 ± 0.0017
IP-V-1-71-2	250.14 ± 0.32	0.1766 ± 0.0013

Table 3.7: Measured Specific Heat in J/gK of the TKP and THKP Pellets Found with the Pocographite Reference.

Pellet Label	Temperature (C)	Shot #1	Shot #2	Shot #3	Shot #4	Shot #5	Shot #6	Shot #7
IP-V-1-68-1	24.58 ± 0.26	0.7375 ± 0.0277	0.7316 ± 0.0278	0.7145 ± 0.0268	0.7177 ± 0.0271	0.7473 ± 0.0282	-	-
IP-V-1-68-2	25.16 ± 0.43	0.7853 ± 0.0257	0.7882 ± 0.0260	0.7915 ± 0.0254	0.7746 ± 0.0253	0.7668 ± 0.0255	-	-
IP-V-1-68-3	25.18 ± 0.36	0.7572 ± 0.0281	0.7232 ± 0.0270	0.7267 ± 0.0270	0.7273 ± 0.0274	0.7092 ± 0.0266	-	-
IP-V-1-71-1	24.56 ± 0.28	0.8672 ± 0.0421	0.8493 ± 0.0414	0.8298 ± 0.0405	0.8158 ± 0.0397	0.8558 ± 0.0414	-	-
IP-V-1-71-1	49.92 ± 0.18	0.9843 ± 0.0469	0.9928 ± 0.0477	1.0093 ± 0.0487	1.0169 ± 0.0491	0.9671 ± 0.0461	-	-
IP-V-1-71-1	100.02 ± 0.18	0.9897 ± 0.0469	0.9908 ± 0.0473	1.0176 ± 0.0481	0.9716 ± 0.0462	0.9620 ± 0.0451	-	-
IP-V-1-71-1	150.02 ± 0.18	1.0779 ± 0.0518	1.0764 ± 0.0511	1.0912 ± 0.0528	1.0948 ± 0.0532	1.1137 ± 0.0534	-	-
IP-V-1-71-1	199.74 ± 0.42	1.1515 ± 0.0554	1.1483 ± 0.0555	1.1258 ± 0.0548	1.1731 ± 0.0557	1.1045 ± 0.0530	-	-
IP-V-1-71-1	250.74 ± 0.30	1.3124 ± 0.0633	1.2720 ± 0.0616	1.2966 ± 0.0620	1.3014 ± 0.0629	1.2466 ± 0.0607	-	-
IP-V-1-71-2	25.18 ± 0.36	0.8066 ± 0.0246	0.7672 ± 0.0238	0.7512 ± 0.0231	0.7561 ± 0.0234	0.7740 ± 0.0237	-	-
IP-V-1-71-2	49.96 ± 0.21	0.8219 ± 0.0238	0.8022 ± 0.0231	0.7614 ± 0.0223	0.8011 ± 0.0229	0.8071 ± 0.0238	-	-
IP-V-1-71-2	100.02 ± 0.19	0.8885 ± 0.0260	0.9158 ± 0.0270	0.8971 ± 0.0265	0.8989 ± 0.0266	0.9034 ± 0.0266	-	-
IP-V-1-71-2	150.02 ± 0.19	1.0208 ± 0.0293	1.0416 ± 0.0304	1.0130 ± 0.0297	0.9921 ± 0.0296	1.0286 ± 0.0300	-	-
IP-V-1-71-2	200.26 ± 0.51	1.0364 ± 0.0307	1.0515 ± 0.0309	1.0325 ± 0.0307	1.0322 ± 0.0310	1.0288 ± 0.0301	-	-
IP-V-1-71-2	250.14 ± 0.32	1.1417 ± 0.0337	1.1209 ± 0.0335	1.1628 ± 0.0346	1.1314 ± 0.0337	1.1403 ± 0.0335	-	-
IP-V-1-71-3	25.20 ± 0.64	0.8368 ± 0.0412	0.8178 ± 0.0401	0.8114 ± 0.0395	0.8442 ± 0.0414	0.8023 ± 0.0395	-	-
IP-V-1-76-1	25.38 ± 0.19	0.7278 ± 0.0285	0.7324 ± 0.0281	0.7645 ± 0.0293	0.7612 ± 0.0292	0.7491 ± 0.0290	-	-
IP-V-1-76-2	24.82 ± 0.88	0.7570 ± 0.0281	0.7785 ± 0.0282	0.7409 ± 0.0269	0.7437 ± 0.0271	0.7407 ± 0.0271	-	-
IP-V-1-76-3	24.82 ± 0.69	0.7400 ± 0.0271	0.7595 ± 0.0281	0.7311 ± 0.0265	0.7211 ± 0.0266	0.7363 ± 0.0269	-	-
IP-V-1-79-1	25.04 ± 0.57	0.7971 ± 0.0241	0.7715 ± 0.0230	0.7773 ± 0.0230	0.8166 ± 0.0248	0.7921 ± 0.0238	-	-
IP-V-1-79-2	24.84 ± 0.80	0.7856 ± 0.0292	0.7878 ± 0.0294	0.7784 ± 0.0286	0.7748 ± 0.0287	0.7701 ± 0.0282	-	-
IP-V-1-79-3	25.26 ± 0.28	0.7444 ± 0.0375	0.7327 ± 0.0374	0.7366 ± 0.0377	0.7446 ± 0.0382	0.7380 ± 0.0377	-	-
IP-A-1-71-1	24.76 ± 0.35	0.7092 ± 0.0314	0.7357 ± 0.0322	0.7452 ± 0.0321	0.7529 ± 0.0327	0.7513 ± 0.0332	0.7438 ± 0.0324	0.7390 ± 0.0321
IP-A-3-71-1	24.90 ± 0.30	0.9546 ± 0.0669	0.9218 ± 0.0622	0.8786 ± 0.0629	0.8165 ± 0.0579	0.8307 ± 0.0538	-	-
IP-A-3-71-2	25.12 ± 0.36	1.0292 ± 0.0729	1.0721 ± 0.0949	0.9402 ± 0.0758	1.0087 ± 0.0724	0.9238 ± 0.0592	-	-
IP-A-3-71-3	25.08 ± 1.30	0.8748 ± 0.3713	0.9950 ± 0.0719	0.9716 ± 0.0621	0.8474 ± 0.0512	0.8542 ± 0.0550	-	-
OP-1-80-1	25.08 ± 0.48	0.6583 ± 0.0243	0.6613 ± 0.0242	0.6513 ± 0.0239	0.6533 ± 0.0241	0.6407 ± 0.0239	-	-
OP-1-80-2	25.38 ± 0.39	0.6554 ± 0.0258	0.6537 ± 0.0254	0.6264 ± 0.0249	0.6327 ± 0.0253	0.6544 ± 0.0257	-	-
OP-1-80-3	25.30 ± 0.41	0.6499 ± 0.0350	0.6419 ± 0.0347	0.6648 ± 0.0356	0.6335 ± 0.0345	0.6591 ± 0.0353	-	-
THKP-1-80-1	24.88 ± 0.26	0.7229 ± 0.0232	0.7222 ± 0.0230	0.6999 ± 0.0224	0.7244 ± 0.0233	0.6904 ± 0.0220	-	-
THKP-1-80-1	25.12 ± 1.37	0.7050 ± 0.0336	0.7161 ± 0.0338	0.7212 ± 0.0343	0.7472 ± 0.0349	0.7477 ± 0.0353	-	-
THKP-1-80-1	25.14 ± 0.40	0.7627 ± 0.0220	0.7734 ± 0.0218	0.7964 ± 0.0228	0.7691 ± 0.0219	0.7358 ± 0.0210	-	-

Table 3.8: Average Measured Specific Heat in J/gK of Each TKP and THKP Formulation Using the Pocographite Reference.

Pellet Label	Temperature (C)	Average Specific Heat	Formulation Specific Heat
IP-V-1-68-1	24.58 ± 0.26	0.7297 ± 0.0243	
IP-V-1-68-2	25.16 ± 0.43	0.7813 ± 0.0205	0.7466 ± 0.0480
IP-V-1-68-3	25.18 ± 0.36	0.7287 ± 0.0276	
IP-V-1-71-1	24.56 ± 0.28	0.8436 ± 0.0364	
IP-V-1-71-2	25.18 ± 0.36	0.7710 ± 0.0297	0.8124 ± 0.0615
IP-V-1-71-3	25.20 ± 0.64	0.8225 ± 0.0334	
IP-V-1-76-1	25.38 ± 0.19	0.7491 ± 0.0290	
IP-V-1-76-2	24.82 ± 0.88	0.7407 ± 0.0271	0.7456 ± 0.0234
IP-V-1-76-3	24.82 ± 0.69	0.7363 ± 0.0269	
IP-V-1-79-1	25.04 ± 0.57	0.7909 ± 0.0262	
IP-V-1-79-2	24.84 ± 0.80	0.7793 ± 0.0194	0.7694 ± 0.0446
IP-V-1-79-3	25.26 ± 0.28	0.7380 ± 0.0223	
IP-A-1-71-1	24.76 ± 0.35	0.7388 ± 0.0302	0.7388 ± 0.02302
IP-A-3-71-1	24.90 ± 0.30	0.8804 ± 0.0787	
IP-A-3-71-2	25.12 ± 0.36	0.9948 ± 0.0883	0.9279 ± 0.1283
IP-A-3-71-3	25.08 ± 1.30	0.9086 ± 0.1390	
OP-1-80-1	25.08 ± 0.48	0.6530 ± 0.0177	
OP-1-80-2	25.38 ± 0.39	0.6445 ± 0.0235	0.6491 ± 0.0181
OP-1-80-3	25.30 ± 0.41	0.6498 ± 0.0268	
THKP-1-80-1	24.88 ± 0.26	0.7120 ± 0.0240	
THKP-1-80-2	25.12 ± 1.37	0.7274 ± 0.0322	0.7356 ± 0.0489
THKP-1-80-3	25.14 ± 0.40	0.7675 ± 0.0289	

Table 3.9: Measured Specific Heat in J/gK of the TKP and THKP Pellets Found with the Pyroceram® Reference.

Pellet Label	Temperature (C)	Shot #1	Shot #2	Shot #3	Shot #4	Shot #5	Shot #6	Shot #7
IP-V-1-68-1	24.58 ± 0.26	0.6031 ± 0.0256	0.5982 ± 0.0256	0.5842 ± 0.0248	0.5869 ± 0.0250	0.6110 ± 0.0260	-	-
IP-V-1-68-2	25.16 ± 0.43	0.6421 ± 0.0245	0.6445 ± 0.0247	0.6472 ± 0.0243	0.6333 ± 0.0242	0.6270 ± 0.0242	-	-
IP-V-1-68-3	25.18 ± 0.36	0.6192 ± 0.0239	0.5913 ± 0.0229	0.5942 ± 0.0229	0.5947 ± 0.0231	0.5798 ± 0.0225	-	-
IP-V-1-71-1	24.56 ± 0.28	0.7091 ± 0.0372	0.6945 ± 0.0365	0.6785 ± 0.0357	0.6671 ± 0.0350	0.6998 ± 0.0365	-	-
IP-V-1-71-1	49.92 ± 0.18	0.7822 ± 0.0389	0.7889 ± 0.0395	0.8021 ± 0.0404	0.8081 ± 0.0407	0.7685 ± 0.0383	-	-
IP-V-1-71-1	100.02 ± 0.18	0.7587 ± 0.0366	0.7596 ± 0.0369	0.7801 ± 0.0375	0.7448 ± 0.0361	0.7375 ± 0.0352	-	-
IP-V-1-71-1	150.02 ± 0.18	0.7900 ± 0.0382	0.7888 ± 0.0377	0.7997 ± 0.0390	0.8023 ± 0.0393	0.8161 ± 0.0394	-	-
IP-V-1-71-1	199.74 ± 0.42	0.8237 ± 0.0399	0.8214 ± 0.0400	0.8053 ± 0.0395	0.8391 ± 0.0402	0.7901 ± 0.0382	-	-
IP-V-1-71-1	250.74 ± 0.30	0.9410 ± 0.0456	0.9120 ± 0.0444	0.9296 ± 0.0447	0.9331 ± 0.0453	0.8938 ± 0.0437	-	-
IP-V-1-71-2	25.18 ± 0.36	0.6595 ± 0.0239	0.6273 ± 0.0230	0.6142 ± 0.0224	0.6182 ± 0.0226	0.6329 ± 0.0230	-	-
IP-V-1-71-2	49.96 ± 0.21	0.6529 ± 0.0211	0.6372 ± 0.0205	0.6048 ± 0.0197	0.6363 ± 0.0204	0.6411 ± 0.0210	-	-
IP-V-1-71-2	100.02 ± 0.19	0.6808 ± 0.0208	0.7017 ± 0.0217	0.6874 ± 0.0212	0.6888 ± 0.0213	0.6922 ± 0.0213	-	-
IP-V-1-71-2	150.02 ± 0.19	0.7477 ± 0.0217	0.7630 ± 0.0225	0.7420 ± 0.0220	0.7267 ± 0.0220	0.7535 ± 0.0223	-	-
IP-V-1-71-2	200.26 ± 0.51	0.7421 ± 0.0224	0.7529 ± 0.0225	0.7393 ± 0.0224	0.7391 ± 0.0226	0.7366 ± 0.0220	-	-
IP-V-1-71-2	250.14 ± 0.32	0.8186 ± 0.0244	0.8037 ± 0.0243	0.8338 ± 0.0251	0.8112 ± 0.0245	0.8176 ± 0.0243	-	-
IP-V-1-71-3	25.20 ± 0.64	0.6842 ± 0.0363	0.6687 ± 0.0353	0.6635 ± 0.0348	0.6903 ± 0.0365	0.6560 ± 0.0348	-	-
IP-V-1-76-1	25.38 ± 0.19	0.5951 ± 0.0265	0.5989 ± 0.0263	0.6251 ± 0.0274	0.6224 ± 0.0273	0.6125 ± 0.0270	-	-
IP-V-1-76-2	24.82 ± 0.88	0.6190 ± 0.0265	0.6366 ± 0.0267	0.6058 ± 0.0255	0.6081 ± 0.0257	0.6056 ± 0.0256	-	-
IP-V-1-76-3	25.26 ± 0.28	0.6051 ± 0.0256	0.6211 ± 0.0264	0.5978 ± 0.0250	0.5896 ± 0.0251	0.6021 ± 0.0254	-	-
IP-V-1-79-1	25.04 ± 0.57	0.6518 ± 0.0237	0.6308 ± 0.0227	0.6356 ± 0.0228	0.6677 ± 0.0243	0.6477 ± 0.0234	-	-
IP-V-1-79-2	24.84 ± 0.80	0.6424 ± 0.0274	0.6441 ± 0.0276	0.6465 ± 0.0270	0.6335 ± 0.0270	0.6297 ± 0.0266	-	-
IP-V-1-79-3	25.26 ± 0.28	0.6087 ± 0.0322	0.5991 ± 0.0328	0.6023 ± 0.0330	0.6088 ± 0.0334	0.5984 ± 0.0330	-	-
IP-A-1-71-1	24.76 ± 0.35	0.5799 ± 0.0281	0.6015 ± 0.0289	0.6093 ± 0.0288	0.6156 ± 0.0293	0.6143 ± 0.0297	0.6082 ± 0.0290	0.6042 ± 0.0288
IP-A-3-71-1	24.90 ± 0.30	0.8127 ± 0.0584	0.7848 ± 0.0543	0.7480 ± 0.0548	0.6951 ± 0.0505	0.7072 ± 0.0471	-	-
IP-A-3-71-2	25.12 ± 0.36	0.8763 ± 0.0636	0.9128 ± 0.0820	0.8004 ± 0.0657	0.8588 ± 0.0631	0.7866 ± 0.0519	-	-
IP-A-3-71-3	25.08 ± 1.30	0.7448 ± 0.3164	0.8471 ± 0.0627	0.8272 ± 0.0544	0.7215 ± 0.0450	0.7273 ± 0.0482	-	-
OP-1-80-1	25.08 ± 0.48	0.5383 ± 0.0225	0.5407 ± 0.0225	0.5326 ± 0.0222	0.5341 ± 0.0223	0.5239 ± 0.0221	-	-
OP-1-80-2	25.38 ± 0.39	0.5359 ± 0.0235	0.5345 ± 0.0233	0.5122 ± 0.0227	0.5173 ± 0.0231	0.5351 ± 0.0235	-	-
OP-1-80-3	25.30 ± 0.41	0.5314 ± 0.0304	0.5248 ± 0.0302	0.5436 ± 0.0310	0.5180 ± 0.0300	0.5389 ± 0.0308	-	-
THKP-1-80-1	24.88 ± 0.26	0.5911 ± 0.0222	0.5905 ± 0.0221	0.5722 ± 0.0215	0.5923 ± 0.0223	0.5646 ± 0.0211	-	-
THKP-1-80-2	25.12 ± 1.37	0.5765 ± 0.0297	0.5855 ± 0.0299	0.5897 ± 0.0304	0.6110 ± 0.0309	0.6114 ± 0.0313	-	-
THKP-1-80-3	25.14 ± 0.40	0.6236 ± 0.0217	0.6324 ± 0.0217	0.6511 ± 0.0226	0.6289 ± 0.0218	0.6016 ± 0.0208	-	-

Table 3.10: Average Measured Specific Heat in J/gK of Each TKP and THKP Formulation Using the Pyroceram® Reference.

Pellet Label	Temperature (C)	Average Specific Heat	Formulation Specific Heat
IP-V-1-68-1	24.58 ± 0.26	0.5967 ± 0.0211	
IP-V-1-68-2	25.16 ± 0.43	0.6388 ± 0.0183	0.6104 ± 0.0398
IP-V-1-68-3	25.18 ± 0.36	0.5958 ± 0.0229	
IP-V-1-71-1	24.56 ± 0.28	0.6898 ± 0.0310	
IP-V-1-71-2	25.18 ± 0.36	0.6304 ± 0.0259	0.6642 ± 0.0510
IP-V-1-71-3	25.20 ± 0.64	0.6725 ± 0.0285	
IP-V-1-76-1	25.38 ± 0.19	0.6108 ± 0.0239	
IP-V-1-76-2	24.82 ± 0.88	0.6150 ± 0.0232	0.6097 ± 0.0200
IP-V-1-76-3	25.26 ± 0.28	0.6031 ± 0.0216	
IP-V-1-79-1	25.04 ± 0.57	0.6467 ± 0.0232	
IP-V-1-79-2	24.84 ± 0.80	0.6372 ± 0.0174	0.6291 ± 0.0373
IP-V-1-79-3	25.26 ± 0.28	0.6035 ± 0.0191	
IP-A-1-71-1	24.76 ± 0.35	0.6041 ± 0.0258	0.6041 ± 0.0258
IP-A-3-71-1	24.90 ± 0.30	0.7496 ± 0.0676	
IP-A-3-71-2	25.12 ± 0.36	0.8470 ± 0.0758	0.7900 ± 0.1094
IP-A-3-71-3	25.08 ± 1.30	0.7736 ± 0.1185	
OP-1-80-1	25.08 ± 0.48	0.5339 ± 0.0157	
OP-1-80-2	25.38 ± 0.39	0.5270 ± 0.0203	0.5308 ± 0.0154
OP-1-80-3	25.30 ± 0.41	0.5313 ± 0.0227	
THKP-1-80-1	24.88 ± 0.26	0.5821 ± 0.0210	
THKP-1-80-2	25.12 ± 1.37	0.5948 ± 0.0274	0.6015 ± 0.0408
THKP-1-80-3	25.14 ± 0.40	0.6275 ± 0.0253	

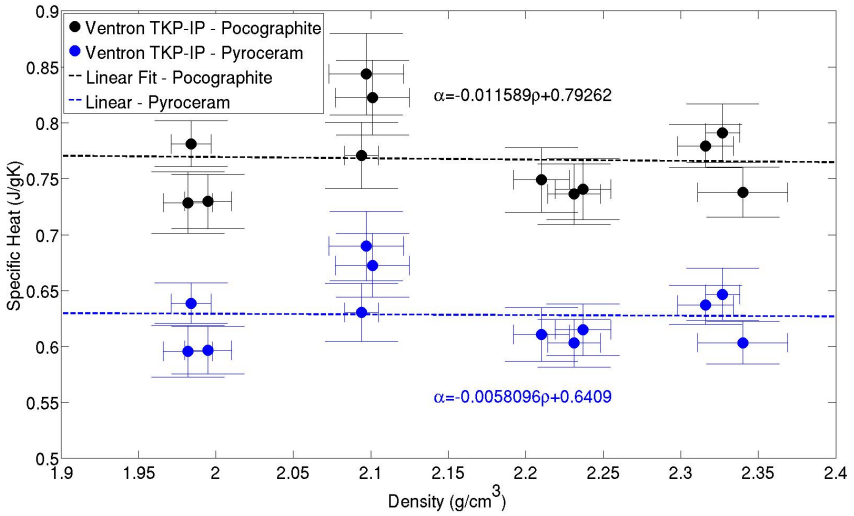

Figure 3.4: Specific heat as a function of density for the Ventron TKP-IP at 25 °C. The data shows a shallow downward trend in specific heat as density increases. The results also show a dependence on the reference material. The specific heat found with pocographite (black) is $\sim$ 15% higher than that found with Pyroceram® (blue).

3.3.2.1 Effect of Density on Specific Heat

The change in specific heat as a function density at 25 °C for the Ventron TKP-IP pellets is presented graphically Figure 3.4. The data shows a shallow downward trend in specific heat with density that is fit to a linear equation. Since the specific heats found with pocographite are a consistent percentage off from those found with Pyroceram®, both exhibit shallow slopes.

3.3.2.2 Effect of Temperature on Specific Heat

The average specific heat of the Ventron TKP-IP at each temperature measured using the pocographite reference are listed in Table 3.11, while those found using Pyroceram® are in Table 3.12. Once again, each pellet was compared to the average of 5 shots on the reference materials at identical NanoFlash® machine parameters and temperatures. There is still the observed variability in specific heat with reference material. The change is specific heat as a function temperature for the Ventron TKP-IP pellets is presented graphically in Figure 3.5. The data shows an upward trend in specific heat with temperature that is fit to a linear equation. Since the specific heats found with pocographite are a consistent percentage off from those found with Pyroceram®, similar slopes are seen in both linear fits.

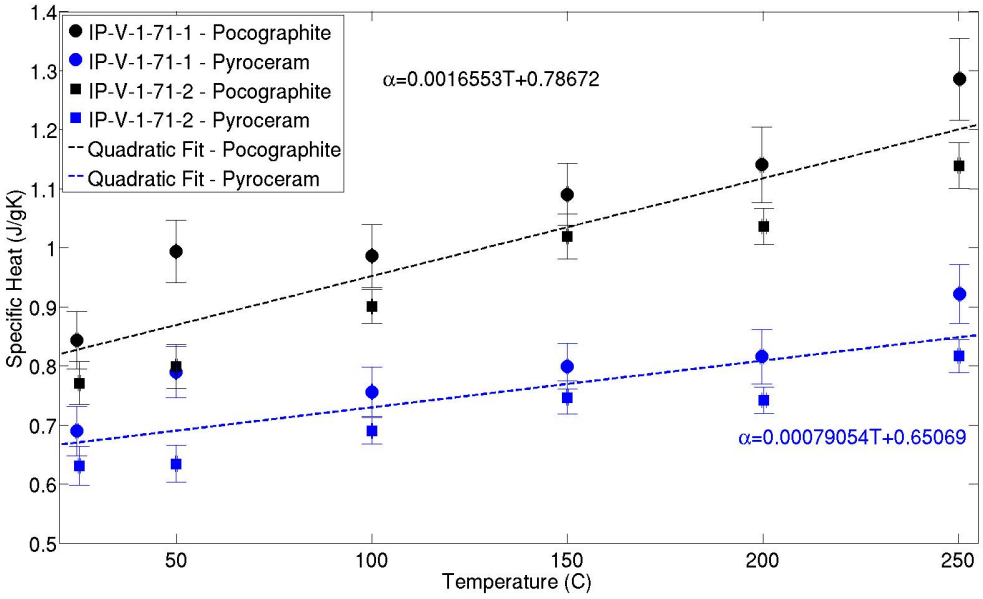

Figure 3.5: Specific heat as a function of temperature for Ventron TKP-IP samples IP-V-1-71-1 and IP-V-1-71-2. The data shows an upward trend in specific heat with increasing temperature, which is fit to a linear equation. The specific heat found with pocographite (black) is consistently higher than that found with Pyroceram® (blue).

Table 3.11: Average Measured Specific Heat in J/gK of Ventron TKP-IP at Temperature Using the Pocographite Reference.

Pellet Label	Temperature (C)	Average Specific Heat
IP-V-1-71-1	24.56 ± 0.28	0.8436 ± 0.0487
IP-V-1-71-1	49.92 ± 0.18	0.9941 ± 0.0530
IP-V-1-71-1	100.02 ± 0.18	0.9863 ± 0.0535
IP-V-1-71-1	150.02 ± 0.18	1.0908 ± 0.0524
IP-V-1-71-1	199.74 ± 0.42	1.1406 ± 0.0639
IP-V-1-71-1	250.24 ± 0.30	1.2858 ± 0.0695
IP-V-1-71-2	25.18 ± 0.36	0.7710 ± 0.0368
IP-V-1-71-2	49.96 ± 0.21	0.7987 ± 0.0370
IP-V-1-71-2	100.02 ± 0.19	0.9007 ± 0.0285
IP-V-1-71-2	150.02 ± 0.19	1.0192 ± 0.0384
IP-V-1-71-2	200.26 ± 0.51	1.0363 ± 0.0307
IP-V-1-71-2	250.14 ± 0.32	1.1394 ± 0.0388

3.3.2.3 Comparison to a Specific Heat Found with Mass Averaging

The specific heat measured at 25 °C with the flash technique can be compared to an analytical value determined through mass averaging of the constituents using JANNAF tables [10]. Assuming a 0.5 °C temperature error in the tabular data, the specific heat of Potassium Perchlorate, Titanium, and Titanium Hydride at 25 °C are $c_{p_{KP}} = 0.7954 \pm 0.0054$ J/gK, $c_{p_{Ti}} = 0.5271 \pm 0.0002$ J/gK, and $c_{p_{TiH}} = 0.6030 \pm 0.0009$ J/gK, respectively. Using the compositions of each TKP and THKP formulation listed in Section 3.1, a mass averaged specific heat was calculated. These values are given in Table 3.13 and tend to lie between those calculated with the pocographite and Pyroceram® standards. The exception to this is TKP-OP, which is below this analytical value for both standards.

3.3.3 Comparison to the Proteus® Software

In order to verify the MATLAB® routine, it was desired to compere it to the Proteus® LFA analysis software [17] provided with the NanoFlash® machine. The thermal diffusivities found at 25 °C using the Cowan model with both the Proteus® software and MATLAB® code are presented in Table 3.14. The two methods are within 5% for all cases and within 3% for most pellets. As a result, the MATLAB® code is considered to be an appropriate analysis method for determining thermal diffusivity.

The specific heats found with the Proteus® software and the MATLAB® code using the pocographite reference are presented in Table 3.15, while those found using the Pyroceram®

Table 3.12: Average Measured Specific Heat in J/gK of Ventron TKP-IP at Temperature Using the Pyroceram® Reference.

Pellet Label	Temperature (C)	Average Specific Heat
IP-V-1-71-1	24.56 ± 0.28	0.6898 ± 0.0417
IP-V-1-71-1	49.92 ± 0.18	0.7900 ± 0.0433
IP-V-1-71-1	100.02 ± 0.18	0.7561 ± 0.0415
IP-V-1-71-1	150.02 ± 0.18	0.7994 ± 0.0386
IP-V-1-71-1	199.74 ± 0.42	0.8159 ± 0.0459
IP-V-1-71-1	250.24 ± 0.30	0.9219 ± 0.0499
IP-V-1-71-2	25.18 ± 0.36	0.6304 ± 0.0259
IP-V-1-71-2	49.96 ± 0.21	0.6344 ± 0.0309
IP-V-1-71-2	100.02 ± 0.19	0.6902 ± 0.0226
IP-V-1-71-2	150.02 ± 0.19	0.7466 ± 0.0284
IP-V-1-71-2	200.26 ± 0.51	0.7420 ± 0.0223
IP-V-1-71-2	250.14 ± 0.32	0.8170 ± 0.0280

Table 3.13: Analytically Determined Specific Heat in J/gK of Each TKP and THKP Formulation Using Mass Averaging.

Energetic Material	Percentage Ti	Percentage $TiH_{1.65}$	Percentage KP	Specific Heat
TKP-IP (Ventron)	33	0	67	0.7069 ± 0.0036
TKP-IP (ATK)	33	0	67	0.7069 ± 0.0036
TKP-OP	41	0	59	0.6854 ± 0.0032
THKP	0	33	67	0.7319 ± 0.0036

reference are presented in Table 3.16. The two methods are within 5% for all 1 mm pellets with most being within 2% . The error in the 3 mm pellets is much larger due teh large noise present in the signals. The MATLAB® and Proteus® packages have different methods for signal conditioning. Despite this difference, the results have overlapping errors and can be considered essentially the same values. As a result, the MATLAB® code is considered to be an appropriate analysis method for determining specific heat.

Table 3.14: Comparisons of the Thermal Diffusivity in mm^2/s Found with Each Analysis Program for Each TKP and THKP Formulation.

Pellet Label	Energetic Material	MATLAB® Thermal Diffusivity	Proteus® Thermal Diffusivity	Percentage Difference
IP-V-1-68-1	TKP-IP (Ventron)	0.3076 ± 0.0024	0.2988 ± 0.0013	-2.95
IP-V-1-68-2	TKP-IP (Ventron)	0.3011 ± 0.0020	0.2888 ± 0.0015	-4.26
IP-V-1-68-3	TKP-IP (Ventron)	0.3015 ± 0.0031	0.2934 ± 0.0008	-2.75
IP-V-1-71-1	TKP-IP (Ventron)	0.3041 ± 0.0019	0.2964 ± 0.0016	-2.60
IP-V-1-71-2	TKP-IP (Ventron)	0.2932 ± 0.0040	0.2854 ± 0.0014	-2.75
IP-V-1-71-3	TKP-IP (Ventron)	0.3019 ± 0.0027	0.2964 ± 0.0016	-1.86
IP-V-1-76-1	TKP-IP (Ventron)	0.3753 ± 0.0054	0.3658 ± 0.0012	-2.61
IP-V-1-76-2	TKP-IP (Ventron)	0.3729 ± 0.0047	0.3624 ± 0.0020	-2.90
IP-V-1-76-3	TKP-IP (Ventron)	0.3660 ± 0.0042	0.3652 ± 0.0030	-0.23
IP-V-1-79-1	TKP-IP (Ventron)	0.4312 ± 0.0031	0.4212 ± 0.0023	-2.38
IP-V-1-79-2	TKP-IP (Ventron)	0.4494 ± 0.0056	0.4378 ± 0.0024	-2.65
IP-V-1-79-3	TKP-IP (Ventron)	0.4485 ± 0.0047	0.4408 ± 0.0023	-1.74
IP-A-1-71-1	TKP-IP (ATK) 1mm	0.2457 ± 0.0019	0.2420 ± 0.0009	-1.54
IP-A-3-71-1	TKP-IP (ATK) 3mm	0.2239 ± 0.0042	0.2248 ± 0.0026	0.41
IP-A-3-71-2	TKP-IP (ATK) 3mm	0.2151 ± 0.0066	0.2076 ± 0.0047	-3.63
IP-A-3-71-3	TKP-IP (ATK) 3mm	0.2074 ± 0.0113	0.2036 ± 0.0089	-1.86
OP-1-80-1	TKP-OP	0.3050 ± 0.0021	0.2964 ± 0.0014	-2.90
OP-1-80-2	TKP-OP	0.3290 ± 0.0045	0.3228 ± 0.0015	-1.93
OP-1-80-3	TKP-OP	0.3369 ± 0.0040	0.3314 ± 0.0018	-1.65
THKP-1-80-1	THKP	0.2964 ± 0.0040	0.2926 ± 0.0019	-1.29
THKP-1-80-2	THKP	0.3048 ± 0.0037	0.3042 ± 0.0018	-0.20
THKP-1-80-3	THKP	0.3159 ± 0.0025	0.3062 ± 0.0012	-3.16

Table 3.15: Comparisons of the Specific Heat in J/gK Found with Each Analysis Program for Each TKP and THKP Formulation Using the Pocographite Reference.

Pellet Label	Energetic Material	MATLAB® Specific Heat	Proteus® Specific Heat	Percentage Difference
IP-V-1-68-1	TKP-IP (Ventron)	0.7297 ± 0.0243	0.7364 ± 0.0206	0.91
IP-V-1-68-2	TKP-IP (Ventron)	0.7813 ± 0.0205	0.7718 ± 0.0206	-1.23
IP-V-1-68-3	TKP-IP (Ventron)	0.7287 ± 0.0276	0.7362 ± 0.0177	1.02
IP-V-1-71-1	TKP-IP (Ventron)	0.8436 ± 0.0364	0.8540 ± 0.0354	1.22
IP-V-1-71-2	TKP-IP (Ventron)	0.7710 ± 0.0297	0.7804 ± 0.0371	1.21
IP-V-1-71-3	TKP-IP (Ventron)	0.8225 ± 0.0334	0.8454 ± 0.0346	2.71
IP-V-1-76-1	TKP-IP (Ventron)	0.7470 ± 0.0274	0.7586 ± 0.0130	1.53
IP-V-1-76-2	TKP-IP (Ventron)	0.7521 ± 0.0265	0.7610 ± 0.0190	1.16
IP-V-1-76-3	TKP-IP (Ventron)	0.7376 ± 0.0245	0.7520 ± 0.0285	1.91
IP-V-1-79-1	TKP-IP (Ventron)	0.7909 ± 0.0262	0.8066 ± 0.0375	1.94
IP-V-1-79-2	TKP-IP (Ventron)	0.7793 ± 0.0194	0.7922 ± 0.0379	1.63
IP-V-1-79-3	TKP-IP (Ventron)	0.7380 ± 0.0223	0.7602 ± 0.0127	2.91
IP-A-1-71-1	TKP-IP (ATK) 1mm	0.7388 ± 0.0302	0.7606 ± 0.0214	2.86
IP-A-3-71-1	TKP-IP (ATK) 3mm	0.8804 ± 0.0787	0.8500 ± 0.1087	-3.58
IP-A-3-71-2	TKP-IP (ATK) 3mm	0.9948 ± 0.0883	0.8774 ± 0.0884	-13.38
IP-A-3-71-3	TKP-IP (ATK) 3mm	0.9086 ± 0.1390	0.8256 ± 0.1194	-10.05
OP-1-80-1	TKP-OP	0.6530 ± 0.0177	0.6683 ± 0.0146	1.63
OP-1-80-2	TKP-OP	0.6445 ± 0.0235	0.6612 ± 0.0120	2.52
OP-1-80-3	TKP-OP	0.6498 ± 0.0268	0.6690 ± 0.0180	2.87
THKP-1-80-1	THKP	0.7120 ± 0.0240	0.7380 ± 0.0212	3.53
THKP-1-80-2	THKP	0.7274 ± 0.0322	0.7666 ± 0.0233	5.11
THKP-1-80-3	THKP	0.7675 ± 0.0289	0.7736 ± 0.0301	0.79

Table 3.16: Comparisons of the Specific Heat in J/gK Found with Each Analysis Program for Each TKP and THKP Formulation Using the Pyroceram® Reference.

Pellet Label	Energetic Material	MATLAB® Specific Heat	Proteus® Specific Heat	Percentage Difference
IP-V-1-68-1	TKP-IP (Ventron)	0.5967 ± 0.0211	0.5926 ± 0.0168	-0.69
IP-V-1-68-2	TKP-IP (Ventron)	0.6388 ± 0.0183	0.6210 ± 0.0164	-2.87
IP-V-1-68-3	TKP-IP (Ventron)	0.5958 ± 0.0229	0.5922 ± 0.0141	-0.61
IP-V-1-71-1	TKP-IP (Ventron)	0.6898 ± 0.0310	0.6874 ± 0.0282	-0.34
IP-V-1-71-2	TKP-IP (Ventron)	0.6304 ± 0.0259	0.6276 ± 0.0301	-0.45
IP-V-1-71-3	TKP-IP (Ventron)	0.6725 ± 0.0285	0.6780 ± 0.0274	-0.81
IP-V-1-76-1	TKP-IP (Ventron)	0.6108 ± 0.0239	0.6100 ± 0.0101	-0.13
IP-V-1-76-2	TKP-IP (Ventron)	0.6150 ± 0.0232	0.6126 ± 0.0150	-0.39
IP-V-1-76-3	TKP-IP (Ventron)	0.6031 ± 0.0216	0.6050 ± 0.0230	0.31
IP-V-1-79-1	TKP-IP (Ventron)	0.6467 ± 0.0232	0.6488 ± 0.0301	0.32
IP-V-1-79-2	TKP-IP (Ventron)	0.6372 ± 0.0174	0.6374 ± 0.0302	0.03
IP-V-1-79-3	TKP-IP (Ventron)	0.6035 ± 0.0191	0.6116 ± 0.0110	1.33
IP-A-1-71-1	TKP-IP (ATK) 1mm	0.6041 ± 0.0258	0.6120 ± 0.0168	1.29
IP-A-3-71-1	TKP-IP (ATK) 3mm	0.7496 ± 0.0676	0.7210 ± 0.0911	-3.97
IP-A-3-71-2	TKP-IP (ATK) 3mm	0.8470 ± 0.0758	0.7446 ± 0.0752	-13.75
IP-A-3-71-4	TKP-IP (ATK) 3mm	0.7736 ± 0.1185	0.7006 ± 0.1019	-10.42
OP-1-80-1	TKP-OP	0.5339 ± 0.0157	0.5326 ± 0.0138	-0.25
OP-1-80-2	TKP-OP	0.5270 ± 0.0203	0.5320 ± 0.0092	0.94
OP-1-80-3	TKP-OP	0.5313 ± 0.0227	0.5382 ± 0.0148	1.27
THKP-1-80-1	THKP	0.5821 ± 0.0210	0.5936 ± 0.0167	1.93
THKP-1-80-2	THKP	0.5948 ± 0.0274	0.6168 ± 0.0189	3.57
THKP-1-80-3	THKP	0.6275 ± 0.0253	0.6226 ± 0.0238	-0.79

Chapter 4

Measurements on 9013 Glass

4.1 Material Properties

A 1 mm and a 2 mm sample of 9013 glass sealed at 1000 °C and annealed at 465 °C were measured at temperatures ranging from 25 to 300 °C. The properties of each sample are presented in Table 4.1. The uncertainty in the sample weights are taken as the uncertainty of the scale used. The uncertainty of the height and diameter are obtained from 4 independent measurements at different locations on the sample. The density was calculated assuming a perfect cylindrical geometry. The density measured for each sample is well below the 2.64 g/cm^3 reported by the Corning company [5]. This discrepancy could be the result of differing heat treatments, casting imperfections, or deviations from a perfect cylindrical geometry. For all calculations below, the measured densities and associated errors are used.

Table 4.1: Parameters of the 9013 Glass Samples.

Sample Number	Diameter (mm)	Weight (g)	Height (mm)	Density (g/cm^3)
9013-1	12.683 ± 0.010	0.281 ± 0.0005	0.997 ± 0.004	2.231 ± 0.013
9013-2	12.690 ± 0.007	0.561 ± 0.0005	2.001 ± 0.021	2.217 ± 0.024

4.2 Experimental Arrangement

The thermal diffusivity of each sample was measured 5 times at 25, 50, 100, 150, 200, 250, and 300 °C. The samples were coated with graphite ($\sim$ 5 microns) to ensure uniform and thorough absorption of the Xenon flash energy. In all tests, the flash duration was significantly less than the half rise time ($\sim$ 300 ms for 1 mm sample and $\sim$ 1000 ms for 2 mm sample), so no correction for the pulse duration was needed [2]. The NanoFlash® machine parameters used for the 9013 glass samples are listed in Table 4.2.

Table 4.2: NanoFlash® Machine Parameters for Both 9013 Glass Samples.

Sample Number	Temperature (C)	Shots	Volts (V)	Filter (%)	Flash Duration (μs)	Preamp Gain	Main Gain	Recording Time (ms)
9013-1	25.33 ± 0.59	3	270	100 (5)	250	10	2520	3094
9013-1	49.90 ± 0.10	3	270	100 (5)	250	10	1260	3094
9013-1	100.00 ± 0.10	3	270	100 (5)	250	10	623	3400
9013-1	150.00 ± 0.10	3	270	100 (5)	250	10	315	3360
9013-1	200.40 ± 0.40	3	270	100 (5)	250	10	155	3360
9013-1	250.00 ± 0.21	3	270	100 (5)	250	10	78.8	3360
9013-1	300.10 ± 0.21	3	270	100 (5)	250	10	78.8	3360
9013-2	24.70 ± 0.44	3	270	100 (5)	450	10	2520	11680
9013-2	49.90 ± 0.10	3	270	100 (5)	450	10	1260	11680
9013-2	100.00 ± 0.10	3	270	100 (5)	450	10	315	13050
9013-2	150.00 ± 0.10	3	270	100 (5)	450	10	315	12072
9013-2	200.00 ± 0.10	3	270	100 (5)	450	10	155	12246
9013-2	250.07 ± 0.33	3	270	100 (5)	450	10	78.8	12246
9013-2	300.10 ± 0.30	3	270	100 (5)	450	10	78.8	12246

4.3 Experimental Results

4.3.1 Thermal Diffusivity

All shots on the 9013 glass samples were analyzed with the MATLAB® routine using the Cowan model [7, 8]. Using data from the Corning Company, the coefficient of linear thermal expansion, CTE, of 9013 glass is approximately $8.85 \times 10^{-6}\ C^{-1}$ [5]. Using the same procedure as in Section 3.3.1.2, thermal expansion is found to have a negligible effect (*i.e.* $< 0.5\%$) on the measured thermal diffusivity and specific heat. For this reason, the effects of thermal expansion are considered to be included in the conservative error estimations reported.

The thermal diffusivity and accompanying error for each shot on the 9013 glass samples are presented in Table 4.3. The average thermal diffusivity at each temperature is also reported. The average values at each temperature are presented graphically in Figure 4.1. For most temperatures, the thermal diffusivities for the 1 mm and 2 mm samples have overlapping errors and can be considered essentially the same value. The results show a downward trend in thermal diffusivity with temperature. This trend is fit to a quadratic equation using the data from both samples, and is shown in Figure 4.1.

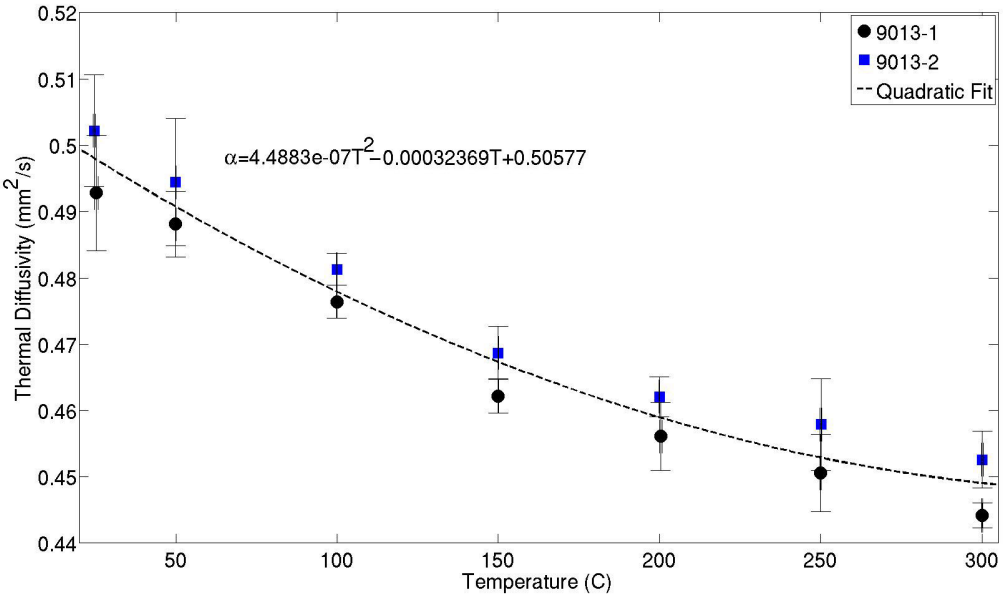

Figure 4.1: Thermal diffusivity as a function of temperature for both 9013 glass samples. The data shows a downward trend in thermal diffusivity with increasing temperature, which is fit to a quadratic equation.

4.3.2 Specific Heat

The specific heats measured with the MATLAB® for each shot on the 9013 glass samples along with the average at each temperature are presented in Table 4.4. The average specific heat at each temperature is presented graphically in Figure 4.2. To calculate the specific heat, each 9013 glass shot was compared to the average of 3 shots on the pocographite and Pyroceram® reference materials at identical machine parameters and temperatures. There is an observed variability in specific heat with reference material. Specific heats found with pocographite have a $\sim 15\%$ higher value when compared to those found with Pyroceram®. The specific heat of each 9013 glass sample is seen to increase with temperature for both reference materials. The increase in specific heat with temperature is fit to a quadratic equation, which is shown in Figure 4.2. The differing thermal and physical properties between the reference and sample make measuring the specific heat of a sample to a high degree of accuracy difficult. These considerations must be kept in mind when using this data.

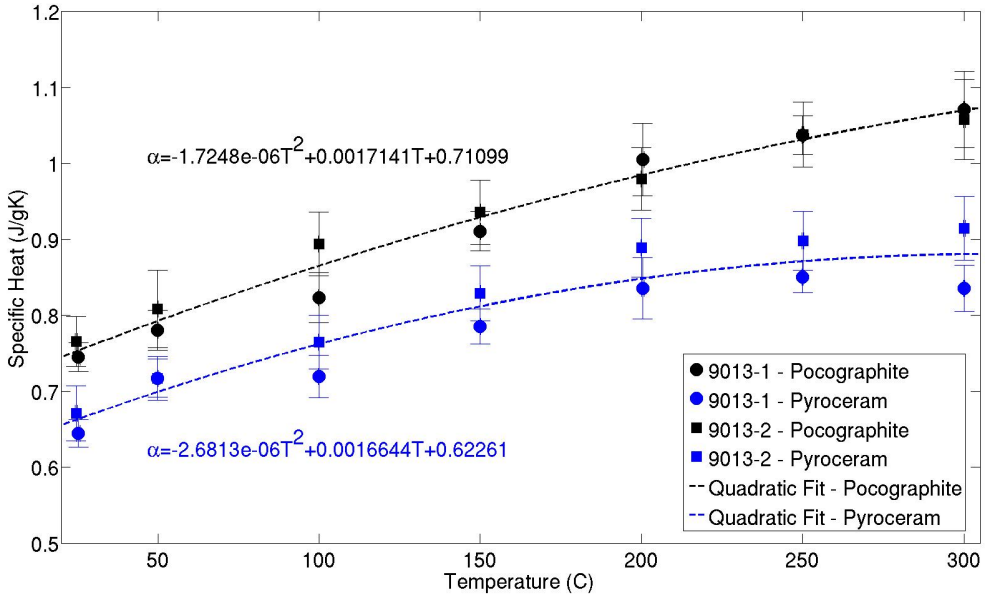

Figure 4.2: Specific heat as a function of temperature for both 9013 glass samples. The data shows an upward trend in specific heat as temperature increases. The results also show a dependence on the reference used for comparison. The specific heat found with pocographite (black) is $\sim 15\%$ higher than that found with Pyroceram® (blue).

Table 4.3: Measured Thermal Diffusivity in mm^2/s of the 9013 Glass Samples.

Sample Number	Temperature (C)	Shot #1	Shot #2	Shot #3	Average
9013-1	25.33 ± 0.59	0.4922 ± 0.0025	0.4866 ± 0.0023	0.4996 ± 0.0025	0.4928 ± 0.0087
9013-1	49.90 ± 0.10	0.4845 ± 0.0020	0.4907 ± 0.0023	0.4890 ± 0.0022	0.4881 ± 0.0049
9013-1	100.00 ± 0.10	0.4757 ± 0.0020	0.4768 ± 0.0020	0.4782 ± 0.0018	0.4764 ± 0.0025
9013-1	150.00 ± 0.10	0.4610 ± 0.0019	0.4622 ± 0.0020	0.4635 ± 0.0019	0.4622 ± 0.0026
9013-1	200.40 ± 0.40	0.4598 ± 0.0018	0.4560 ± 0.0019	0.4526 ± 0.0017	0.4561 ± 0.0051
9013-1	250.00 ± 0.21	0.4485 ± 0.0019	0.4554 ± 0.0020	0.4479 ± 0.0019	0.4506 ± 0.0058
9013-1	300.10 ± 0.21	0.4447 ± 0.0020	0.4446 ± 0.0020	0.4434 ± 0.0018	0.4442 ± 0.0019
9013-2	24.70 ± 0.44	0.5065 ± 0.0030	0.5047 ± 0.0030	0.4955 ± 0.0029	0.5022 ± 0.0084
9013-2	49.90 ± 0.10	0.4949 ± 0.0025	0.4870 ± 0.0025	0.5013 ± 0.0027	0.4944 ± 0.0096
9013-2	100.00 ± 0.10	0.4823 ± 0.0023	0.4806 ± 0.0024	0.4810 ± 0.0024	0.4813 ± 0.0024
9013-2	150.00 ± 0.10	0.4699 ± 0.0024	0.4702 ± 0.0027	0.4661 ± 0.0022	0.4687 ± 0.0040
9013-2	200.00 ± 0.10	0.4623 ± 0.0026	0.4634 ± 0.0024	0.4607 ± 0.0024	0.4621 ± 0.0030
9013-2	250.07 ± 0.33	0.4530 ± 0.0024	0.4580 ± 0.0022	0.4627 ± 0.0027	0.4579 ± 0.0069
9013-2	300.10 ± 0.30	0.4498 ± 0.0024	0.4534 ± 0.0024	0.4546 ± 0.0024	0.4526 ± 0.0043

Table 4.4: Measured Specific Heat in J/gK of the 9013 Glass Samples.

Sample Number	Standard Material	Temperature (C)	Shot #1	Shot #2	Shot #3	Average
9013-1	Pocographite	25.33 ± 0.59	0.7472 ± 0.0250	0.7439 ± 0.0224	0.7521 ± 0.0247	0.7477 ± 0.0189
9013-1	Pocographite	49.90 ± 0.10	0.7931 ± 0.0236	0.7753 ± 0.0233	0.7725 ± 0.0230	0.7803 ± 0.0261
9013-1	Pocographite	100.00 ± 0.10	0.8138 ± 0.0222	0.8433 ± 0.0231	0.8125 ± 0.0220	0.8232 ± 0.0327
9013-1	Pocographite	150.00 ± 0.10	0.9158 ± 0.0265	0.9172 ± 0.0266	0.8999 ± 0.0259	0.9109 ± 0.0261
9013-1	Pocographite	200.40 ± 0.40	1.0298 ± 0.0286	0.9981 ± 0.0278	0.9736 ± 0.0270	1.0005 ± 0.0479
9013-1	Pocographite	250.00 ± 0.21	1.0293 ± 0.0298	1.0407 ± 0.0302	1.0422 ± 0.0301	1.0374 ± 0.0253
9013-1	Pocographite	300.10 ± 0.21	1.0426 ± 0.0311	1.0989 ± 0.0318	1.0723 ± 0.0316	1.0713 ± 0.0501
9013-1	Pyroceram®	25.33 ± 0.59	0.6443 ± 0.0250	0.6414 ± 0.0246	0.6485 ± 0.0248	0.6447 ± 0.0183
9013-1	Pyroceram®	49.90 ± 0.10	0.7291 ± 0.0241	0.7128 ± 0.0238	0.7102 ± 0.0236	0.7174 ± 0.0254
9013-1	Pyroceram®	100.00 ± 0.10	0.7111 ± 0.0118	0.7369 ± 0.0223	0.7100 ± 0.0213	0.7193 ± 0.0282
9013-1	Pyroceram®	150.00 ± 0.10	0.7896 ± 0.0233	0.7908 ± 0.0233	0.7759 ± 0.0227	0.7854 ± 0.0227
9013-1	Pyroceram®	200.40 ± 0.40	0.8601 ± 0.0248	0.8337 ± 0.0240	0.8132 ± 0.0234	0.8357 ± 0.0405
9013-1	Pyroceram®	250.00 ± 0.21	0.8442 ± 0.0249	0.8536 ± 0.0252	0.8548 ± 0.0251	0.8508 ± 0.0210
9013-1	Pyroceram®	300.10 ± 0.21	0.8196 ± 0.0247	0.8448 ± 0.0252	0.8429 ± 0.0251	0.8357 ± 0.0303
9013-2	Pocographite	24.70 ± 0.44	0.7736 ± 0.0393	0.7552 ± 0.0383	0.7676 ± 0.0393	0.7655 ± 0.0331
9013-2	Pocographite	49.90 ± 0.10	0.8196 ± 0.0404	0.7802 ± 0.0391	0.8257 ± 0.0408	0.8085 ± 0.0511
9013-2	Pocographite	100.00 ± 0.10	0.9052 ± 0.0567	0.8911 ± 0.0561	0.8848 ± 0.0430	0.8937 ± 0.0420
9013-2	Pocographite	150.00 ± 0.10	0.9507 ± 0.0465	0.9337 ± 0.0464	0.9229 ± 0.0448	0.9358 ± 0.0424
9013-2	Pocographite	200.00 ± 0.10	0.9936 ± 0.0491	0.9738 ± 0.0474	0.9723 ± 0.0475	0.9799 ± 0.0412
9013-2	Pocographite	250.07 ± 0.33	1.0463 ± 0.0519	1.0251 ± 0.0501	1.0439 ± 0.0519	1.0384 ± 0.0427
9013-2	Pocographite	300.10 ± 0.30	1.0763 ± 0.0536	1.0370 ± 0.0516	1.0603 ± 0.0536	1.0579 ± 0.0529
9013-2	Pyroceram®	24.70 ± 0.44	0.6779 ± 0.0361	0.6618 ± 0.0341	0.6726 ± 0.0361	0.6708 ± 0.0298
9013-2	Pyroceram®	49.90 ± 0.10	0.7268 ± 0.0365	0.6918 ± 0.0353	0.7322 ± 0.0368	0.7169 ± 0.0457
9013-2	Pyroceram®	100.00 ± 0.10	0.7742 ± 0.0383	0.7621 ± 0.0381	0.7568 ± 0.0375	0.7644 ± 0.0320
9013-2	Pyroceram®	150.00 ± 0.10	0.8421 ± 0.0411	0.8271 ± 0.0410	0.8175 ± 0.0396	0.8289 ± 0.0375
9013-2	Pyroceram®	200.00 ± 0.10	0.9015 ± 0.0451	0.8836 ± 0.0435	0.8822 ± 0.0436	0.8891 ± 0.0377
9013-2	Pyroceram®	250.07 ± 0.33	0.9050 ± 0.0450	0.8866 ± 0.0435	0.9029 ± 0.0450	0.8982 ± 0.0371
9013-2	Pyroceram®	300.10 ± 0.30	0.9303 ± 0.0466	0.8963 ± 0.0448	0.9165 ± 0.0466	0.9144 ± 0.0459

Chapter 5

Measurements on 7052 Glass

5.1 Material Properties

Two 1 mm and two 3 mm samples of 7052 glass were measured at temperatures ranging from 25 to 300 °C. The properties of each sample are presented in Table 5.1. The uncertainty in the sample weights are taken as the uncertainty of the scale used. The uncertainty of the height and diameter are obtained from 4 independent measurements at different locations on the sample. The density was calculated assuming a perfect cylindrical geometry. The density measured for each sample is well below the 2.27 g/cm^3 reported by the Corning company [6]. This discrepancy could be the result of differing heat treatments, casting imperfections, or deviations from a perfect cylindrical geometry. For all calculations below, the measured densities and associated errors are used.

Table 5.1: Parameters of the 7052 Glass Samples.

Sample Number	Diameter (mm)	Weight (g)	Height (mm)	Density (g/cm^3)
7052-1-1	12.560 ± 0.086	0.254 ± 0.0005	1.008 ± 0.007	2.035 ± 0.032
7052-1-2	12.475 ± 0.065	0.255 ± 0.0005	0.997 ± 0.014	2.094 ± 0.038
7052-3-1	12.706 ± 0.055	0.766 ± 0.0005	3.005 ± 0.003	2.011 ± 0.018
7052-3-2	12.695 ± 0.096	0.764 ± 0.0005	2.983 ± 0.015	2.023 ± 0.032

5.2 Experimental Arrangement

The thermal diffusivity of each sample was measured 5 times at 25, 50, 100, 150, 200, 250, and 300 °C. The samples were coated with graphite ($\sim$ 5 microns) to ensure uniform and thorough absorption of the Xenon flash energy. A higher flash voltage was used for the 3 mm samples to reduce signal noise. In all tests, the flash duration was significantly less than the half rise time ($\sim$ 200 ms for 1 mm samples and $\sim$ 2000 ms for 3 mm samples), so

no correction for the pulse duration was needed [2]. The NanoFlash® machine parameters are listed in Table 5.2.

Table 5.2: NanoFlash® Machine Parameters for the 7052 Glass Samples.

Sample Number	Temperature (C)	Shots	Volts (V)	Filter (%)	Flash Duration (μs)	Preamp Gain	Main Gain	Recording Time (ms)
7052-1-1	25.02 ± 0.19	5	270	100 (5)	250	10	2520	2740
7052-1-1	50.00 ± 0.10	5	270	100 (5)	250	10	1260	2740
7052-1-1	100.00 ± 0.10	5	270	100 (5)	250	10	623	2740
7052-1-1	150.00 ± 0.10	5	270	100 (5)	250	10	315	2740
7052-1-1	200.00 ± 0.10	5	270	100 (5)	250	10	155	3028
7052-1-1	250.00 ± 0.10	5	270	100 (5)	250	10	78.8	3028
7052-1-1	300.00 ± 0.10	5	270	100 (5)	250	10	78.8	3028
7052-1-2	24.98 ± 0.19	5	270	100 (5)	250	10	2520	2750
7052-1-2	50.00 ± 0.10	5	270	100 (5)	250	10	1260	2750
7052-1-2	100.00 ± 0.10	5	270	100 (5)	250	10	623	2750
7052-1-2	150.00 ± 0.10	5	270	100 (5)	250	10	315	2750
7052-1-2	200.00 ± 0.10	5	270	100 (5)	250	10	155	2750
7052-1-2	249.96 ± 0.21	5	270	100 (5)	250	10	78.8	3094
7052-1-2	300.00 ± 0.10	5	270	100 (5)	250	10	78.8	3094
7052-3-1	25.14 ± 0.40	5	292	100 (5)	450	10	5002	23464
7052-3-1	49.98 ± 0.19	5	292	100 (5)	450	10	2520	23464
7052-3-1	100.00 ± 0.10	5	292	100 (5)	450	10	1260	23414
7052-3-1	150.00 ± 0.10	5	292	100 (5)	450	10	623	23414
7052-3-1	200.00 ± 0.10	5	292	100 (5)	450	10	315	23414
7052-3-1	250.02 ± 0.19	5	292	100 (5)	450	10	155	23414
7052-3-1	300.06 ± 0.28	5	292	100 (5)	450	10	155	23414
7052-3-2	24.94 ± 0.21	5	292	100 (5)	450	10	5002	23464
7052-3-2	49.98 ± 0.19	5	292	100 (5)	450	10	2520	23464
7052-3-2	100.00 ± 0.10	5	292	100 (5)	450	10	1260	21586
7052-3-2	150.00 ± 0.10	5	292	100 (5)	450	10	623	21586
7052-3-2	200.00 ± 0.10	5	292	100 (5)	450	10	315	23852
7052-3-2	249.96 ± 0.20	5	292	100 (5)	450	10	155	23852
7052-3-2	300.00 ± 0.10	5	292	100 (5)	450	10	155	23852

5.3 Experimental Results

5.3.1 Thermal Diffusivity

All shots on the 7052 glass samples were analyzed with the MATLAB® routine using the Cowan model [7, 8]. Using data from the Corning Company, the coefficient of linear thermal expansion, CTE, of 7052 glass is approximately $4.6 \times 10^{-6}\ C^{-1}$ [6]. Using the same

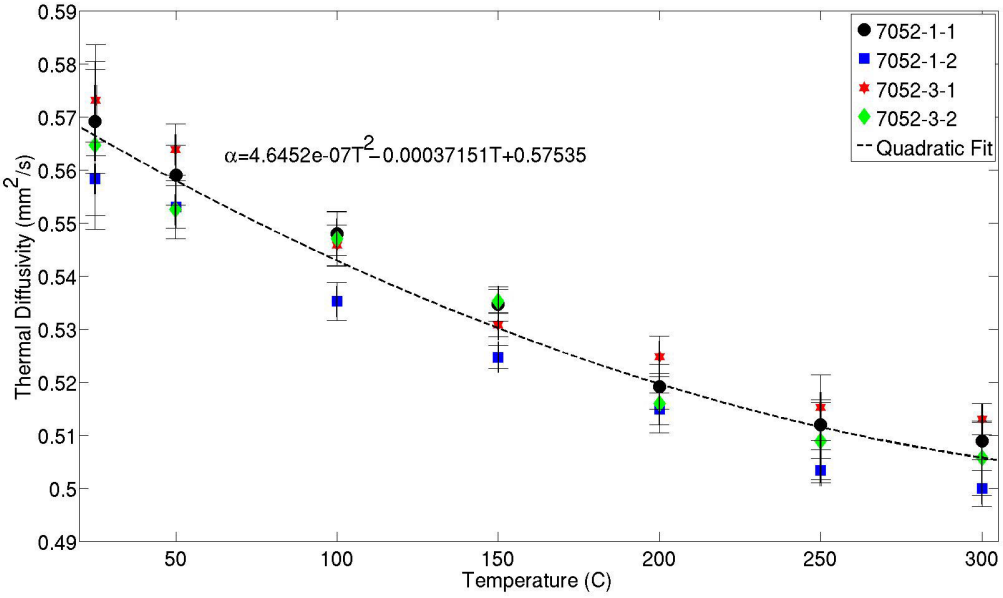

Figure 5.1: Thermal diffusivity as a function of temperature for all four 7052 glass samples. The data shows a downward trend in thermal diffusivity with increasing temperature, which is fit to a quadratic equation.

procedure as in Section 3.3.1.2, thermal expansion has a negligible effect (*i.e.* $< 0.5\%$) on the measured thermal diffusivity and specific heat. For this reason, the effects of thermal expansion are considered to be included in the conservative error estimations reported.

The thermal diffusivity and accompanying error for each shot on the 7052 glass samples are presented in Table 5.3. The average thermal diffusivity at each temperature is also reported. The average values at each temperature are presented graphically in Figure 5.1. The results show a downward trend in thermal diffusivity with temperature. This trend is fit to a quadratic equation using the data from all four samples, and is shown in Figure 5.1.

5.3.2 Specific Heat

The specific heats measured with the MATLAB® for each shot on the 7052 glass samples along with the average at each temperature are presented in Tables 5.4 and 5.5. The average specific heat at each temperature is presented graphically in Figure 5.2. To calculate the specific heat, each 7052 glass shot was compared to the average of 3 shots for the 1 mm samples and 5 shots for the 3 mm samples on the reference materials at identical machine parameters and temperatures. There is an observed variability in specific heat with reference material and sample thickness. Specific heats found with pocographite have a $\sim 15\%$ higher value when compared to those found with Pyroceram®. Also, the 3 mm samples tend to give

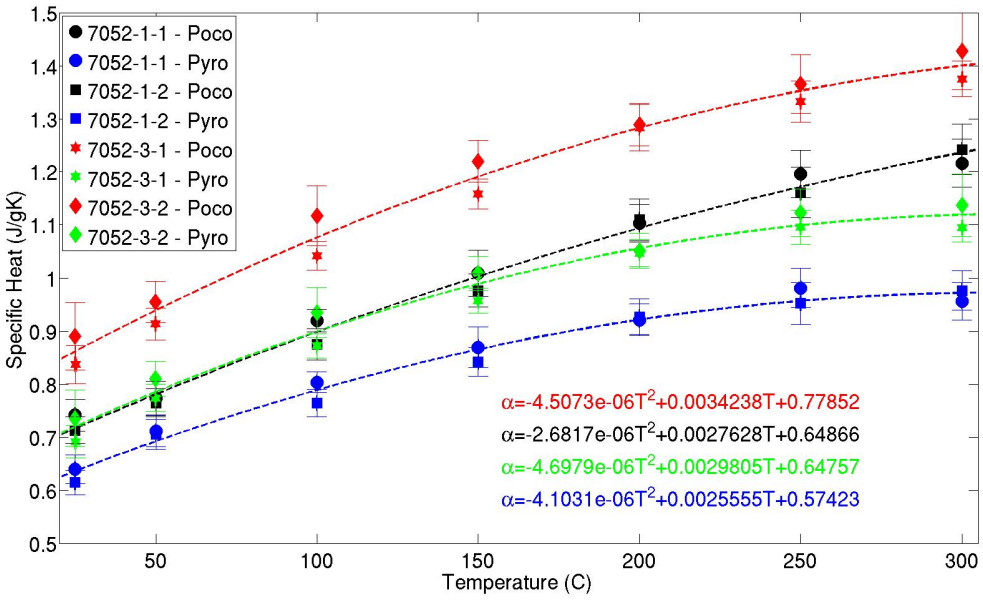

Figure 5.2: Specific heat as a function of temperature for all four 7052 glass samples. The data shows an upward trend in specific heat as temperature increases for all samples. The specific heat found with pocographite is $\sim$ 15% higher than that found using Pyroceram® for samples at similar thicknesses. In addition, the 3 mm samples are seen to have a $\sim$ 10% higher specific heat than the 1 mm samples using the same reference.

a $\sim$ 10% higher specific heat than the 1 mm samples. The specific heat of each 7052 glass sample is seen to increase with temperature. This increase in specific heat with temperature for samples of similar thickness and identical references are fit to quadratic equations, which are shown in Figure 5.2. The differing thermal and physical properties between the reference and sample make measuring the specific heat of a sample to a high degree of accuracy difficult. These considerations must be kept in mind when using this data.

Table 5.3: Measured Thermal Diffusivity in mm^2/s of the 7052 Glass Samples.

Sample Number	Temperature (C)	Shot #1	Shot #2	Shot #3	Shot #4	Shot #5	Average
7052-1-1	25.02 ± 0.19	0.5804 ± 0.0021	0.5707 ± 0.0031	0.5680 ± 0.0029	0.5727 ± 0.0030	0.5538 ± 0.0029	0.5691 ± 0.0098
7052-1-1	50.00 ± 0.10	0.5641 ± 0.0028	0.5521 ± 0.0029	0.5616 ± 0.0028	0.5618 ± 0.0030	0.5556 ± 0.0026	0.5590 ± 0.0056
7052-1-1	100.00 ± 0.10	0.5446 ± 0.0026	0.5483 ± 0.0027	0.5511 ± 0.0027	0.5444 ± 0.0026	0.5513 ± 0.0028	0.5479 ± 0.0041
7052-1-1	150.00 ± 0.10	0.5374 ± 0.0019	0.5324 ± 0.0028	0.5328 ± 0.0026	0.5372 ± 0.0023	0.5339 ± 0.0027	0.5347 ± 0.0032
7052-1-1	200.00 ± 0.10	0.5160 ± 0.0024	0.5206 ± 0.0024	0.5239 ± 0.0025	0.5151 ± 0.0024	0.5198 ± 0.0024	0.5191 ± 0.0042
7052-1-1	250.00 ± 0.10	0.5081 ± 0.0024	0.5077 ± 0.0023	0.5146 ± 0.0026	0.5120 ± 0.0025	0.5171 ± 0.0024	0.5119 ± 0.0047
7052-1-1	300.00 ± 0.10	0.5089 ± 0.0024	0.5058 ± 0.0023	0.5119 ± 0.0023	0.5045 ± 0.0023	0.5107 ± 0.0026	0.5089 ± 0.0035
7052-1-2	24.98 ± 0.19	0.5502 ± 0.0034	0.5651 ± 0.0036	0.5558 ± 0.0034	0.5639 ± 0.0035	0.5567 ± 0.0035	0.5583 ± 0.0069
7052-1-2	50.00 ± 0.10	0.5558 ± 0.0034	0.5535 ± 0.0034	0.5549 ± 0.0035	0.5522 ± 0.0033	0.5485 ± 0.0035	0.5530 ± 0.0040
7052-1-2	100.00 ± 0.10	0.5347 ± 0.0033	0.5325 ± 0.0031	0.5334 ± 0.0032	0.5366 ± 0.0032	0.5386 ± 0.0032	0.5352 ± 0.0036
7052-1-2	150.00 ± 0.10	0.5259 ± 0.0023	0.5233 ± 0.0032	0.5255 ± 0.0031	0.5244 ± 0.0033	0.5245 ± 0.0032	0.5247 ± 0.0022
7052-1-2	200.00 ± 0.10	0.5140 ± 0.0028	0.5158 ± 0.0036	0.5169 ± 0.0032	0.5158 ± 0.0023	0.5120 ± 0.0031	0.5149 ± 0.0030
7052-1-2	249.96 ± 0.21	0.5025 ± 0.0029	0.5023 ± 0.0031	0.5046 ± 0.0031	0.5042 ± 0.0030	0.5028 ± 0.0028	0.5033 ± 0.0023
7052-1-2	300.00 ± 0.10	0.5016 ± 0.0030	0.4985 ± 0.0030	0.4969 ± 0.0029	0.5030 ± 0.0029	0.4995 ± 0.0028	0.4999 ± 0.0034
7052-3-1	25.14 ± 0.40	0.5558 ± 0.0024	0.5812 ± 0.0027	0.5720 ± 0.0028	0.5747 ± 0.0030	0.5820 ± 0.0028	0.5731 ± 0.0105
7052-3-1	49.98 ± 0.19	0.5624 ± 0.0022	0.5705 ± 0.0026	0.5629 ± 0.0025	0.5642 ± 0.0023	0.5589 ± 0.0023	0.5638 ± 0.0048
7052-3-1	100.00 ± 0.10	0.5403 ± 0.0023	0.5482 ± 0.0025	0.5466 ± 0.0021	0.5473 ± 0.0020	0.5468 ± 0.0025	0.5458 ± 0.0038
7052-3-1	150.00 ± 0.10	0.5311 ± 0.0021	0.5328 ± 0.0020	0.5285 ± 0.0023	0.5308 ± 0.0023	0.5310 ± 0.0019	0.5308 ± 0.0023
7052-3-1	200.00 ± 0.10	0.5234 ± 0.0024	0.5293 ± 0.0021	0.5268 ± 0.0024	0.5216 ± 0.0021	0.5231 ± 0.0023	0.5248 ± 0.0038
7052-3-1	250.02 ± 0.19	0.5176 ± 0.0023	0.5134 ± 0.0025	0.5146 ± 0.0025	0.5232 ± 0.0021	0.5070 ± 0.0024	0.5152 ± 0.0062
7052-3-1	300.06 ± 0.28	0.5133 ± 0.0023	0.5123 ± 0.0022	0.5112 ± 0.0023	0.5118 ± 0.0021	0.5167 ± 0.0023	0.5130 ± 0.0029
7052-3-2	24.94 ± 0.21	0.5683 ± 0.0032	0.5525 ± 0.0035	0.5645 ± 0.0035	0.5896 ± 0.0040	0.5480 ± 0.0032	0.5646 ± 0.0158
7052-3-2	49.98 ± 0.19	0.5538 ± 0.0030	0.5555 ± 0.0029	0.5487 ± 0.0028	0.5582 ± 0.0026	0.5466 ± 0.0026	0.5525 ± 0.0055
7052-3-2	100.00 ± 0.10	0.5407 ± 0.0027	0.5499 ± 0.0028	0.5449 ± 0.0031	0.5523 ± 0.0030	0.5472 ± 0.0026	0.5470 ± 0.0052
7052-3-2	150.00 ± 0.10	0.5340 ± 0.0030	0.5370 ± 0.0031	0.5353 ± 0.0024	0.5342 ± 0.0026	0.5357 ± 0.0026	0.5352 ± 0.0023
7052-3-2	200.00 ± 0.10	0.5165 ± 0.0025	0.5122 ± 0.0024	0.5128 ± 0.0026	0.5139 ± 0.0025	0.5246 ± 0.0028	0.5160 ± 0.0056
7052-3-2	249.96 ± 0.20	0.5183 ± 0.0028	0.5037 ± 0.0022	0.5116 ± 0.0023	0.5108 ± 0.0026	0.5002 ± 0.0026	0.5089 ± 0.0073
7052-3-2	300.00 ± 0.10	0.4993 ± 0.0026	0.5102 ± 0.0023	0.5078 ± 0.0024	0.4981 ± 0.0023	0.5133 ± 0.0028	0.5057 ± 0.0070

Table 5.4: Measured Specific Heat in J/gK of the 7052 Glass Samples 7052-1-1 and 7052-1-2.

Sample Number	Standard Material	Temperature (C)	Shot #1	Shot #2	Shot #3	Shot #4	Shot #5	Average
7052-1-1	Pocographite	25.02 ± 0.19	0.7457 ± 0.0298	0.7446 ± 0.0298	0.7489 ± 0.0297	0.7599 ± 0.0302	0.7094 ± 0.0287	0.7417 ± 0.0300
7052-1-1	Pocographite	50.00 ± 0.10	0.7855 ± 0.0305	0.7571 ± 0.0298	0.8019 ± 0.0312	0.7711 ± 0.0302	0.7518 ± 0.0293	0.7735 ± 0.0316
7052-1-1	Pocographite	100.00 ± 0.10	0.9267 ± 0.0344	0.9200 ± 0.0343	0.9192 ± 0.0342	0.9224 ± 0.0342	0.9077 ± 0.0339	0.9192 ± 0.0215
7052-1-1	Pocographite	150.00 ± 0.10	1.0367 ± 0.0382	1.0081 ± 0.0389	0.9809 ± 0.0375	1.0402 ± 0.0391	0.9756 ± 0.0374	1.0083 ± 0.0435
7052-1-1	Pocographite	200.00 ± 0.10	1.0877 ± 0.0408	1.1235 ± 0.0420	1.0981 ± 0.0410	1.0817 ± 0.0407	1.1215 ± 0.0420	1.1025 ± 0.0353
7052-1-1	Pocographite	250.00 ± 0.10	1.2066 ± 0.0460	1.2180 ± 0.0465	1.2189 ± 0.0465	1.1821 ± 0.0451	1.1541 ± 0.0436	1.1959 ± 0.0447
7052-1-1	Pocographite	300.00 ± 0.10	1.2078 ± 0.0467	1.1750 ± 0.0453	1.2392 ± 0.0473	1.2425 ± 0.0481	1.2171 ± 0.0474	1.2163 ± 0.0450
7052-1-1	Pyroceram®	25.02 ± 0.19	0.6430 ± 0.0293	0.6420 ± 0.0293	0.6457 ± 0.0293	0.6552 ± 0.0298	0.6116 ± 0.0282	0.6395 ± 0.0274
7052-1-1	Pyroceram®	50.00 ± 0.10	0.7221 ± 0.0299	0.6960 ± 0.0292	0.7372 ± 0.0306	0.7089 ± 0.0296	0.6911 ± 0.0287	0.7111 ± 0.0299
7052-1-1	Pyroceram®	100.00 ± 0.10	0.8098 ± 0.0318	0.8039 ± 0.0316	0.8032 ± 0.0316	0.8060 ± 0.0316	0.7932 ± 0.0313	0.8032 ± 0.0195
7052-1-1	Pyroceram®	150.00 ± 0.10	0.8939 ± 0.0333	0.8692 ± 0.0339	0.8458 ± 0.0326	0.8969 ± 0.0341	0.8412 ± 0.0326	0.8694 ± 0.0377
7052-1-1	Pyroceram®	200.00 ± 0.10	0.9085 ± 0.0348	0.9384 ± 0.0358	0.9172 ± 0.0350	0.9035 ± 0.0347	0.9367 ± 0.0358	0.9209 ± 0.0298
7052-1-1	Pyroceram®	250.00 ± 0.10	0.9896 ± 0.0381	0.9989 ± 0.0385	0.9997 ± 0.0385	0.9695 ± 0.0374	0.9466 ± 0.0361	0.9809 ± 0.0368
7052-1-1	Pyroceram®	300.00 ± 0.10	0.9494 ± 0.0369	0.9236 ± 0.0358	0.9740 ± 0.0374	0.9767 ± 0.0380	0.9567 ± 0.0375	0.9561 ± 0.0354
7052-1-2	Pocographite	24.98 ± 0.19	0.7135 ± 0.0419	0.7132 ± 0.0410	0.7054 ± 0.0412	0.7252 ± 0.0418	0.7060 ± 0.0411	0.7126 ± 0.0255
7052-1-2	Pocographite	50.00 ± 0.10	0.7706 ± 0.0441	0.7574 ± 0.0431	0.7617 ± 0.0437	0.7748 ± 0.0445	0.7590 ± 0.0438	0.7647 ± 0.0263
7052-1-2	Pocographite	100.00 ± 0.10	0.8711 ± 0.0490	0.8713 ± 0.0490	0.8690 ± 0.0490	0.8708 ± 0.0488	0.8897 ± 0.0498	0.8744 ± 0.0295
7052-1-2	Pocographite	150.00 ± 0.10	0.9701 ± 0.0531	0.9743 ± 0.0556	0.9786 ± 0.0551	0.9698 ± 0.0554	0.9882 ± 0.0566	0.9762 ± 0.0313
7052-1-2	Pocographite	200.00 ± 0.10	1.1076 ± 0.0615	1.0963 ± 0.0629	1.1305 ± 0.0638	1.0988 ± 0.0600	1.1143 ± 0.0629	1.1095 ± 0.0399
7052-1-2	Pocographite	249.96 ± 0.21	1.1322 ± 0.0647	1.1537 ± 0.0659	1.1789 ± 0.0674	1.1561 ± 0.0660	1.1830 ± 0.0668	1.1608 ± 0.0477
7052-1-2	Pocographite	300.00 ± 0.10	1.2708 ± 0.0727	1.2328 ± 0.0714	1.2309 ± 0.0708	1.2477 ± 0.0712	1.2281 ± 0.0701	1.2421 ± 0.0474
7052-1-2	Pyroceram®	24.98 ± 0.19	0.6152 ± 0.0386	0.6149 ± 0.0378	0.6082 ± 0.0379	0.6253 ± 0.0386	0.6087 ± 0.0378	0.6145 ± 0.0231
7052-1-2	Pyroceram®	50.00 ± 0.10	0.7084 ± 0.0419	0.6964 ± 0.0409	0.7003 ± 0.0415	0.7224 ± 0.0423	0.6977 ± 0.0415	0.7050 ± 0.0281
7052-1-2	Pyroceram®	100.00 ± 0.10	0.7612 ± 0.0439	0.7614 ± 0.0439	0.7593 ± 0.0439	0.7610 ± 0.0437	0.7775 ± 0.0446	0.7641 ± 0.0263
7052-1-2	Pyroceram®	150.00 ± 0.10	0.8365 ± 0.0460	0.8401 ± 0.0481	0.8438 ± 0.0478	0.8362 ± 0.0480	0.8521 ± 0.0487	0.8417 ± 0.0271
7052-1-2	Pyroceram®	200.00 ± 0.10	0.9251 ± 0.0519	0.9157 ± 0.0530	0.9443 ± 0.0538	0.9177 ± 0.0506	0.9307 ± 0.0530	0.9267 ± 0.0336
7052-1-2	Pyroceram®	249.96 ± 0.21	0.9286 ± 0.0533	0.9463 ± 0.0543	0.9669 ± 0.0555	0.9482 ± 0.0544	0.9703 ± 0.0550	0.9521 ± 0.0393
7052-1-2	Pyroceram®	300.00 ± 0.10	0.9989 ± 0.0573	0.9691 ± 0.0563	0.9675 ± 0.0558	0.9807 ± 0.0561	0.9653 ± 0.0552	0.9763 ± 0.0373

Table 5.5: Measured Specific Heat in J/gK of the 7052 Glass Samples 7052-3-1 and 7052-3-2.

Sample Number	Standard Material	Temperature (C)	Shot #1	Shot #2	Shot #3	Shot #4	Shot #5	Average
7052-3-1	Pocographite	25.14 ± 0.40	0.7991 ± 0.0290	0.8656 ± 0.0312	0.8338 ± 0.0307	0.8320 ± 0.0301	0.8535 ± 0.0310	0.8368 ± 0.0358
7052-3-1	Pocographite	49.98 ± 0.19	0.9110 ± 0.0291	0.9148 ± 0.0293	0.9322 ± 0.0302	0.9257 ± 0.0301	0.8829 ± 0.0282	0.9133 ± 0.0298
7052-3-1	Pocographite	100.00 ± 0.10	1.0433 ± 0.0321	1.0164 ± 0.0314	1.0462 ± 0.0314	1.0492 ± 0.0314	1.0532 ± 0.0326	1.0417 ± 0.0270
7052-3-1	Pocographite	150.00 ± 0.10	1.1650 ± 0.0352	1.1653 ± 0.0350	1.1569 ± 0.0350	1.1703 ± 0.0356	1.1331 ± 0.0343	1.1581 ± 0.0286
7052-3-1	Pocographite	200.00 ± 0.10	1.2933 ± 0.0400	1.2805 ± 0.0390	1.2731 ± 0.0394	1.2439 ± 0.0383	1.3248 ± 0.0408	1.2831 ± 0.0435
7052-3-1	Pocographite	250.02 ± 0.52	1.3553 ± 0.0428	1.3144 ± 0.0416	1.3495 ± 0.0428	1.3391 ± 0.0418	1.3019 ± 0.0415	1.3320 ± 0.0390
7052-3-1	Pocographite	300.06 ± 0.51	1.3770 ± 0.0441	1.3672 ± 0.0435	1.3566 ± 0.0434	1.3990 ± 0.0449	1.3757 ± 0.0439	1.3751 ± 0.0334
7052-3-1	Pyroceram®	25.14 ± 0.40	0.6602 ± 0.0259	0.7152 ± 0.0279	0.6889 ± 0.0274	0.6874 ± 0.0270	0.7052 ± 0.0277	0.6914 ± 0.0305
7052-3-1	Pyroceram®	49.98 ± 0.19	0.7722 ± 0.0257	0.7754 ± 0.0259	0.7901 ± 0.0267	0.7846 ± 0.0266	0.7484 ± 0.0250	0.7741 ± 0.0257
7052-3-1	Pyroceram®	100.00 ± 0.10	0.8733 ± 0.0271	0.8508 ± 0.0265	0.8757 ± 0.0265	0.8783 ± 0.0265	0.8816 ± 0.0275	0.8719 ± 0.0227
7052-3-1	Pyroceram®	150.00 ± 0.10	0.9629 ± 0.0289	0.9631 ± 0.0288	0.9562 ± 0.0288	0.9672 ± 0.0293	0.9365 ± 0.0282	0.9572 ± 0.0236
7052-3-1	Pyroceram®	200.00 ± 0.10	1.0553 ± 0.0328	1.0448 ± 0.0320	1.0388 ± 0.0323	1.0150 ± 0.0314	1.0810 ± 0.0335	1.0470 ± 0.0356
7052-3-1	Pyroceram®	250.02 ± 0.52	1.1146 ± 0.0354	1.0810 ± 0.0343	1.1099 ± 0.0353	1.1014 ± 0.0345	1.0707 ± 0.0342	1.0955 ± 0.0321
7052-3-1	Pyroceram®	300.06 ± 0.51	1.0960 ± 0.0351	1.0881 ± 0.0346	1.0798 ± 0.0345	1.1135 ± 0.0357	1.0949 ± 0.0349	1.0945 ± 0.0266
7052-3-2	Pocographite	24.94 ± 0.21	0.8802 ± 0.0411	0.8738 ± 0.0420	0.8833 ± 0.0423	0.9748 ± 0.0461	0.8362 ± 0.0389	0.8897 ± 0.0637
7052-3-2	Pocographite	49.98 ± 0.19	0.9453 ± 0.0404	0.9517 ± 0.0405	0.9330 ± 0.0399	0.9946 ± 0.0418	0.9505 ± 0.0402	0.9550 ± 0.0386
7052-3-2	Pocographite	100.00 ± 0.10	1.0528 ± 0.0435	1.1307 ± 0.0466	1.1206 ± 0.0469	1.1662 ± 0.0484	1.1137 ± 0.0457	1.1168 ± 0.0567
7052-3-2	Pocographite	150.00 ± 0.10	1.2232 ± 0.0510	1.2317 ± 0.0513	1.2243 ± 0.0497	1.1862 ± 0.0482	1.2348 ± 0.0498	1.2200 ± 0.0395
7052-3-2	Pocographite	200.00 ± 0.10	1.2725 ± 0.0525	1.2817 ± 0.0528	1.2876 ± 0.0533	1.2805 ± 0.0528	1.3216 ± 0.0542	1.2888 ± 0.0405
7052-3-2	Pocographite	249.96 ± 0.20	1.3895 ± 0.0574	1.3185 ± 0.0534	1.3920 ± 0.0568	1.3869 ± 0.0574	1.3398 ± 0.0559	1.3653 ± 0.0549
7052-3-2	Pocographite	300.00 ± 0.10	1.3700 ± 0.0583	1.4430 ± 0.0601	1.4550 ± 0.0603	1.3771 ± 0.0581	1.4960 ± 0.0624	1.4282 ± 0.0738
7052-3-2	Pyroceram®	24.94 ± 0.21	0.7272 ± 0.0357	0.7219 ± 0.0364	0.7298 ± 0.0366	0.8055 ± 0.0400	0.6909 ± 0.0338	0.7351 ± 0.0535
7052-3-2	Pyroceram®	49.98 ± 0.19	0.8013 ± 0.0351	0.8066 ± 0.0352	0.7908 ± 0.0346	0.8430 ± 0.0363	0.8057 ± 0.0350	0.8095 ± 0.0331
7052-3-2	Pyroceram®	100.00 ± 0.10	0.8812 ± 0.0366	0.9464 ± 0.0392	0.9380 ± 0.0394	0.9762 ± 0.0407	0.9323 ± 0.0384	0.9348 ± 0.0475
7052-3-2	Pyroceram®	150.00 ± 0.10	1.0110 ± 0.0420	1.0180 ± 0.0423	1.0119 ± 0.0409	0.9804 ± 0.0397	1.0206 ± 0.0410	1.0084 ± 0.0326
7052-3-2	Pyroceram®	200.00 ± 0.10	1.0383 ± 0.0430	1.0458 ± 0.0432	1.0506 ± 0.0436	1.0448 ± 0.0432	1.0784 ± 0.0444	1.0516 ± 0.0331
7052-3-2	Pyroceram®	249.96 ± 0.20	1.1428 ± 0.0473	1.0844 ± 0.0440	1.1448 ± 0.0468	1.1407 ± 0.0473	1.1019 ± 0.0461	1.1229 ± 0.0452
7052-3-2	Pyroceram®	300.00 ± 0.10	1.0904 ± 0.0464	1.1485 ± 0.0479	1.1580 ± 0.0480	1.0960 ± 0.0462	1.1907 ± 0.0497	1.1367 ± 0.0588

This page intentionally left blank.

Chapter 6

Measurements on SB-14 Glass

6.1 Material Properties

Two 1 mm and two 2 mm samples of SB-14 glass were measured at temperatures ranging from 25 to 300 °C. The properties of each sample are presented in Table 6.1. The uncertainty in the sample weights are taken as the uncertainty of the scale used. The uncertainty of the height and diameter are obtained from 4 independent measurements at different locations on the sample. The density was calculated assuming a perfect cylindrical geometry.

Table 6.1: Parameters of the SB-14 Glass Samples.

Sample Number	Diameter (mm)	Weight (g)	Height (mm)	Density (g/cm^3)
SB-1-1	12.607 ± 0.001	0.305 ± 0.0005	1.039 ± 0.002	2.352 ± 0.008
SB-1-2	12.600 ± 0.011	0.304 ± 0.0005	1.033 ± 0.001	2.360 ± 0.009
SB-2-1	12.607 ± 0.024	0.595 ± 0.0005	2.016 ± 0.001	2.364 ± 0.001
SB-2-2	12.598 ± 0.006	0.595 ± 0.0005	2.017 ± 0.002	2.367 ± 0.005

6.2 Experimental Arrangement

The thermal diffusivity of each sample was measured 5 times at 25, 50, 100, 150, 200, 250, and 300 °C. The samples were coated with graphite ($\sim$ 5 microns) to ensure uniform and thorough absorption of the Xenon flash energy. A higher flash voltage was used for the 2 mm samples to reduce signal noise. In all tests, the flash duration was significantly less than the half rise time ($\sim$ 100 ms for 1 mm samples and $\sim$ 500 ms for 3 mm samples), so no correction for the pulse duration was needed [2]. The NanoFlash® machine parameters are listed in Table 6.2.

Table 6.2: NanoFlash® Machine Parameters for the SB-14 Glass Samples.

Sample Number	Temperature (C)	Shots	Volts (V)	Filter (%)	Flash Duration (μs)	Preamp Gain	Main Gain	Recording Time (ms)
SB-1-1	25.40 ± 0.34	5	270	100 (5)	250	10	2520	1304
SB-1-1	49.92 ± 0.26	5	270	100 (5)	250	10	1260	1304
SB-1-1	99.94 ± 0.21	5	270	100 (5)	250	10	623	1304
SB-1-1	150.00 ± 0.10	5	270	100 (5)	250	10	315	1620
SB-1-1	200.02 ± 0.19	5	270	100 (5)	250	10	155	1774
SB-1-1	250.00 ± 0.10	5	270	100 (5)	250	10	78.8	1774
SB-1-1	300.08 ± 0.26	5	270	100 (5)	250	10	78.8	1774
SB-1-2	25.02 ± 0.36	5	270	100 (5)	250	10	2520	1380
SB-1-2	50.00 ± 0.10	5	270	100 (5)	250	10	1260	1380
SB-1-2	100.00 ± 0.10	5	270	100 (5)	250	10	623	1380
SB-1-2	150.00 ± 0.10	5	270	100 (5)	250	10	315	1518
SB-1-2	200.00 ± 0.10	5	270	100 (5)	250	10	155	1722
SB-1-2	250.00 ± 0.10	5	270	100 (5)	250	10	78.8	1722
SB-1-2	300.04 ± 0.21	5	270	100 (5)	250	10	78.8	1894
SB-2-1	24.94 ± 0.21	5	292	100 (5)	450	10	2520	4340
SB-2-1	50.00 ± 0.10	5	292	100 (5)	450	10	1260	4774
SB-2-1	100.00 ± 0.10	5	292	100 (5)	450	10	623	4774
SB-2-1	150.00 ± 0.10	5	292	100 (5)	450	10	315	5538
SB-2-1	200.00 ± 0.10	5	292	100 (5)	450	10	155	6314
SB-2-1	250.00 ± 0.10	5	292	100 (5)	450	10	155	6314
SB-2-1	300.00 ± 0.10	5	292	100 (5)	450	10	78.8	6314
SB-2-2	25.00 ± 0.10	5	292	100 (5)	450	10	2520	4190
SB-2-2	50.00 ± 0.10	5	292	100 (5)	450	10	1260	4798
SB-2-2	100.00 ± 0.10	5	292	100 (5)	450	10	623	4798
SB-2-2	150.00 ± 0.10	5	292	100 (5)	450	10	315	5566
SB-2-2	200.00 ± 0.10	5	292	100 (5)	450	10	155	6344
SB-2-2	250.00 ± 0.10	5	292	100 (5)	450	10	155	6344
SB-2-2	300.00 ± 0.10	5	292	100 (5)	450	10	78.8	6946

6.3 Experimental Results

6.3.1 Thermal Diffusivity

All shots on the SB-14 glass samples were analyzed with the MATLAB® routine using the Cowan model [7, 8]. Taking the coefficient of linear thermal expansion, CTE, of SB-14 glass to be as high as $15 \times 10^{-6}\ C^{-1}$ leads to a negligible change (*i.e.* $< 0.8\%$) in the measured thermal diffusivity and specific heat. For this reason, the effects of thermal expansion are considered to be included in the conservative error estimations reported.

The thermal diffusivity and accompanying error for each shot on the SB-14 glass samples are presented in Table 6.3. The average thermal diffusivity at each temperature is also

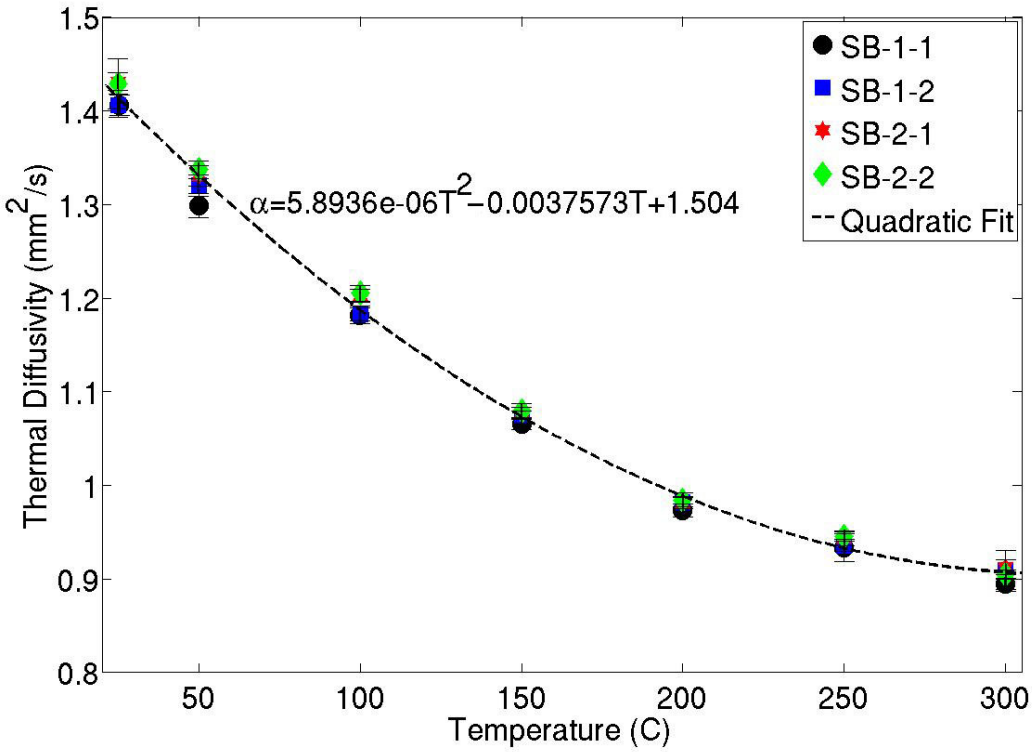

Figure 6.1: Thermal diffusivity as a function of temperature for all four SB-14 glass samples. The data shows a downward trend in thermal diffusivity with increasing temperature, which is fit to a quadratic equation.

reported. The average values at each temperature are presented graphically in Figure 6.1. The results show a downward trend in thermal diffusivity with temperature. This trend is fit to a quadratic equation using the data from all four samples, and is shown in Figure 6.1.

6.3.2 Specific Heat

The specific heats measured with the MATLAB® for each shot on the SB-14 glass samples along with the average at each temperature are presented in Tables 6.4 and 6.5. The average specific heat at each temperature is presented graphically in Figure 6.2. To calculate the specific heat, each SB-14 glass shot was compared to the average of 3 shots for the 1 mm samples and 5 shots for the 2 mm samples on the reference materials at identical machine parameters and temperatures. There is an observed variability in specific heat with reference material. Specific heats found with pocographite have a $\sim 15\%$ higher value when compared to those found with Pyroceram®. Also, the 2 mm samples tend to give a $\sim 10\%$ higher specific heat than the 1 mm samples. The specific heat of each SB-14 glass sample is seen

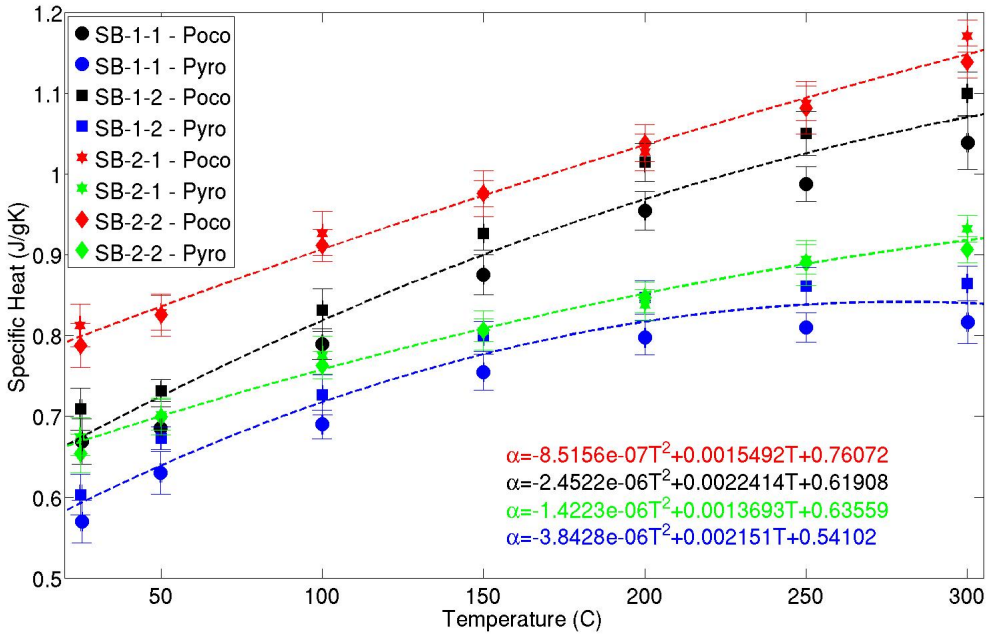

Figure 6.2: Specific heat as a function of temperature for all four SB-14 glass samples. The data shows an upward trend in specific heat as temperature increases for all samples. The specific heat found with pocographite is $\sim 15\%$ higher than that found using Pyroceram® for samples at similar thicknesses. In addition, the 2 mm samples are seen to have a $\sim 10\%$ higher specific heat than the 1 mm samples using the same reference.

to increase with temperature. This increase in specific heat with temperature for samples of similar thickness and identical references are fit to quadratic equations, which are shown in Figure 6.2. The differing thermal and physical properties between the reference and sample make measuring the specific heat of a sample to a high degree of accuracy difficult. These considerations must be kept in mind when using this data.

Table 6.3: Measured Thermal Diffusivity in mm^2/s of the SB-14 Glass Samples.

Sample Number	Temperature (C)	Shot #1	Shot #2	Shot #3	Shot #4	Shot #5	Average
SB-1-1	25.40 ± 0.34	1.4062 ± 0.0058	1.4109 ± 0.0061	1.4131 ± 0.0062	1.4114 ± 0.0059	1.3890 ± 0.0056	1.4091 ± 0.0113
SB-1-1	49.92 ± 0.26	1.3136 ± 0.0054	1.3061 ± 0.0053	1.3007 ± 0.0050	1.2883 ± 0.0053	1.2864 ± 0.0049	1.2990 ± 0.0125
SB-1-1	99.94 ± 0.21	1.1816 ± 0.0055	1.1954 ± 0.0059	1.1827 ± 0.0045	1.1782 ± 0.0039	1.1731 ± 0.0050	1.1822 ± 0.0095
SB-1-1	150.00 ± 0.10	1.0620 ± 0.0041	1.0628 ± 0.0040	1.0738 ± 0.0041	1.0697 ± 0.0039	1.0618 ± 0.0042	1.0660 ± 0.0066
SB-1-1	200.02 ± 0.19	0.9779 ± 0.0036	0.9804 ± 0.0038	0.9672 ± 0.0034	0.9738 ± 0.0035	0.9684 ± 0.0038	0.9735 ± 0.0067
SB-1-1	250.00 ± 0.10	0.9254 ± 0.0035	0.9588 ± 0.0038	0.9340 ± 0.0039	0.9323 ± 0.0038	0.9192 ± 0.0037	0.9339 ± 0.0149
SB-1-1	300.08 ± 0.26	0.8892 ± 0.0035	0.8946 ± 0.0038	0.8972 ± 0.0026	0.9001 ± 0.0038	0.8918 ± 0.0036	0.8946 ± 0.0053
SB-1-2	25.02 ± 0.36	1.4047 ± 0.0055	1.3983 ± 0.0054	1.4085 ± 0.0054	1.3943 ± 0.0054	1.4232 ± 0.0049	1.4058 ± 0.0122
SB-1-2	50.00 ± 0.10	1.3181 ± 0.0053	1.3106 ± 0.0049	1.3109 ± 0.0047	1.3292 ± 0.0038	1.3325 ± 0.0052	1.3203 ± 0.0111
SB-1-2	100.00 ± 0.10	1.1912 ± 0.0040	1.1847 ± 0.0037	1.1775 ± 0.0043	1.1828 ± 0.0045	1.1781 ± 0.0046	1.1829 ± 0.0068
SB-1-2	150.00 ± 0.10	1.0728 ± 0.0040	1.0760 ± 0.0041	1.0715 ± 0.0042	1.0765 ± 0.0041	1.0787 ± 0.0042	1.0751 ± 0.0044
SB-1-2	200.00 ± 0.10	0.9775 ± 0.0036	0.9791 ± 0.0036	0.9875 ± 0.0035	0.9869 ± 0.0038	0.9820 ± 0.0036	0.9826 ± 0.0056
SB-1-2	250.00 ± 0.10	0.9281 ± 0.0036	0.9437 ± 0.0037	0.9358 ± 0.0036	0.9353 ± 0.0038	0.9353 ± 0.0037	0.9356 ± 0.0065
SB-1-2	300.04 ± 0.21	0.9870 ± 0.0035	0.8976 ± 0.0033	0.9023 ± 0.0035	0.8956 ± 0.0033	0.9506 ± 0.0033	0.9086 ± 0.0222
SB-2-1	24.94 ± 0.21	1.4409 ± 0.0068	1.4288 ± 0.0058	1.4364 ± 0.0062	1.4309 ± 0.0063	1.4201 ± 0.0054	1.4314 ± 0.0097
SB-2-1	50.00 ± 0.10	1.3388 ± 0.0050	1.3230 ± 0.0054	1.3409 ± 0.0051	1.3334 ± 0.0051	1.3172 ± 0.0047	1.3307 ± 0.0112
SB-2-1	100.00 ± 0.10	1.2061 ± 0.0041	1.1992 ± 0.0045	1.1957 ± 0.0049	1.2100 ± 0.0046	1.2008 ± 0.0049	1.2024 ± 0.0070
SB-2-1	150.00 ± 0.10	1.0702 ± 0.0039	1.0786 ± 0.0039	1.0830 ± 0.0039	1.0780 ± 0.0041	1.0763 ± 0.0039	1.0772 ± 0.0058
SB-2-1	200.00 ± 0.10	0.9866 ± 0.0031	0.9836 ± 0.0034	0.9797 ± 0.0033	0.9833 ± 0.0033	0.9736 ± 0.0032	0.9814 ± 0.0058
SB-2-1	250.00 ± 0.10	0.9439 ± 0.0037	0.9420 ± 0.0033	0.9325 ± 0.0032	0.9521 ± 0.0037	0.9458 ± 0.0035	0.9432 ± 0.0078
SB-2-1	300.00 ± 0.10	0.9086 ± 0.0033	0.9061 ± 0.0035	0.9152 ± 0.0037	0.9103 ± 0.0038	0.9232 ± 0.0038	0.9127 ± 0.0075
SB-2-2	25.00 ± 0.10	1.4218 ± 0.0068	1.4073 ± 0.0056	1.4558 ± 0.0079	1.4009 ± 0.0061	1.4606 ± 0.0057	1.4293 ± 0.0270
SB-2-2	50.00 ± 0.10	1.3348 ± 0.0053	1.3385 ± 0.0054	1.3352 ± 0.0053	1.3498 ± 0.0054	1.3279 ± 0.0049	1.3372 ± 0.0094
SB-2-2	100.00 ± 0.10	1.2033 ± 0.0050	1.2152 ± 0.0048	1.2094 ± 0.0050	1.1986 ± 0.0047	1.1998 ± 0.0048	1.2053 ± 0.0083
SB-2-2	150.00 ± 0.10	1.0818 ± 0.0039	1.0702 ± 0.0036	1.0899 ± 0.0041	1.0791 ± 0.0043	1.0776 ± 0.0037	1.0797 ± 0.0080
SB-2-2	200.00 ± 0.10	0.9899 ± 0.0033	0.9917 ± 0.0035	0.9814 ± 0.0033	0.9839 ± 0.0035	0.9761 ± 0.0034	0.9846 ± 0.0071
SB-2-2	250.00 ± 0.10	0.9440 ± 0.0036	0.9428 ± 0.0036	0.9444 ± 0.0038	0.9527 ± 0.0037	0.9444 ± 0.0034	0.9457 ± 0.0051
SB-2-2	300.00 ± 0.10	0.8993 ± 0.0033	0.9075 ± 0.0030	0.9059 ± 0.0034	0.9059 ± 0.0029	0.9064 ± 0.0035	0.9050 ± 0.0043

Table 6.4: Measured Specific Heat in J/gK of the SB-14 Glass Samples SB-1-1 and SB-1-2.

Sample Number	Standard Material	Temperature (C)	Shot #1	Shot #2	Shot #3	Shot #4	Shot #5	Average
SB-1-1	Pocographite	25.40 ± 0.34	0.6850 ± 0.0174	0.6773 ± 0.0174	0.6944 ± 0.0180	0.6481 ± 0.0165	0.6418 ± 0.0163	0.6693 ± 0.0280
SB-1-1	Pocographite	49.92 ± 0.26	0.7222 ± 0.0176	0.6700 ± 0.0163	0.6725 ± 0.0162	0.6729 ± 0.0164	0.6895 ± 0.0168	0.6854 ± 0.0267
SB-1-1	Pocographite	100.00 ± 0.21	0.7991 ± 0.0180	0.8071 ± 0.0183	0.7855 ± 0.0172	0.7776 ± 0.0169	0.7793 ± 0.0175	0.7897 ± 0.0191
SB-1-1	Pocographite	150.00 ± 0.10	0.8766 ± 0.0203	0.8513 ± 0.0195	0.8726 ± 0.0200	0.8747 ± 0.0201	0.9023 ± 0.0209	0.8755 ± 0.0249
SB-1-1	Pocographite	200.02 ± 0.19	0.9465 ± 0.0209	0.9436 ± 0.0210	0.9654 ± 0.0214	0.9787 ± 0.0216	0.9407 ± 0.0209	0.9550 ± 0.0238
SB-1-1	Pocographite	250.00 ± 0.10	0.9748 ± 0.0222	0.9760 ± 0.0226	0.9911 ± 0.0229	1.0050 ± 0.0233	0.9926 ± 0.0229	0.9879 ± 0.0213
SB-1-1	Pocographite	300.08 ± 0.26	1.0111 ± 0.0240	1.0585 ± 0.0253	1.0382 ± 0.0239	1.0691 ± 0.0255	1.0180 ± 0.0243	1.0390 ± 0.0329
SB-1-1	Pyroceram®	25.40 ± 0.34	0.5831 ± 0.0205	0.5766 ± 0.0203	0.5911 ± 0.0209	0.5517 ± 0.0194	0.5463 ± 0.0192	0.5698 ± 0.0263
SB-1-1	Pyroceram®	49.92 ± 0.26	0.6639 ± 0.0197	0.6159 ± 0.0183	0.6183 ± 0.0182	0.6186 ± 0.0183	0.6338 ± 0.0188	0.6301 ± 0.0261
SB-1-1	Pyroceram®	100.00 ± 0.21	0.6983 ± 0.0189	0.7052 ± 0.0192	0.6864 ± 0.0182	0.6795 ± 0.0179	0.6810 ± 0.0183	0.6901 ± 0.0181
SB-1-1	Pyroceram®	150.00 ± 0.10	0.7557 ± 0.0191	0.7340 ± 0.0185	0.7524 ± 0.0189	0.7542 ± 0.0189	0.7780 ± 0.0197	0.7549 ± 0.0222
SB-1-1	Pyroceram®	200.02 ± 0.19	0.7905 ± 0.0195	0.7882 ± 0.0195	0.8063 ± 0.0199	0.8175 ± 0.0201	0.7857 ± 0.0195	0.7976 ± 0.0208
SB-1-1	Pyroceram®	250.00 ± 0.10	0.7995 ± 0.0199	0.8005 ± 0.0202	0.8129 ± 0.0205	0.8242 ± 0.0208	0.8141 ± 0.0205	0.8102 ± 0.0182
SB-1-1	Pyroceram®	300.08 ± 0.26	0.7948 ± 0.0203	0.8320 ± 0.0215	0.8160 ± 0.0203	0.8404 ± 0.0216	0.8002 ± 0.0206	0.8167 ± 0.0266
SB-1-2	Pocographite	25.02 ± 0.36	0.7006 ± 0.0171	0.6939 ± 0.0169	0.6890 ± 0.0167	0.7286 ± 0.0180	0.7346 ± 0.0178	0.7094 ± 0.0260
SB-1-2	Pocographite	50.00 ± 0.10	0.7283 ± 0.0170	0.7318 ± 0.0168	0.7230 ± 0.0166	0.7392 ± 0.0167	0.7388 ± 0.0171	0.7322 ± 0.0136
SB-1-2	Pocographite	100.00 ± 0.10	0.8569 ± 0.0175	0.8301 ± 0.0169	0.8237 ± 0.0170	0.8472 ± 0.0176	0.8012 ± 0.0166	0.8318 ± 0.0266
SB-1-2	Pocographite	150.00 ± 0.10	0.9108 ± 0.0201	0.9350 ± 0.0207	0.9212 ± 0.0203	0.9242 ± 0.0204	0.9444 ± 0.0209	0.9271 ± 0.0205
SB-1-2	Pocographite	200.00 ± 0.10	1.0341 ± 0.0217	1.0219 ± 0.0214	1.0217 ± 0.0213	0.9987 ± 0.0210	0.9982 ± 0.0209	1.0149 ± 0.0234
SB-1-2	Pocographite	250.00 ± 0.10	1.0454 ± 0.0229	1.0694 ± 0.0236	1.0452 ± 0.0228	1.0696 ± 0.0236	1.0234 ± 0.0224	1.0506 ± 0.0273
SB-1-2	Pocographite	300.04 ± 0.21	1.0956 ± 0.0245	1.1256 ± 0.0252	1.1077 ± 0.0247	1.0771 ± 0.0240	1.0950 ± 0.0243	1.1002 ± 0.0267
SB-1-2	Pyroceram®	25.02 ± 0.36	0.5959 ± 0.0205	0.5902 ± 0.0203	0.5861 ± 0.0201	0.6197 ± 0.0214	0.6249 ± 0.0214	0.6033 ± 0.0248
SB-1-2	Pyroceram®	50.00 ± 0.10	0.6695 ± 0.0193	0.6728 ± 0.0192	0.6646 ± 0.0189	0.6795 ± 0.0192	0.6792 ± 0.0195	0.6731 ± 0.0142
SB-1-2	Pyroceram®	100.00 ± 0.10	0.7488 ± 0.0190	0.7253 ± 0.0183	0.7198 ± 0.0184	0.7403 ± 0.0189	0.7001 ± 0.0179	0.7269 ± 0.0248
SB-1-2	Pyroceram®	150.00 ± 0.10	0.7853 ± 0.0191	0.8062 ± 0.0196	0.7943 ± 0.0193	0.7969 ± 0.0194	0.8143 ± 0.0199	0.7994 ± 0.0185
SB-1-2	Pyroceram®	200.00 ± 0.10	0.8637 ± 0.0204	0.8536 ± 0.0201	0.8534 ± 0.0201	0.8341 ± 0.0198	0.8337 ± 0.0197	0.8477 ± 0.0206
SB-1-2	Pyroceram®	250.00 ± 0.10	0.8574 ± 0.0206	0.8771 ± 0.0212	0.8572 ± 0.0206	0.8773 ± 0.0213	0.8394 ± 0.0203	0.8617 ± 0.0233
SB-1-2	Pyroceram®	300.04 ± 0.21	0.8612 ± 0.0210	0.8847 ± 0.0215	0.8707 ± 0.0211	0.8466 ± 0.0205	0.8608 ± 0.0208	0.8648 ± 0.0217

Table 6.5: Measured Specific Heat in J/gK of the SB-14 Glass Samples SB-2-1 and SB-2-2.

Sample Number	Standard Material	Temperature (C)	Shot #1	Shot #2	Shot #3	Shot #4	Shot #5	Average
SB-2-1	Pocographite	24.94 ± 0.21	0.8427 ± 0.0223	0.8104 ± 0.0208	0.8040 ± 0.0208	0.8169 ± 0.0212	0.7899 ± 0.0200	0.8128 ± 0.0265
SB-2-1	Pocographite	50.00 ± 0.10	0.8334 ± 0.0199	0.8115 ± 0.0198	0.8273 ± 0.0198	0.8490 ± 0.0204	0.8201 ± 0.0196	0.8282 ± 0.0214
SB-2-1	Pocographite	100.00 ± 0.10	0.9485 ± 0.0217	0.9286 ± 0.0214	0.9018 ± 0.0210	0.9440 ± 0.0217	0.9113 ± 0.0213	0.9268 ± 0.0273
SB-2-1	Pocographite	150.00 ± 0.10	0.9686 ± 0.0219	0.9779 ± 0.0220	0.9496 ± 0.0213	1.0084 ± 0.0228	0.9751 ± 0.0220	0.9759 ± 0.0285
SB-2-1	Pocographite	200.00 ± 0.10	1.0158 ± 0.0222	1.0197 ± 0.0225	1.0186 ± 0.0224	1.0496 ± 0.0231	1.0332 ± 0.0228	1.0274 ± 0.0225
SB-2-1	Pocographite	250.00 ± 0.10	1.0935 ± 0.0245	1.0926 ± 0.0243	1.0665 ± 0.0237	1.0970 ± 0.0245	1.0893 ± 0.0243	1.0878 ± 0.0216
SB-2-1	Pocographite	300.00 ± 0.10	1.1752 ± 0.0271	1.1760 ± 0.0272	1.1641 ± 0.0269	1.1615 ± 0.0269	1.1824 ± 0.0274	1.1718 ± 0.0198
SB-2-1	Pyroceram®	25.00 ± 0.10	0.6999 ± 0.0222	0.6730 ± 0.0210	0.6677 ± 0.0209	0.6784 ± 0.0213	0.6560 ± 0.0202	0.6750 ± 0.0236
SB-2-1	Pyroceram®	50.00 ± 0.10	0.7064 ± 0.0192	0.6878 ± 0.0190	0.7012 ± 0.0191	0.7196 ± 0.0197	0.6951 ± 0.0189	0.7020 ± 0.0191
SB-2-1	Pyroceram®	100.00 ± 0.10	0.7940 ± 0.0197	0.7773 ± 0.0193	0.7548 ± 0.0190	0.7902 ± 0.0197	0.7628 ± 0.0192	0.7758 ± 0.0235
SB-2-1	Pyroceram®	150.00 ± 0.10	0.8005 ± 0.0192	0.8082 ± 0.0193	0.7849 ± 0.0187	0.8335 ± 0.0200	0.8059 ± 0.0193	0.8066 ± 0.0240
SB-2-1	Pyroceram®	200.00 ± 0.10	0.8289 ± 0.0197	0.8320 ± 0.0199	0.8311 ± 0.0198	0.8565 ± 0.0204	0.8431 ± 0.0201	0.8383 ± 0.0191
SB-2-1	Pyroceram®	250.00 ± 0.10	0.8993 ± 0.0217	0.8986 ± 0.0215	0.8771 ± 0.0210	0.9022 ± 0.0217	0.8959 ± 0.0216	0.8946 ± 0.0184
SB-2-1	Pyroceram®	300.00 ± 0.10	0.9354 ± 0.0230	0.9360 ± 0.0231	0.9265 ± 0.0228	0.9244 ± 0.0228	0.9411 ± 0.0233	0.9327 ± 0.0164
SB-2-2	Pocographite	24.94 ± 0.21	0.7849 ± 0.0208	0.7990 ± 0.0207	0.7537 ± 0.0198	0.7953 ± 0.0206	0.8060 ± 0.0208	0.7878 ± 0.0272
SB-2-2	Pocographite	50.00 ± 0.10	0.8174 ± 0.0200	0.8037 ± 0.0195	0.8213 ± 0.0198	0.8556 ± 0.0208	0.8312 ± 0.0200	0.8258 ± 0.0259
SB-2-2	Pocographite	100.00 ± 0.10	0.9177 ± 0.0215	0.9149 ± 0.0213	0.9259 ± 0.0216	0.8957 ± 0.0208	0.9057 ± 0.0212	0.9120 ± 0.0197
SB-2-2	Pocographite	150.00 ± 0.10	0.9788 ± 0.0223	0.9842 ± 0.0222	0.9798 ± 0.0224	0.9728 ± 0.0223	0.9658 ± 0.0218	0.9763 ± 0.0162
SB-2-2	Pocographite	200.00 ± 0.10	1.0445 ± 0.0231	1.0401 ± 0.0231	1.0149 ± 0.0225	1.0535 ± 0.0234	1.0403 ± 0.0231	1.0387 ± 0.0229
SB-2-2	Pocographite	250.00 ± 0.10	1.1242 ± 0.0254	1.0617 ± 0.0239	1.0763 ± 0.0242	1.0668 ± 0.0242	1.0828 ± 0.0243	1.0824 ± 0.0326
SB-2-2	Pocographite	300.00 ± 0.10	1.1346 ± 0.0259	1.1280 ± 0.0255	1.1361 ± 0.0258	1.1492 ± 0.0257	1.1482 ± 0.0263	1.1392 ± 0.0196
SB-2-2	Pyroceram®	25.00 ± 0.10	0.6518 ± 0.0207	0.6636 ± 0.0208	0.6259 ± 0.0198	0.6604 ± 0.0207	0.6694 ± 0.0209	0.6542 ± 0.0241
SB-2-2	Pyroceram®	50.00 ± 0.10	0.6928 ± 0.0192	0.6812 ± 0.0187	0.6961 ± 0.0191	0.7252 ± 0.0200	0.7045 ± 0.0192	0.7000 ± 0.0230
SB-2-2	Pyroceram®	100.00 ± 0.10	0.7682 ± 0.0194	0.7658 ± 0.0193	0.7750 ± 0.0195	0.7497 ± 0.0189	0.7582 ± 0.0191	0.7634 ± 0.0171
SB-2-2	Pyroceram®	150.00 ± 0.10	0.8090 ± 0.0195	0.8134 ± 0.0195	0.8098 ± 0.0196	0.8040 ± 0.0195	0.7982 ± 0.0192	0.8069 ± 0.0139
SB-2-2	Pyroceram®	200.00 ± 0.10	0.8523 ± 0.0204	0.8487 ± 0.0204	0.8282 ± 0.0199	0.8596 ± 0.0207	0.8489 ± 0.0204	0.8475 ± 0.0194
SB-2-2	Pyroceram®	250.00 ± 0.10	0.9246 ± 0.0225	0.8732 ± 0.0212	0.8852 ± 0.0214	0.8774 ± 0.0214	0.8906 ± 0.0215	0.8902 ± 0.0275
SB-2-2	Pyroceram®	300.00 ± 0.10	0.9031 ± 0.0220	0.8978 ± 0.0217	0.9042 ± 0.0220	0.9147 ± 0.0219	0.9139 ± 0.0224	0.9067 ± 0.0163

This page intentionally left blank.

Chapter 7

Measurements on C-4000 Muscovite Mica

7.1 Material Properties

Measurements of the thermal diffusivity and specific heat of C-4000 Muscovite mica were measured at temperatures ranging from 25 to 300 °C. The properties of the mica sample are presented in Table 7.1. The error in the sample weight is taken as the uncertainty of the scale used. The uncertainty of the height is obtained from 4 independent measurements at different locations on the sample. The sample was made with a high precision die, so negligible error is assumed for the diameter. ThThe density of C-4000 Muscovite Mica has been reported as 2.852 g/cm^3 [9]. This puts the theoretical maximum density (TMD) of the mica sample at around 67%. It should be noted that the mica sample was pressed 1 week before the measurements were taken. The sample was not stored in a desiccator cabinet and no effort was made to determine the level of hydration in the samples at the time of measurement.

Table 7.1: Parameters of the Mica Sample.

Diameter (mm)	Weight (g)	Height (mm)	Density (g/cm^3)
7.980 ± 0.000	0.158 ± 0.0005	1.647 ± 0.004	1.919 ± 0.013

7.2 Experimental Method

The thermal diffusivity of the sample was measured 5 times at 25, 50, 100, 150, 200, 250, and 300 °C. In all tests, the flash duration was significantly less than the half rise time ($\sim$ 4000 ms), so no correction for the pulse duration was needed [2]. The NanoFlash® machine parameters used for the mica sample are listed in Table 7.2.

Table 7.2: NanoFlash® Machine Parameters for the Mica Sample.

Temperature (C)	Shots	Volts (V)	Filter (%)	Flash Duration (μs)	Preamp Gain	Main Gain	Recording Time (ms)
24.86 ± 0.43	5	304	100 (5)	450	10	5002	48644
49.98 ± 0.26	5	304	100 (5)	450	10	5002	48644
100.00 ± 0.10	5	304	100 (5)	450	10	2520	48644
150.00 ± 0.10	5	304	100 (5)	450	10	1260	55454
200.02 ± 0.19	5	304	100 (5)	450	10	623	55454
250.04 ± 0.28	5	304	100 (5)	450	10	623	55454
300.00 ± 0.10	5	304	100 (5)	450	10	315	55864

7.3 Experimental Results

7.3.1 Thermal Diffusivity

All shots on the mica sample were analyzed with the MATLAB® routine using the Cowan model [7, 8]. The coefficient of linear thermal expansion, CTE, of mica changes depending on lattice orientation [15]. The CTE has been reported as $17.8 \times 10^{-6}\ C^{-1}$ perpendicular to the lattice and $3.5 \times 10^{-6}\ C^{-1}$ parallel to the lattice [15]. Since the pellet is pressed from a powder, it is assumed that there is equal thermal transport parallel and perpendicular to the lattice. The sample CTE is taken as the average of the parallel and perpendicular values, $10.65 \times 10^{-6}\ C^{-1}$ and assumed to have a 3% error. Accounting for thermal expansion leads to a negligible change (*i.e.* $< 0.7\%$) in the measured thermal diffusivity and specific heat. For this reason, the effects of thermal expansion are considered to be included in the conservative error estimations reported.

The thermal diffusivity and accompanying error for each shot on the mica sample is presented in Table 7.3. These results are presented graphically in Figure 7.1. The results show a downward trend in thermal diffusivity with temperature. This trend is fit to a quadratic equation, and is shown in Figure 7.1. The mica voltage records (Appendix E) had a large amount of noise, making analysis difficult. Also, the reported lower limit for thermal diffusivity measurements on the NanoFlash® machine is 0.1 mm^2/s [16]. The mica values are seen to be on the very edge of the NanoFlash® machines' capabilities. Both of these factors led to the large amount of error in the reported thermal diffusivities.

7.3.2 Specific Heat

The specific heats measured with the MATLAB® for each mica shot along with the average at each temperature are presented in Table 7.4. To calculate the specific heat, each mica shot was compared to the average of 5 shots on the reference material at identical

Table 7.3: Measured Thermal Diffusivity in mm^2/s of Mica.

Temperature (C)	Shot #1	Shot #2	Shot #3	Shot #4	Shot #5	Average
24.86 ± 0.43	0.0914 ± 0.0011	0.0917 ± 0.0012	0.0855 ± 0.0011	0.0809 ± 0.0012	0.0921 ± 0.0029	0.0883 ± 0.0050
49.98 ± 0.26	0.0821 ± 0.0009	0.1016 ± 0.0122	0.0828 ± 0.0010	0.0840 ± 0.0008	0.0800 ± 0.0009	0.0861 ± 0.0102
100.00 ± 0.10	0.0771 ± 0.0008	0.0771 ± 0.0008	0.0817 ± 0.0009	0.0828 ± 0.0010	0.0800 ± 0.0010	0.0797 ± 0.0027
150.00 ± 0.10	0.0730 ± 0.0008	0.0752 ± 0.0008	0.0770 ± 0.0009	0.0744 ± 0.0008	0.0742 ± 0.0008	0.0747 ± 0.0017
200.02 ± 0.19	0.0769 ± 0.0009	0.0711 ± 0.0009	0.0720 ± 0.0009	0.0735 ± 0.0009	0.0711 ± 0.0009	0.0729 ± 0.0025
250.04 ± 0.28	0.0697 ± 0.0009	0.0718 ± 0.0010	0.0726 ± 0.0009	0.0737 ± 0.0011	0.0716 ± 0.0010	0.0719 ± 0.0017
300.00 ± 0.10	0.0624 ± 0.0015	–	0.0830 ± 0.0010	0.0634 ± 0.0011	0.0727 ± 0.0020	0.0704 ± 0.0090

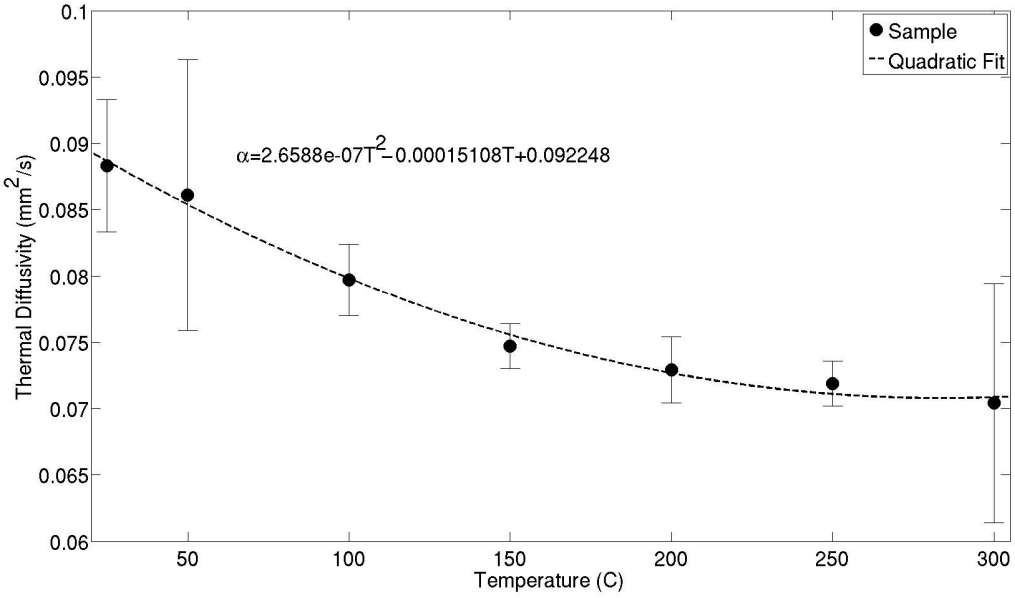

Figure 7.1: Thermal diffusivity as a function of temperature for mica. The data shows a downward trend in thermal diffusivity with increasing temperature.

machine parameters and temperatures. The average specific heat at each temperature is presented graphically in Figure 7.2. It should be noted that the second shot at 300 °C had too much signal error to be analyzed and was removed for this analysis. The specific heat calculations show an increase in specific heat as the temperature increases for both references, which are fit to quadratic equations in Figure 7.2. The specific heat found with pocographite and Pyroceram® are seen to have a similar trend, but the pocographite results report a $\sim 15\%$ higher specific heat value.

The specific heat values reported here are vastly different than those reported in the literature, which are around 0.8 J/gK [19]. This difference was consistent whether the MATLAB® or Proteus® code was used for analysis. The discrepancy could be due to the thermal diffusivity of the mica being at the lower limit of the Nanoflash® capabilities. However, the exact reason is unknown. It is strongly advised to use the literature values for specific heat [19] rather than the data obtained here.

Table 7.4: Measured Specific Heat in J/gK of Mica.

Standard Material	Temperature (C)	Shot #1	Shot #2	Shot #3	Shot #4	Shot #5	Average
Pocographite	24.86 ± 0.43	4.5302 ± 0.4841	4.4420 ± 0.4694	4.0104 ± 0.4427	3.7110 ± 0.4533	4.4739 ± 0.5949	4.2335 ± 0.5336
Pocographite	49.98 ± 0.26	4.1261 ± 0.3840	5.9305 ± 1.2151	4.5396 ± 0.4374	4.3791 ± 0.3857	3.9393 ± 0.3534	4.5829 ± 0.9796
Pocographite	100.00 ± 0.10	5.0035 ± 0.3954	5.0915 ± 0.4183	5.5187 ± 0.4616	5.5582 ± 0.4629	5.2551 ± 0.4728	5.2854 ± 0.4159
Pocographite	150.00 ± 0.10	5.4660 ± 0.4508	5.5205 ± 0.4636	5.8839 ± 0.5072	5.6251 ± 0.4582	5.5794 ± 0.4853	5.6150 ± 0.3536
Pocographite	200.02 ± 0.19	6.5905 ± 0.5598	5.9134 ± 0.5583	6.0184 ± 0.5468	6.4293 ± 0.5582	5.7802 ± 0.5361	6.1464 ± 0.5511
Pocographite	250.04 ± 0.28	6.2273 ± 0.5704	6.5099 ± 0.6141	6.4832 ± 0.5933	6.8947 ± 0.6821	6.4465 ± 0.6204	6.5123 ± 0.4874
Pocographite	300.00 ± 0.10	5.3425 ± 1.1485	–	8.1099 ± 0.6284	5.6873 ± 0.7601	6.9840 ± 0.6702	6.5309 ± 1.4424
Pyroceram®	24.86 ± 0.43	3.7131 ± 0.4022	3.6260 ± 0.3864	3.3343 ± 0.3772	3.0417 ± 0.3754	3.6669 ± 0.4919	3.4764 ± 0.4323
Pyroceram®	49.98 ± 0.26	3.5747 ± 0.3362	5.2207 ± 1.0691	3.9587 ± 0.3828	3.8950 ± 0.3411	3.4129 ± 0.3097	4.0124 ± 0.8782
Pyroceram®	100.00 ± 0.10	4.2615 ± 0.3393	4.3365 ± 0.3588	4.7003 ± 0.3958	4.7340 ± 0.3970	4.4758 ± 0.4050	4.5016 ± 0.3554
Pyroceram®	150.00 ± 0.10	4.7100 ± 0.3908	4.7656 ± 0.4018	5.0701 ± 0.4394	4.8471 ± 0.3972	4.8077 ± 0.4204	4.8401 ± 0.3047
Pyroceram®	200.02 ± 0.19	5.5684 ± 0.4762	4.9962 ± 0.4744	5.0850 ± 0.4647	5.4321 ± 0.4747	4.8837 ± 0.4556	5.1931 ± 0.4669
Pyroceram®	250.04 ± 0.28	5.3170 ± 0.4897	5.5583 ± 0.5270	5.5355 ± 0.5094	5.8869 ± 0.5852	5.5042 ± 0.5323	5.5604 ± 0.4174
Pyroceram®	300.00 ± 0.10	4.2985 ± 0.9250	–	6.5251 ± 0.5096	4.5759 ± 0.6132	5.6193 ± 0.5420	5.2547 ± 1.1614

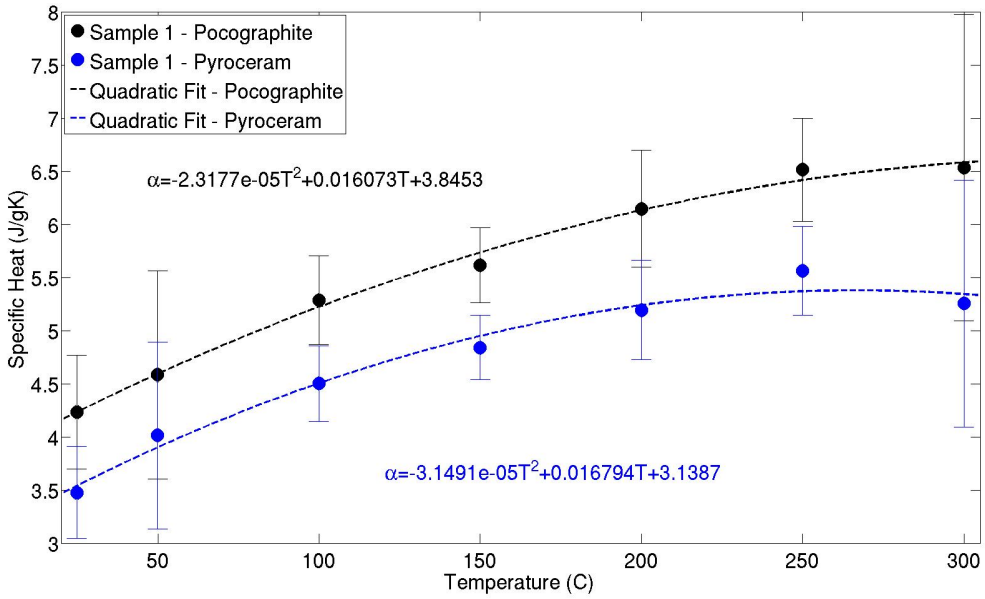

Figure 7.2: Specific heat as a function of temperature for mica. The data shows an upward trend in specific heat as temperature increases. The results also show a dependence on the standard used for comparison. The specific heat found with pocographite (black) is $\sim 15\%$ higher than that found with Pyroceram® (blue).

Chapter 8

Measurements on Pocographite and Pyroceram®

8.1 Physical Properties

The physical properties of the pocographite and Pyroceram® samples are presented in Table 8.1. The error in the weight is taken as the uncertainty of the scale used. The uncertainty of the height is obtained from 4 independent measurements at different locations on the sample. The sample was assumed to have negligible error in diameter.

Table 8.1: Physical Properties of the Pocographite and Pyroceram® Standards.

Material	Diameter (mm)	Weight (g)	Height (mm)	Density (g/cm^3)
Pocographite	12.700	0.223 ± 0.0005	1.007 ± 0.003	1.749 ± 0.009
Pyroceram®	12.700	0.654 ± 0.0005	1.990 ± 0.000	2.594 ± 0.002

8.2 Experimental Arrangement

The thermal diffusivity of each standard was measured at 25, 50, 100, 150, 200, 250, and 300 °C. The NanoFlash® machine allows for a 0.5 °C deviation from the specified temperature with a 0.1 °C accuracy of the reading. This is the source of the temperature error reported in the experimental results. The samples were coated with graphite ($\sim$ 5 microns) to ensure uniform and thorough absorption of the Xenon flash energy. The samples were measured with flash voltages of 270, 292, and 304 V with no filter (NanoFlash® filter option 5). The temperature rise on the back side of each sample was measured with a InSb IR sensor cooled with liquid nitrogen. Flash durations of $\sim$ 250 μs and $\sim$ 450 μs (NanoFlash® pulse options "Medium" and "Long") were both used. Despite the various flash parameters (*i.e.* duration and voltage) the measured thermal diffusivities were similar (*i.e.* $< 5\%$). Given this level of precision, the thermal diffusivities reported are the average

of all measurements taken. The half rise time were ~ 3 ms for pocographite and ~ 300 ms for Pyroceram®. Both of these rise times were long enough to eliminate the need for a pulse correction [2].

8.3 Thermal Diffusivity

The thermal diffusivity of each material was determined with the MATLAB® routine using the Cowan model [7, 8]. The thermal diffusivities of each material at each temperature are presented in Table 8.2.

Table 8.2: Measured Thermal Diffusivity in mm^2/s for Pocographite and Pyroceram®.

Material	Shots	Temperature (C)	Thermal Diffusivity (mm^2/s)
Pocographite	35	24.98 ± 0.55	58.9255 ± 0.6794
Pocographite	21	49.98 ± 0.23	55.0341 ± 0.9698
Pocographite	21	100.00 ± 0.10	48.1284 ± 0.9266
Pocographite	21	149.99 ± 0.15	42.5979 ± 0.5380
Pocographite	21	199.99 ± 0.15	37.8963 ± 0.4674
Pocographite	21	250.00 ± 0.19	34.2292 ± 0.3513
Pocographite	16	300.01 ± 0.16	31.1892 ± 0.1558
Pyroceram®	31	25.03 ± 0.51	2.0184 ± 0.0193
Pyroceram®	21	49.99 ± 0.22	1.8584 ± 0.0101
Pyroceram®	21	99.99 ± 0.15	1.6592 ± 0.0121
Pyroceram®	21	150.00 ± 0.10	1.4957 ± 0.0092
Pyroceram®	21	200.00 ± 0.10	1.4146 ± 0.0065
Pyroceram®	21	250.02 ± 0.21	1.3333 ± 0.0057
Pyroceram®	16	300.02 ± 0.18	1.2788 ± 0.0081

Using data supplied with the NanoFlash® machine, the coefficient of linear thermal expansion, CTE, of pocographite and Pyroceram® are $\sim 7.4 \times 10^{-6}\ C^{-1}$ and $\sim 6.2 \times 10^{-6}\ C^{-1}$, respectively. No effort has been made to verify the accuracy of this data. Accounting for thermal expansion leads to a negligible change (*i.e.* $< 0.5\%$) in the measured thermal diffusivity and specific heat. For this reason, the effects of thermal expansion are considered to be included in the conservative error estimations reported.

Table 8.3: Coefficients of the Numerical Fits for the Specific Heat of Pocographite and Pyroceram®.

Coefficient	Pocographite	Pyroceram®
A_1	$-2.357 \times 10^{-6} \pm 1.015 \times 10^{-7}$	$0.9224 \pm 2.724 \times 10^{-2}$
A_2	$3.037 \times 10^{-3} \pm 3.201 \times 10^{-5}$	$3.671 \times 10^{-4} \pm 8.760 \times 10^{-5}$
A_3	$0.637 \pm 2.156 \times 10^{-3}$	$-0.1924 \pm 3.058 \times 10^{-2}$
A_4	-	$-1.412 \times 10^{-2} \pm 1.850 \times 10^{-3}$

8.4 Specific Heat

The specific heat for each material as a function of temperature was determined from the tabular data accompanying the NanoFlash® machine. No effort have been made to verify the source of this data or its accuracy. The specific heat of pocographite was fit to a quadratic equation, $C_p = A_1T^2 + A_2T + A_3$, while that of Pyroceram® was fit to a double exponential function, $C_P = A_1exp(A_2T) + A_3exp(A_4T)$. These curves gave the best fit to each data set. The values and their 95% confidence intervals were determined and are listed in Table 8.3.

This page intentionally left blank.

References

[1] American Society of Testing and Materials. *Standard Test Method for Thermal Diffusivity by the Flash Method: E1461-13*, 2013.

[2] T. Azumi and Y. Takahashi. Novel finite pulse-width correction in flash thermal diffusivity measurement. *Review of Scientific Instruments*, 52(9):1411, 1981.

[3] Y. Beers. *Introduction to the Theory of Error*. Addison-Wesley, Cambridge Mass., 1953.

[4] Marcia A. Cooper. Flash diffusivity measurements on pyrotechnics. Sandia National Laboratories Work Authorization Form (WAF) #55-0205B, March 2014.

[5] Corning Company. *Corning® Glass Material Properties: Alkali Barium (Low Lead) 9013*, 2014. http://www.corning.com/WorkArea/showcontent.aspx?id=62891.

[6] Corning Company. *Corning® Glass Material Properties: Borosilicate 7052*, 2014. http://www.corning.com/WorkArea/showcontent.aspx?id=62895.

[7] R.D. Cowan. Propsed method of measuring thermal diffusivity at high temperatures. *Journal of Applied Physics*, 32(7):1363, 1961.

[8] R.D. Cowan. Pulse method of measuring thermal diffusivity at high temperatures. *Journal of Applied Physics*, 34(4):926, 1963.

[9] K. Horai and G. Simmons. Thermal conductivity of rock-forming minerals. *Earth and Planetary Science letters*, 6:359, 1969.

[10] M. W. Chase Jr. *NIST-JANNAF Thermochemical Tables*. American Institute of Physics for the National Institute of Standards and Technology, New York, 4 edition, 1998.

[11] K. Levenberg. A method for the solution of certain nonlinear problems in least squares. *Quarterly of Applied Mathematics*, 2:164, 1944.

[12] D.W. Marquardt. An algorithm for least-squares estimations of nonlinear inequalities. *SIAM: Society for Industrial and Applied Mathematics*, 11(2):431, 1963.

[13] MathWorks. Matlab® help: Fit command. http://www.mathworks.com/help/curvefit/fit.html.

[14] MathWorks. *MATLAB® v2013b*, 2013.

[15] H.A. McKinstry. Thermal expansion of clay minerals. *The American Mineralogist*, 50:212, 1965.

[16] Netzsch. *LFA 447 NanoFlash® Operators Manual*, 2005. Appendix: Technical Data.

[17] Netzsch. *Proteus LFA Analysis Program V 6.0.0*, 2012.

[18] W.J. Parker, R. J. Jenkins, C.P. Butler, and G.L. Abbott. Flash method of determining thermal diffusivity, heat capacity, and thermal conductivity. *Journal of Applied Physics*, 32(9):1679, 1961.

[19] R.A. Robie, B.S. Hemmingway, and W.H. Wilson. The heat capacities of calorimetry conference copper and of muscovite $KAl_2(AlSi_3)O_{10}(OH)_2$, pyrophyllite $Al_2Si_4O_{10}(OH)_2$, and illite $K_3(Al_7Mg)(Si_{14}Al_2))_{40}(OH)_8$ between 15 and 375 k and their standard entropies at 29815 k. *Journal of Research of the U.S. Geological Survey*, 4:631, 1976.

Appendix A

Raw Data for the Titanium Potassium Perchlorate and Titanium Subhydride Potassium Perchlorate Pellets

Figure A.1 through A.4 shows the raw data for the various Ventron TKP-IP densities at 25 °C. Figures A.5, A.6, A.7, and A.8 show the raw data for the 1 mm tall ATK TKP-IP, the 3mm tall ATK TKP-IP, the TKP-OP and THKP pellets at 25 °C, respectively. In Figures A.1, A.2, A.3, A.4, A.6, A.7, and A.8, subfigures (a), (b), and (c) show all the recorded shots for each individual pellet. Subfigure (d) corresponds to a comparison of the average response of each pellet. Since in most instances the shot-to-shot variation is low between pellets, this is assumed an appropriate way to graphically compare each pellet. For Figure A.5, only one pellet was measured. Subfigure (a) corresponds to each recorded shot for that pellet. Subfigure (b) represents the average of all 7 shots.

Figure A.9 show the raw data for Ventron TKP-IP pellet IP-V-1-71-1 at temperature. Subfigures (a), (b), (c), (d), and (e) correspond to 50, 100, 150, 200, and 250 °C, respectively. Figures A.10 similarly present the raw data for Ventron TKP-IP pellet IP-V-1-71-2 at temperature.

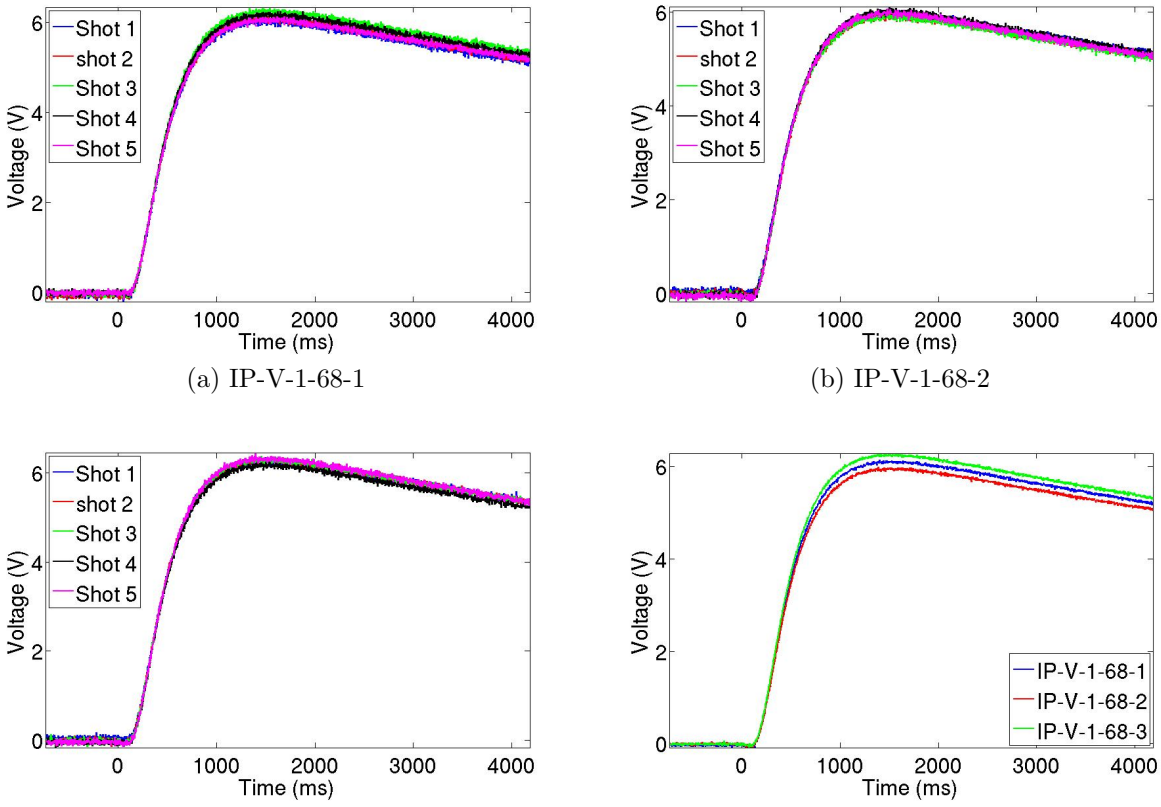

(a) IP-V-1-68-1

(b) IP-V-1-68-2

(c) IP-V-1-68-3

(d) Comparison

Figure A.1: The raw data for all 5 shots for pellets IP-V-1-68-1, IP-V-1-68-2 and IP-V-1-68-3 at 25 °C are shown in (a), (b), and (c), respectively. A comparison of each pellet using the average response obtained from the 5 shots is shown in (d).

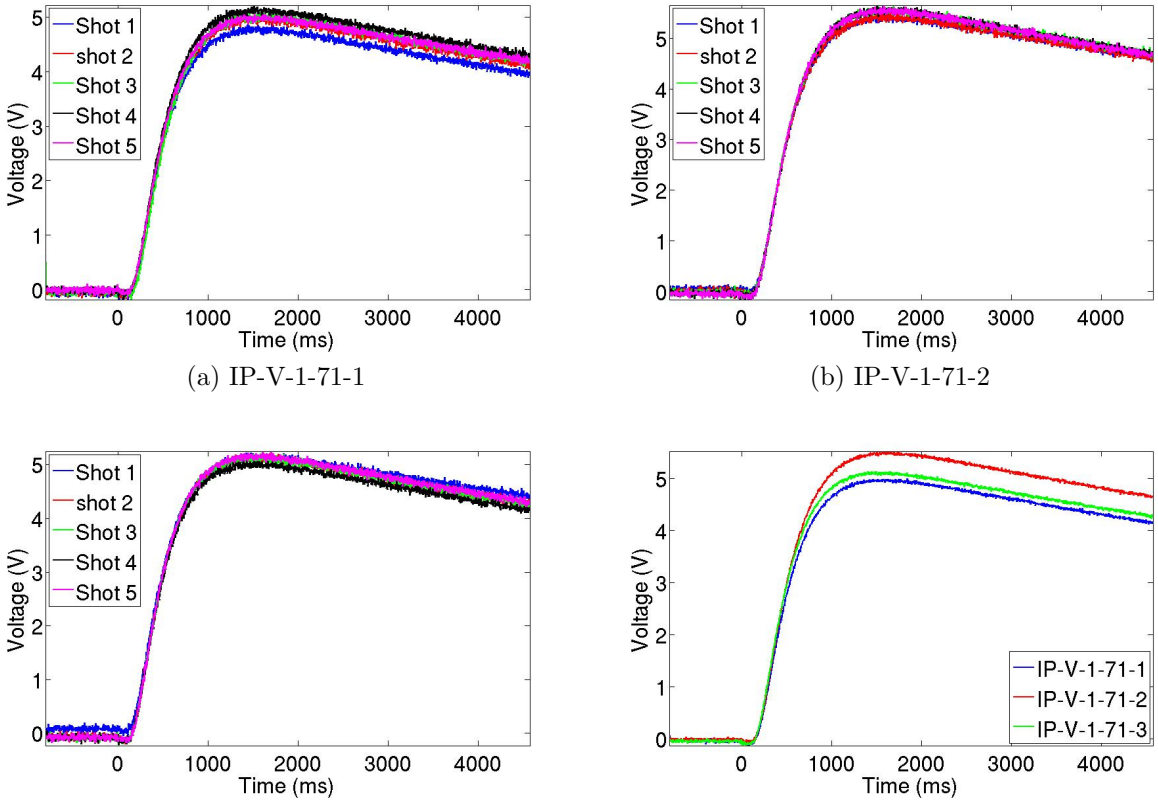

(a) IP-V-1-71-1 (b) IP-V-1-71-2

(c) IP-V-1-71-3 (d) Comparison

Figure A.2: The raw data for all 5 shots for pellets IP-V-1-71-1, IP-V-1-71-2 and IP-V-1-71-3 at 25 °C are shown in (a), (b), and (c), respectively. A comparison of each pellet using the average response obtained from the 5 shots is shown in (d).

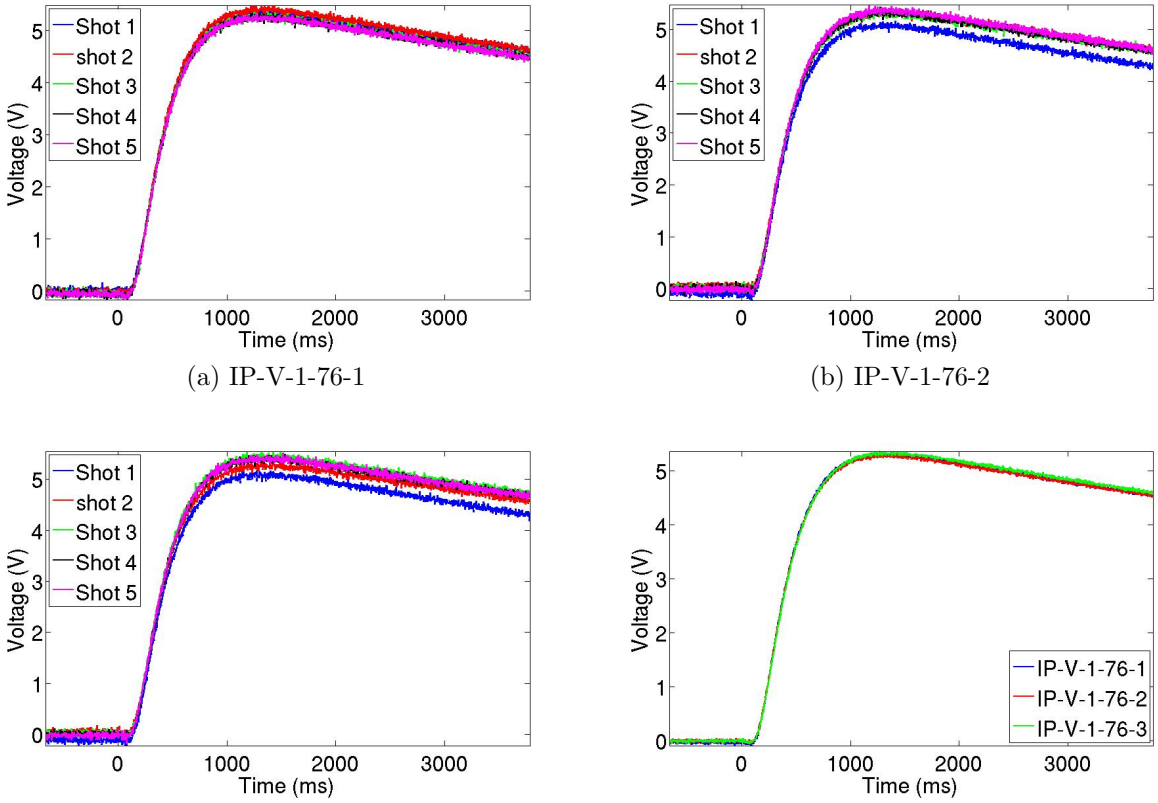

(a) IP-V-1-76-1

(b) IP-V-1-76-2

(c) IP-V-1-76-3

(d) Comparison

Figure A.3: The raw data for all 5 shots for pellets IP-V-1-76-1, IP-V-1-76-2 and IP-V-1-76-3 at 25 °C are shown in (a), (b), and (c), respectively. A comparison of each pellet using the average response obtained from the 5 shots is shown in (d).

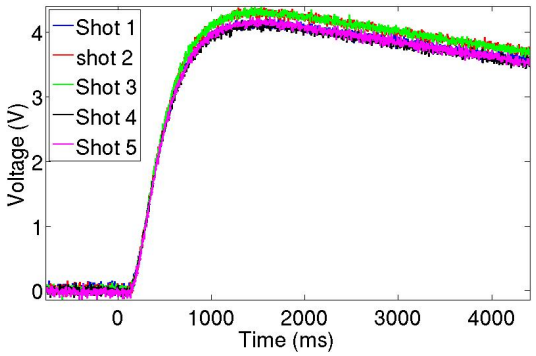

(a) IP-V-1-79-1

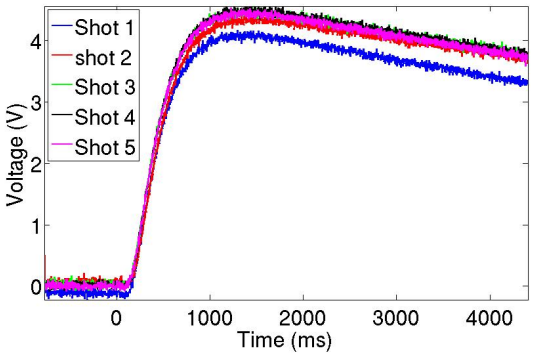

(b) IP-V-1-79-2

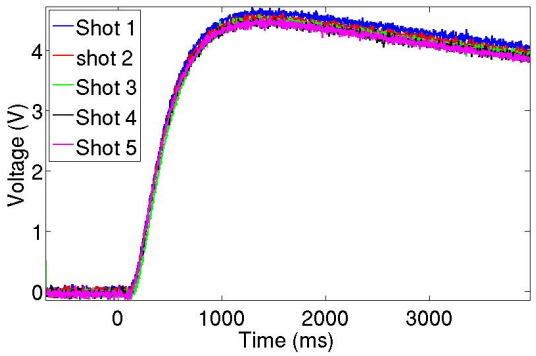

(c) IP-V-1-79-3

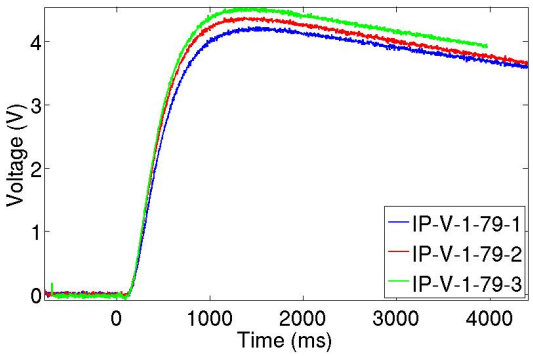

(d) Comparison

Figure A.4: The raw data for all 5 shots for pellets IP-V-1-79-1, IP-V-1-79-2 and IP-V-1-79-3 at 25 °C are shown in (a), (b), and (c), respectively. A comparison of each pellet using the average response obtained from the 5 shots is shown in (d).

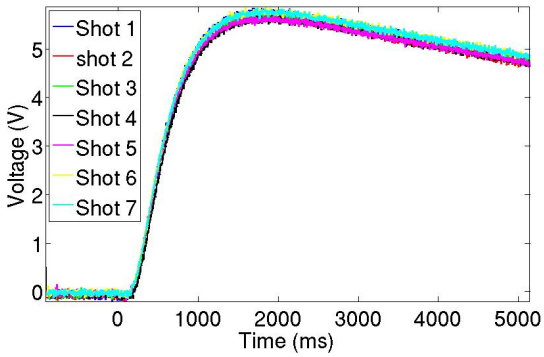

(a) IP-A-1-71-1

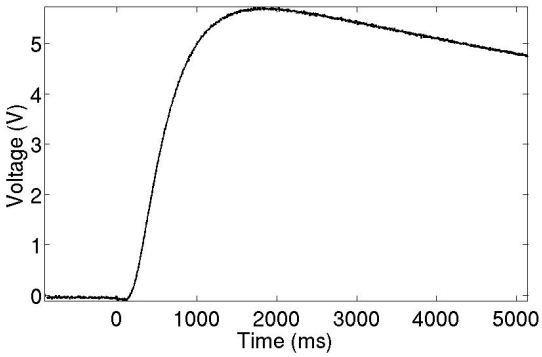

(b) Average

Figure A.5: The raw data for all 7 shots at 25 °C are shown in (a), while the average response of the pellet is given in (b).

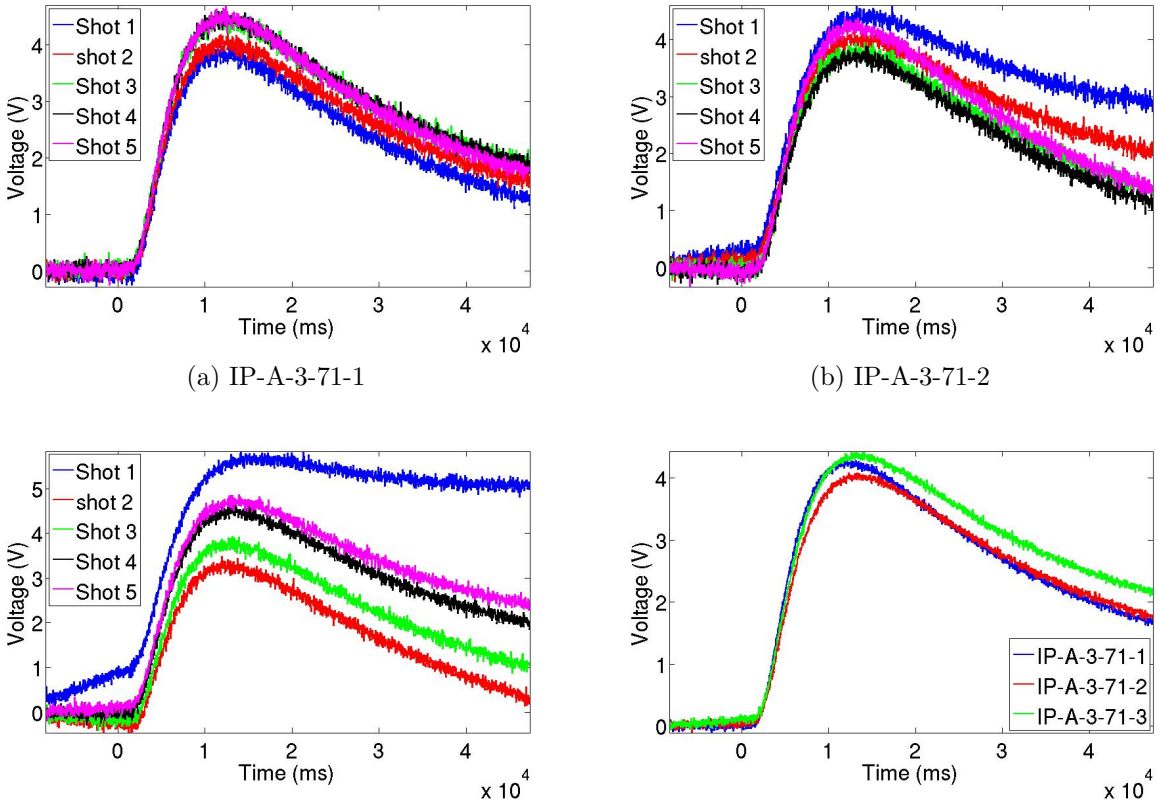

(a) IP-A-3-71-1

(b) IP-A-3-71-2

(c) IP-A-3-71-3

(d) Comparison

Figure A.6: The raw data for all 5 shots for pellets IP-A-3-71-1, IP-A-3-71-2, and IP-A-3-71-3 at 25 °C are shown in (a), (b), and (c), respectively. A comparison of each pellet using the average response obtained from the 5 shots is shown in (d).

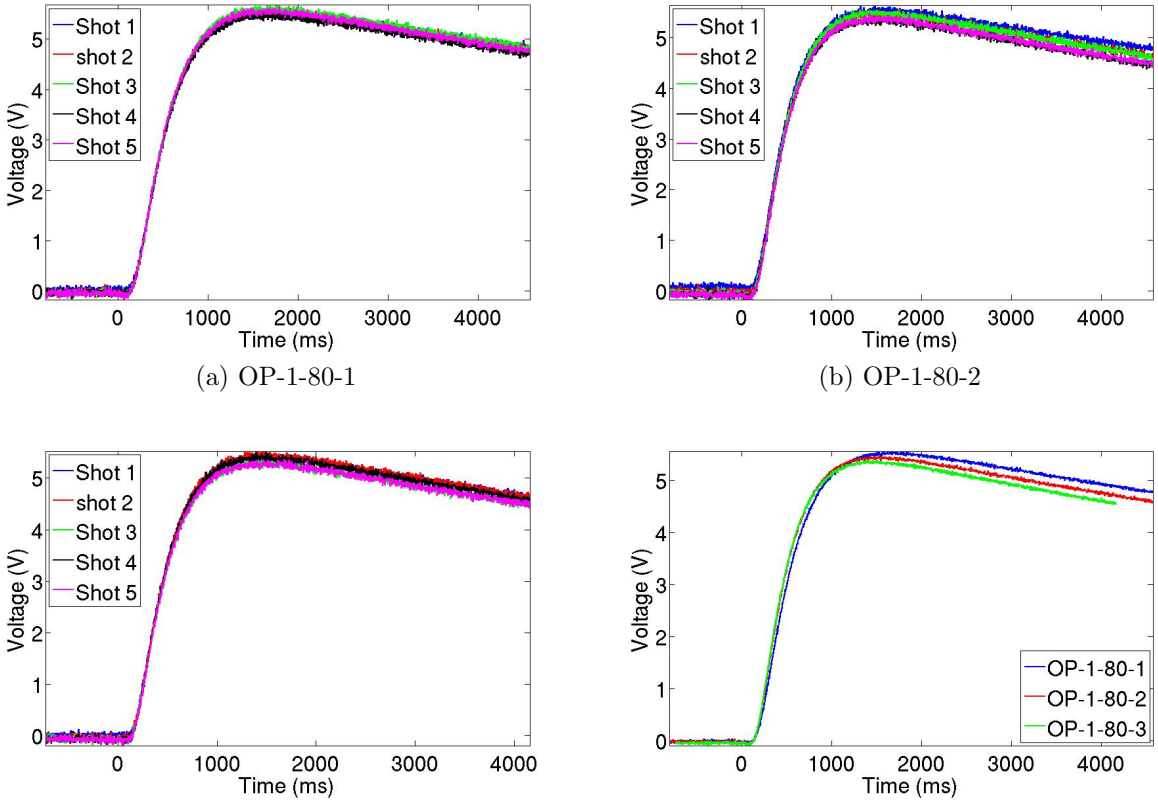

(a) OP-1-80-1 (b) OP-1-80-2

(c) OP-1-80-3 (d) Comparison

Figure A.7: The raw data for all 5 shots for pellets OP-1-80-1, OP-1-80-2 and OP-1-80-3 at 25 °C are shown in (a), (b), and (c), respectively. A comparison of each pellet using the average response obtained from the 5 shots is shown in (d).

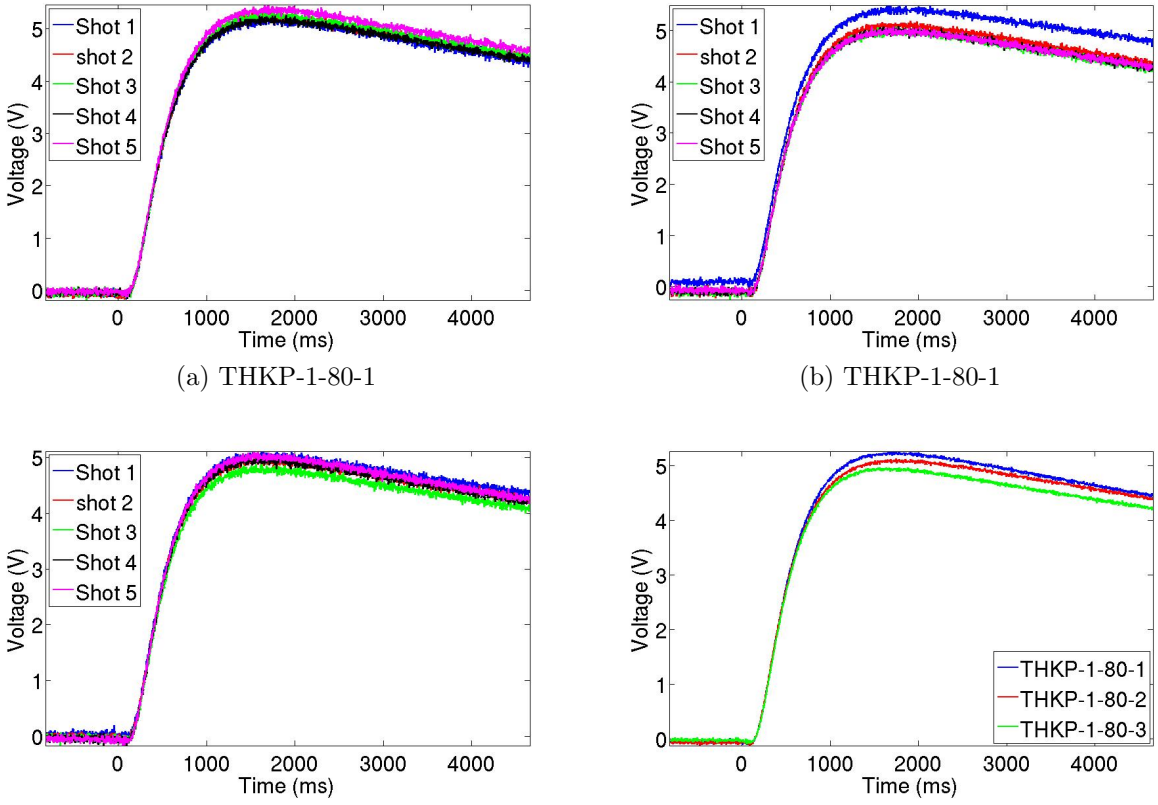

(a) THKP-1-80-1

(b) THKP-1-80-1

(c) THKP-1-80-1

(d) Comparison

Figure A.8: The raw data for all 5 shots for pellets THKP-1-80-1, THKP-1-80-2 and THKP-1-80-3 at 25 °C are shown in (a), (b), and (c), respectively. A comparison of each pellet using the average response obtained from the 5 shots is shown in (d).

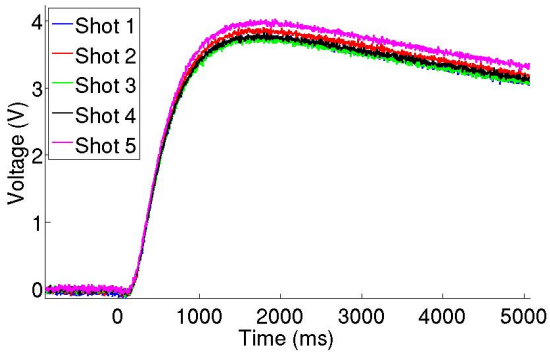

(a) 50 °C

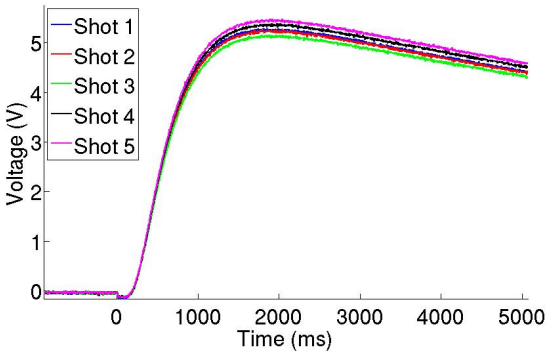

(b) 100 °C

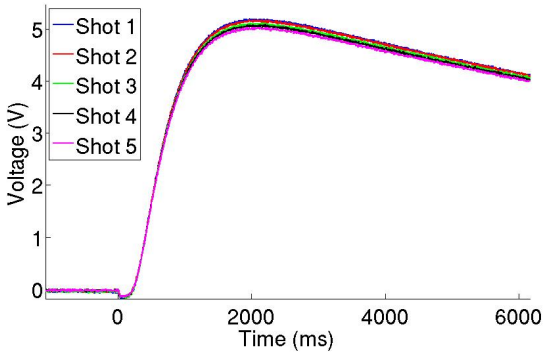

(c) 150 °C

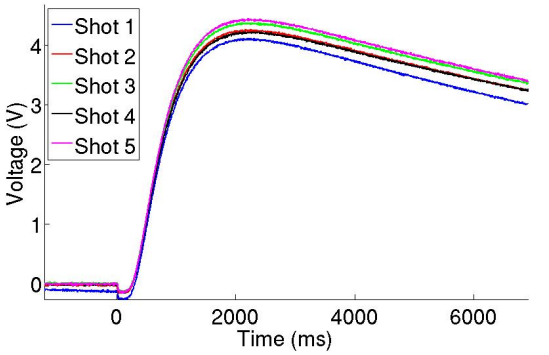

(d) 200 °C

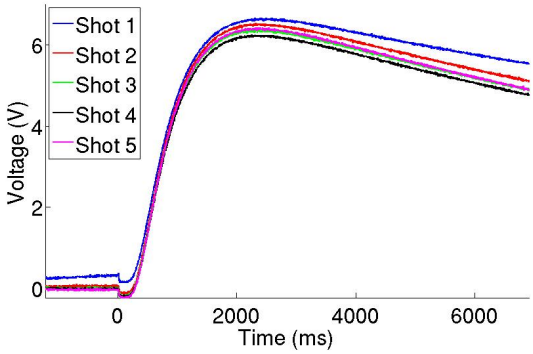

(e) 250 °C

Figure A.9: The raw data for all 5 shots for pellets IP-V-1-71-1 at 50 (a), 100 (b), 150 (c), 200 (d), and 250 °C (e), respectively.

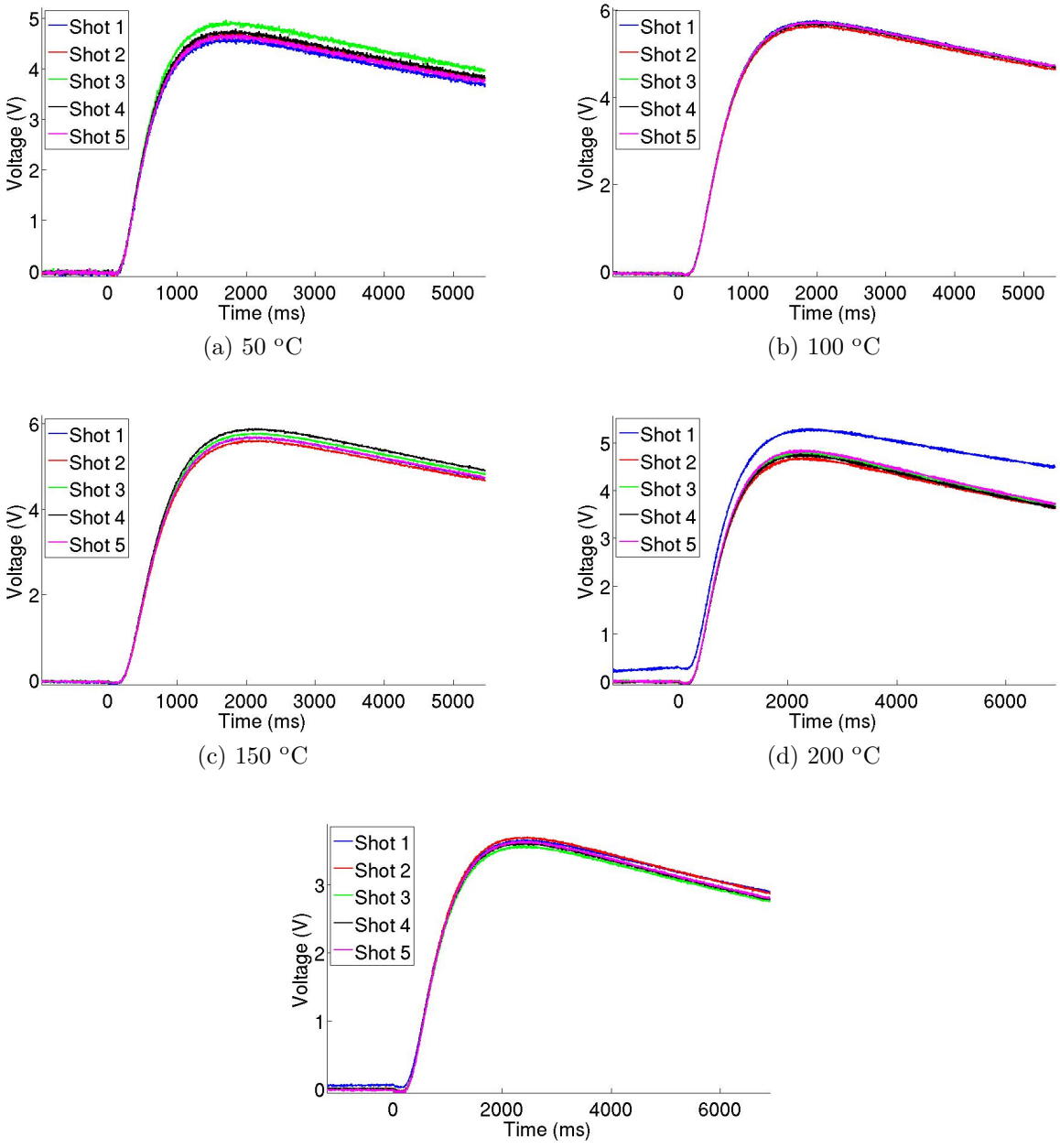

(a) 50 °C

(b) 100 °C

(c) 150 °C

(d) 200 °C

(e) 250 °C

Figure A.10: The raw data for all 5 shots for pellets IP-V-1-71-2 at 50 (a), 100 (b), 150 (c), 200 (d), and 250 °C (e), respectively.

Appendix B

Raw Data for 9013 Glass Samples

Figures B.1 and B.2 shows the results for the 1 mm 9013 glass samples (9013-1). In Figure B.1, subfigures (a), (b), (c), and (d) correspond to 25, 50, 100, and 150 °C, respectively. In Figure B.2, subfigures (a), (b), and (c) correspond to 200, 250, and 300 °C, respectively. Similarly, Figures B.3 and B.4 shows the results for the 2 mm 9013 glass samples (9013-2).

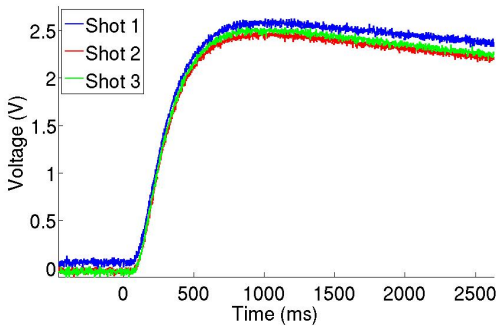

(a) 25 °C

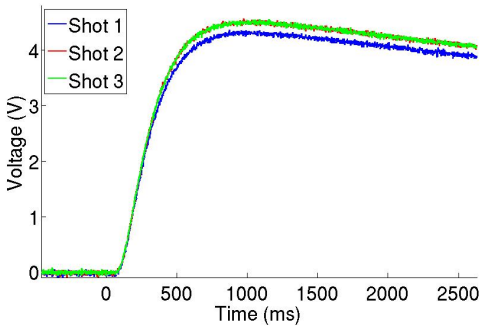

(b) 50 °C

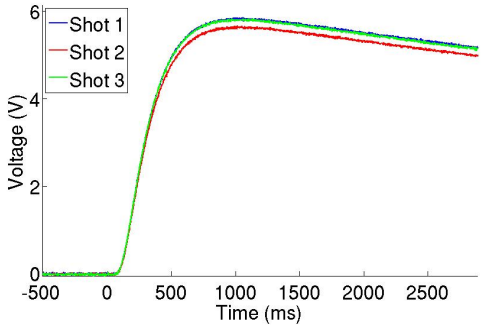

(c) 100 °C

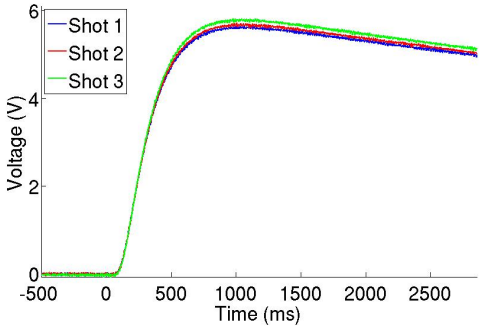

(d) 150 °C

Figure B.1: The raw data for sample 9013-1 at 25, 50, 100, and 150 °C are shown in (a), (b), (c), and (d), respectively.

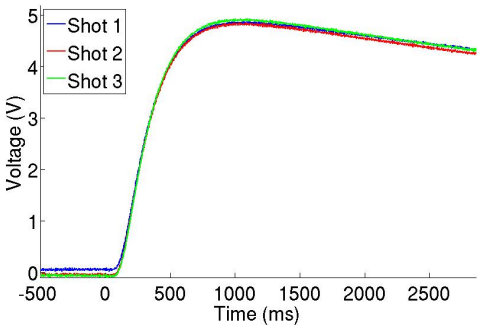

(a) 200 °C

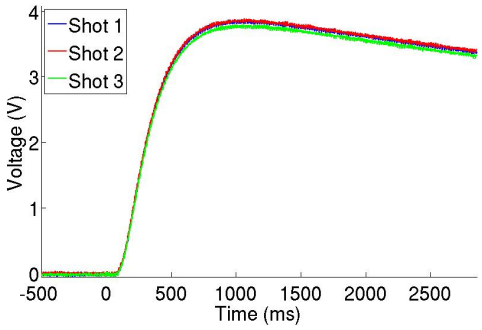

(b) 250 °C

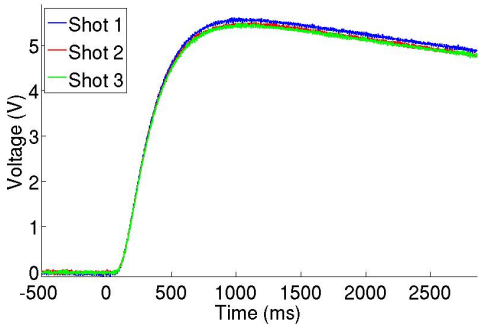

(c) 300 °C

Figure B.2: The raw data for sample 9013-1 at 200, 250, and 300 °C are shown in (a), (b), and (c), respectively.

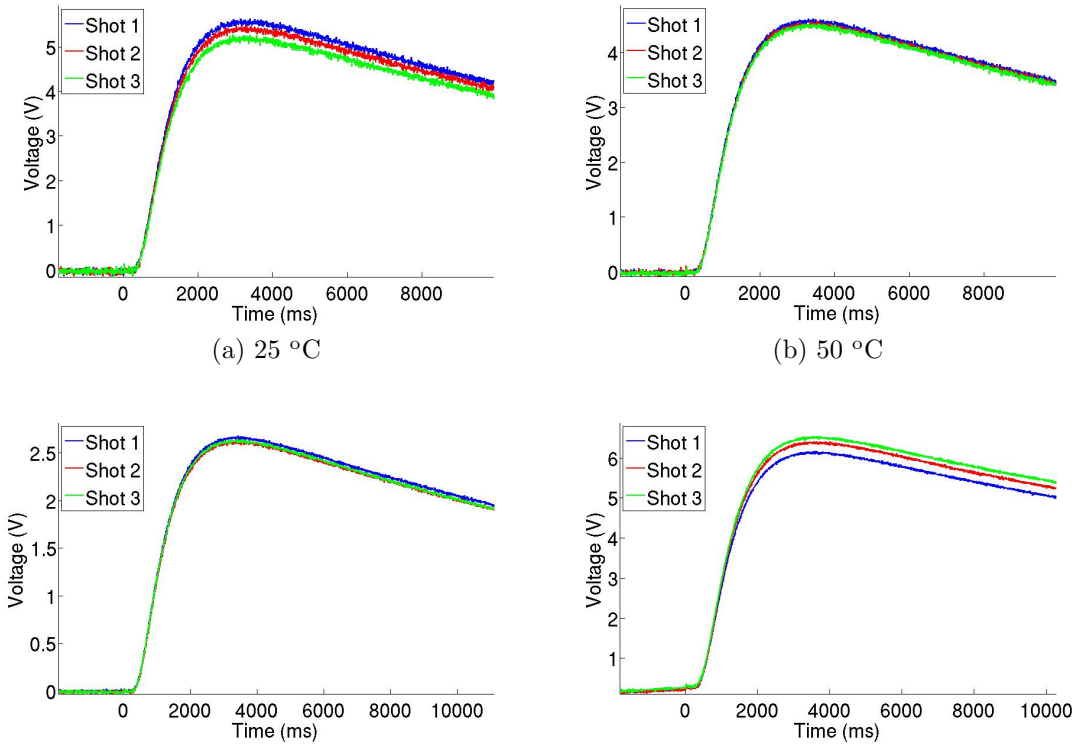

(a) 25 °C (b) 50 °C

(c) 100 °C (d) 150 °C

Figure B.3: The raw data for sample 9013-2 at 25, 50, 100, and 150 °C are shown in (a), (b), (c), and (d), respectively.

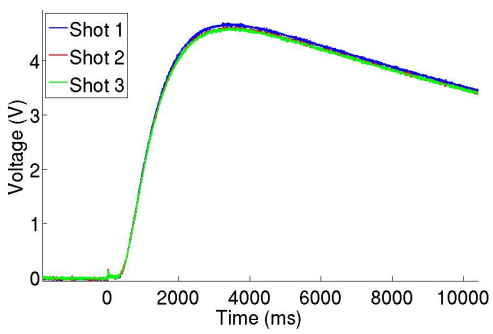

(a) 200 °C

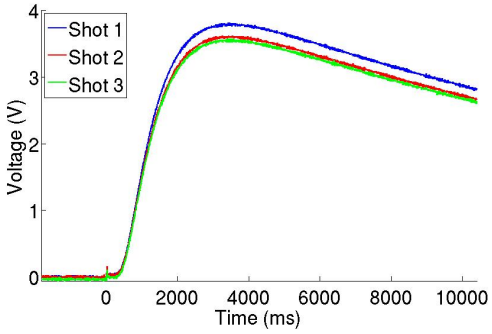

(b) 250 °C

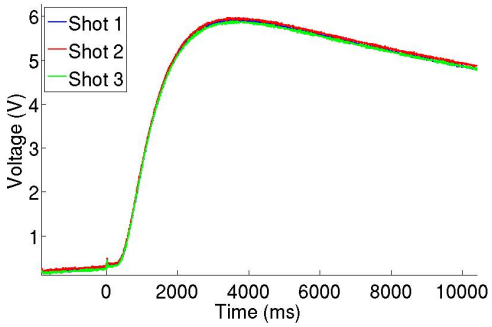

(c) 300 °C

Figure B.4: The raw data for sample 9013-2 at 200, 250, and 300 °C are shown in (a), (b), and (c), respectively.

Appendix C

Raw Data for 7052 Glass Samples

Figures C.1 and C.2 shows the results for the the first 1 mm 7052 glass samples (7052-1-1). In Figure C.1, subfigures (a), (b), (c), and (d) correspond to 25, 50, 100, and 150 °C, respectively. In Figure C.2, subfigures (a), (b), and (c) correspond to 200, 250, and 300 0°C, respectively. A similar pattern holds for Figures C.3 and C.4, Figures C.5 and C.6, and Figures C.7 and C.8, which correspond to sample 7052-1-2, 7052-3-1, and 7052-3-2, respectively.

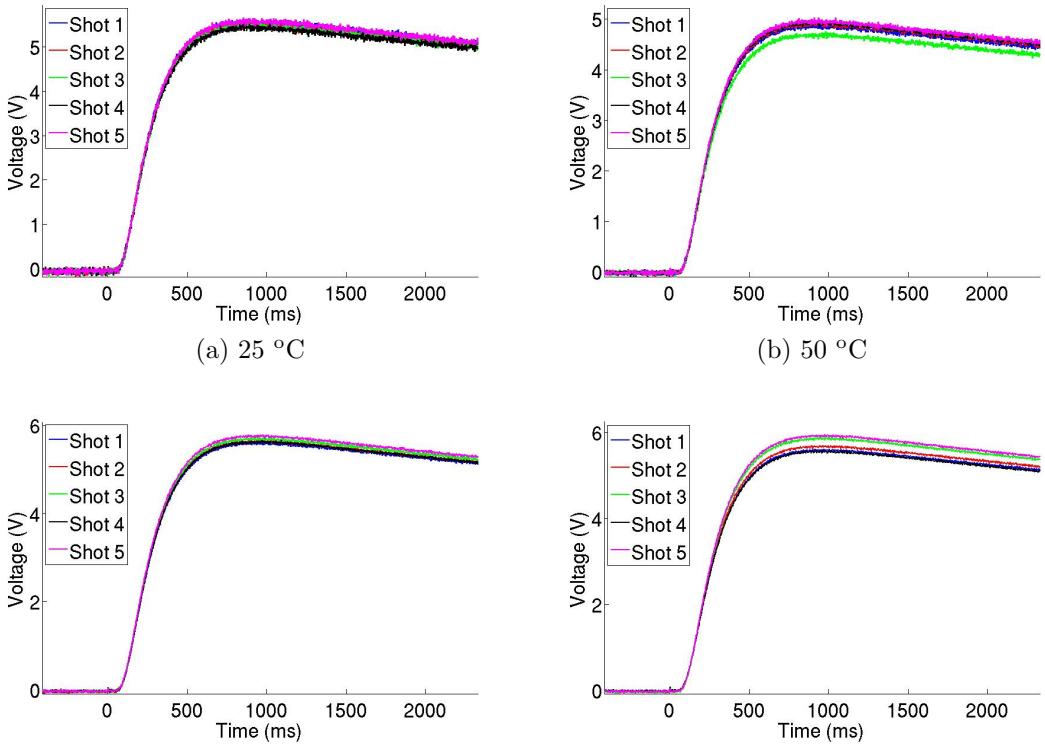

(a) 25 °C (b) 50 °C

(c) 100 °C (d) 150 °C

Figure C.1: The raw data for sample 7052-1-1 at 25, 50, 100, and 150 °C are shown in (a), (b), (c), and (d), respectively.

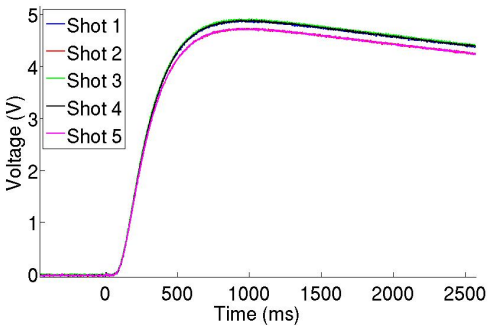

(a) 200 °C

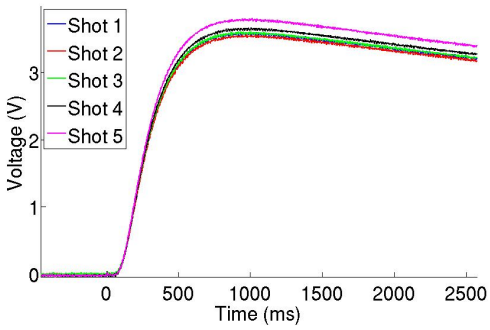

(b) 250 °C

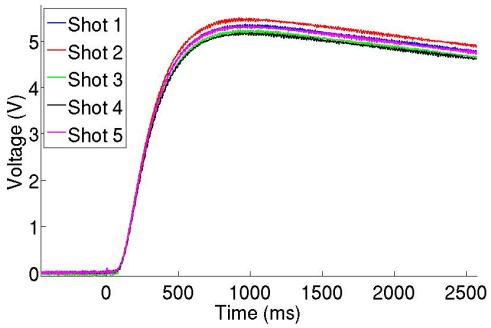

(c) 300 °C

Figure C.2: The raw data for sample 7052-1-1 at 200, 250, and 300 °C are shown in (a), (b), and (c), respectively.

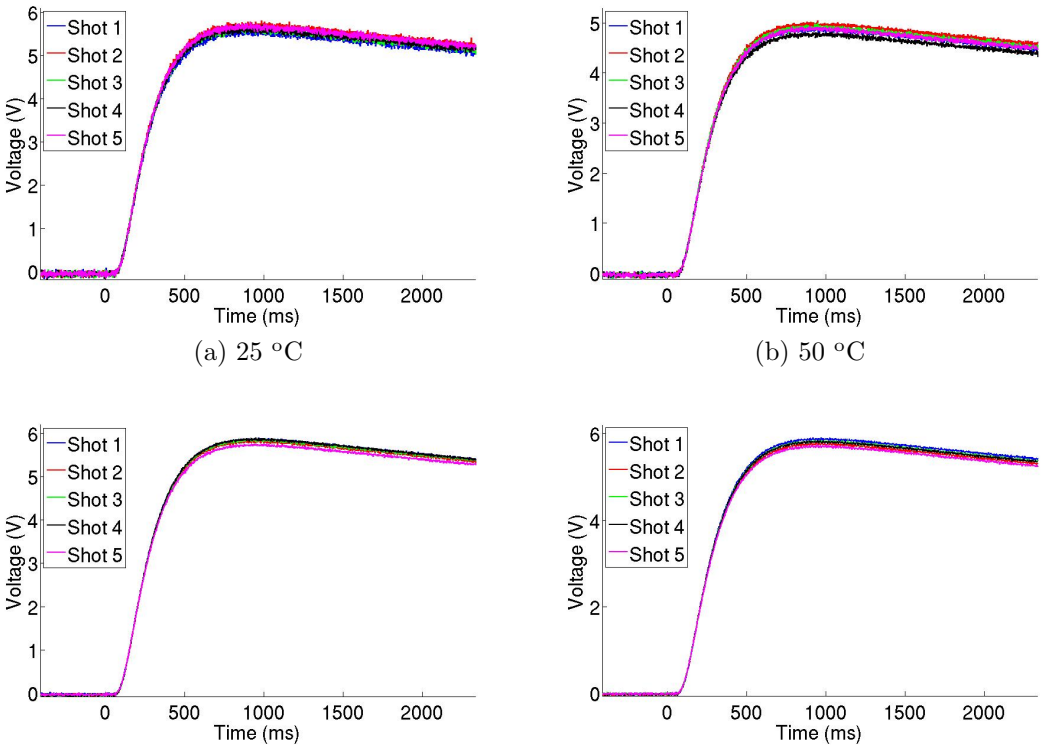

(a) 25 °C (b) 50 °C

(c) 100 °C (d) 150 °C

Figure C.3: The raw data for sample 7052-1-2 at 25, 50, 100, and 150 °C are shown in (a), (b), (c), and (d), respectively.

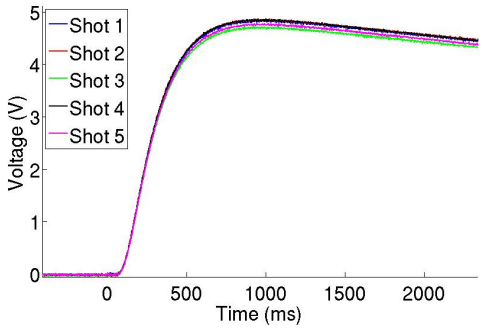

(a) 200 °C

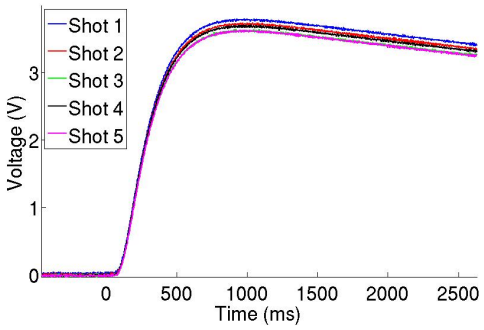

(b) 250 °C

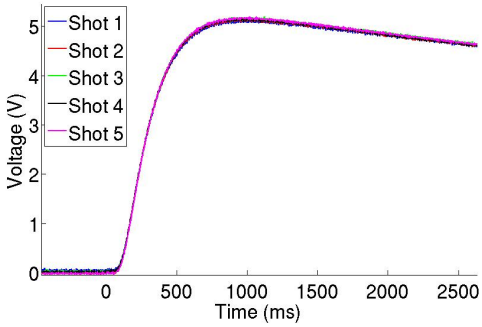

(c) 300 °C

Figure C.4: The raw data for sample 7052-1-2 at 200, 250, and 300 °C are shown in (a), (b), and (c), respectively.

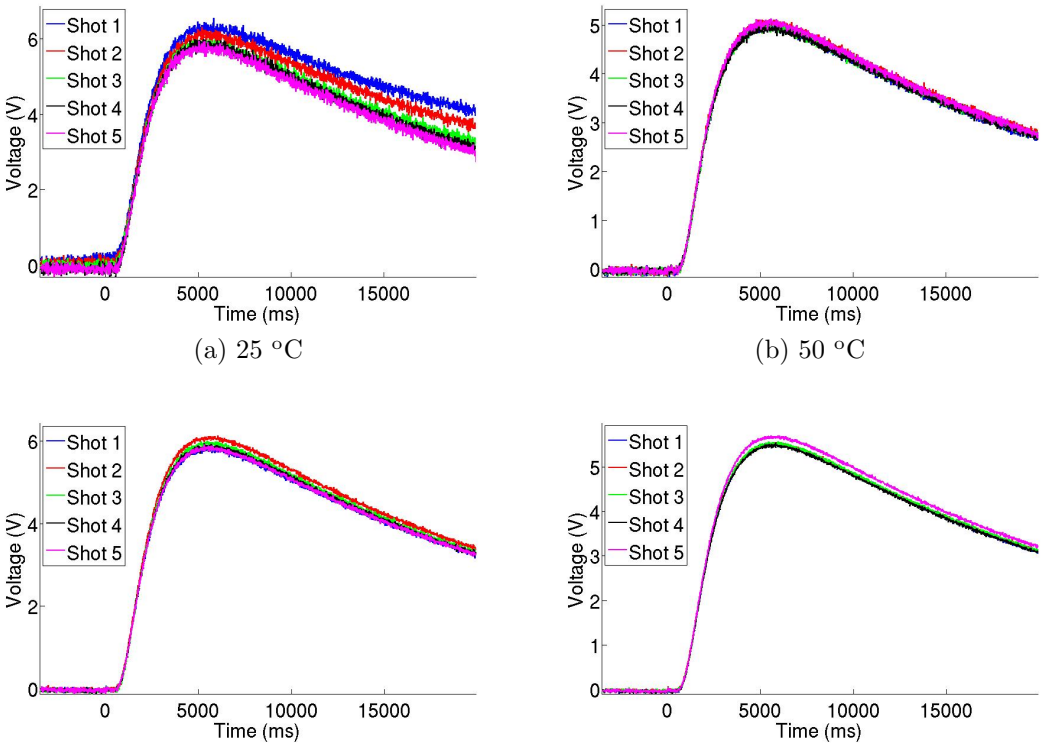

(a) 25 °C (b) 50 °C

(c) 100 °C (d) 150 °C

Figure C.5: The raw data for sample 7052-3-1 at 25, 50, 100, and 150 °C are shown in (a), (b), (c), and (d), respectively.

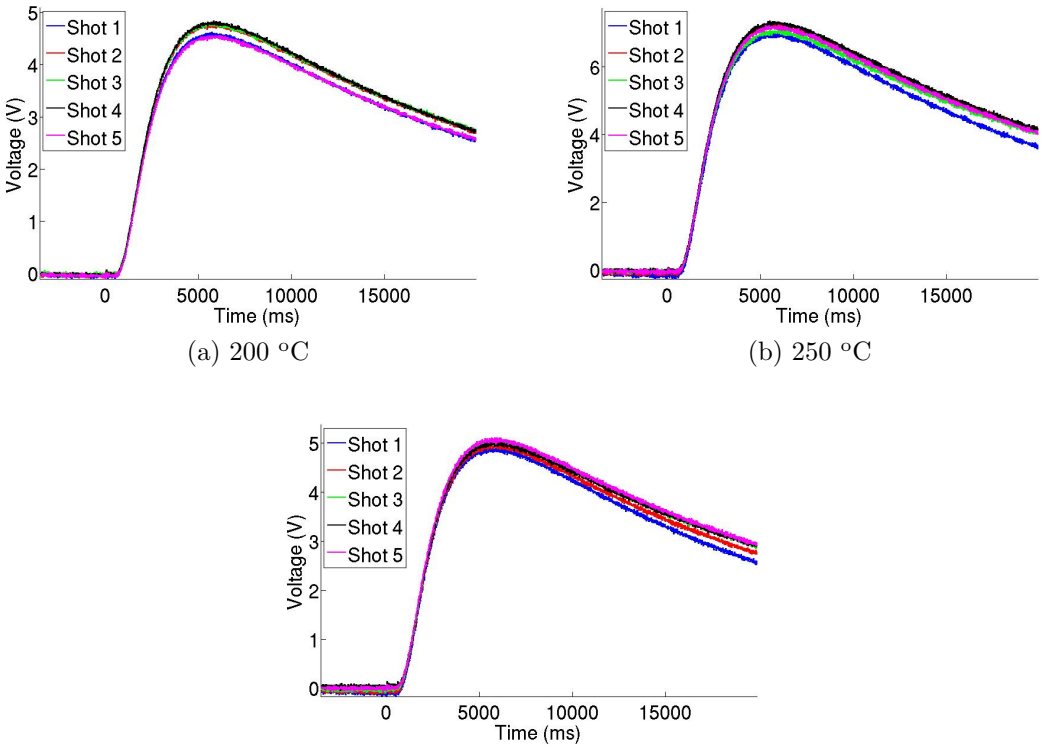

(a) 200 °C

(b) 250 °C

(c) 300 °C

Figure C.6: The raw data for sample 7052-3-1 at 200, 250, and 300 °C are shown in (a), (b), and (c), respectively.

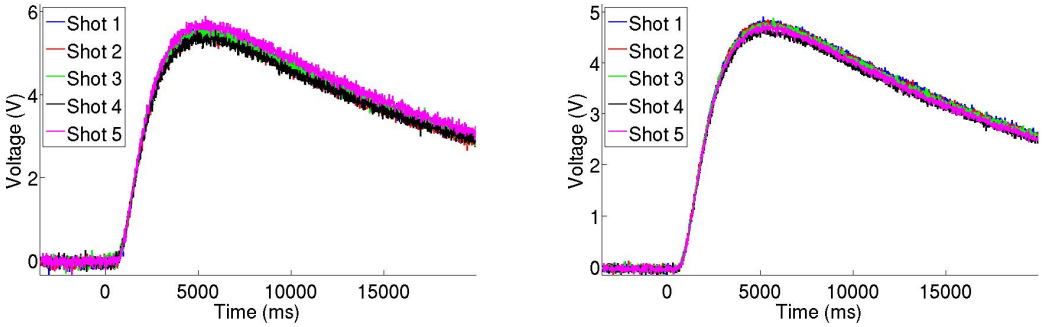

(a) 25 °C

(b) 50 °C

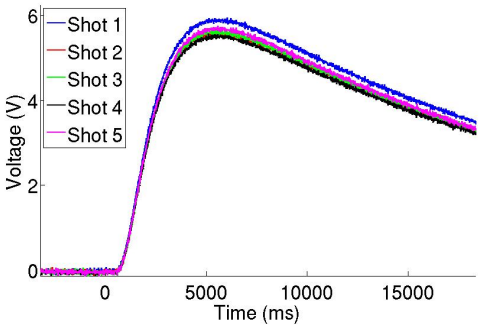

(c) 100 °C

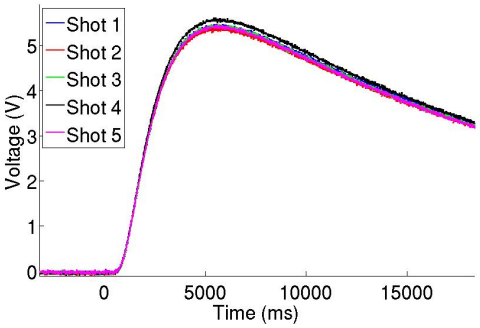

(d) 150 °C

Figure C.7: The raw data for sample 7052-3-2 at 25, 50, 100, and 150 °C are shown in (a), (b), (c), and (d), respectively.

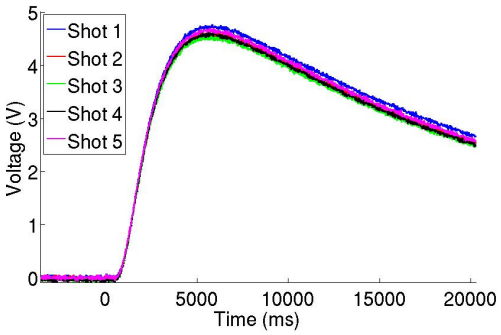

(a) 200 °C

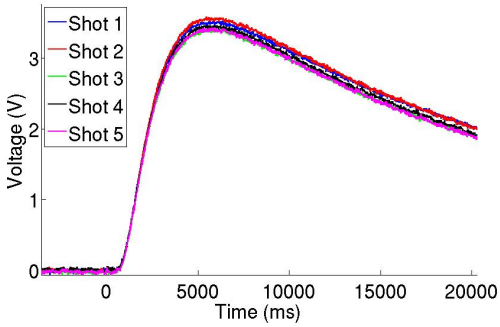

(b) 250 °C

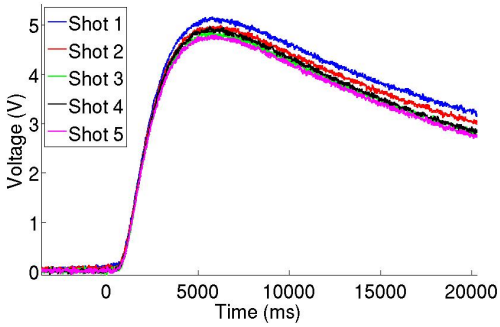

(c) 300 °C

Figure C.8: The raw data for sample 7052-3-2 at 200, 250, and 300 °C are shown in (a), (b), and (c), respectively.

Appendix D

Raw Data for SB-14 Glass Samples

Figures D.1 and D.2 shows the results for the the first 1 mm SB glass samples (SB-1-1). In Figure D.1, subfigures (a), (b), (c), and (d) correspond to 25, 50, 100, and 150 °C, respectively. In Figure D.2, subfigures (a), (b), and (c) correspond to 200, 250, and 300 0°C, respectively. A similar pattern holds for Figures D.3 and D.4, Figures D.5 and D.6, and Figures D.7 and D.8, which correspond to sample SB-1-2, SB-2-1, and SB-2-2, respectively.

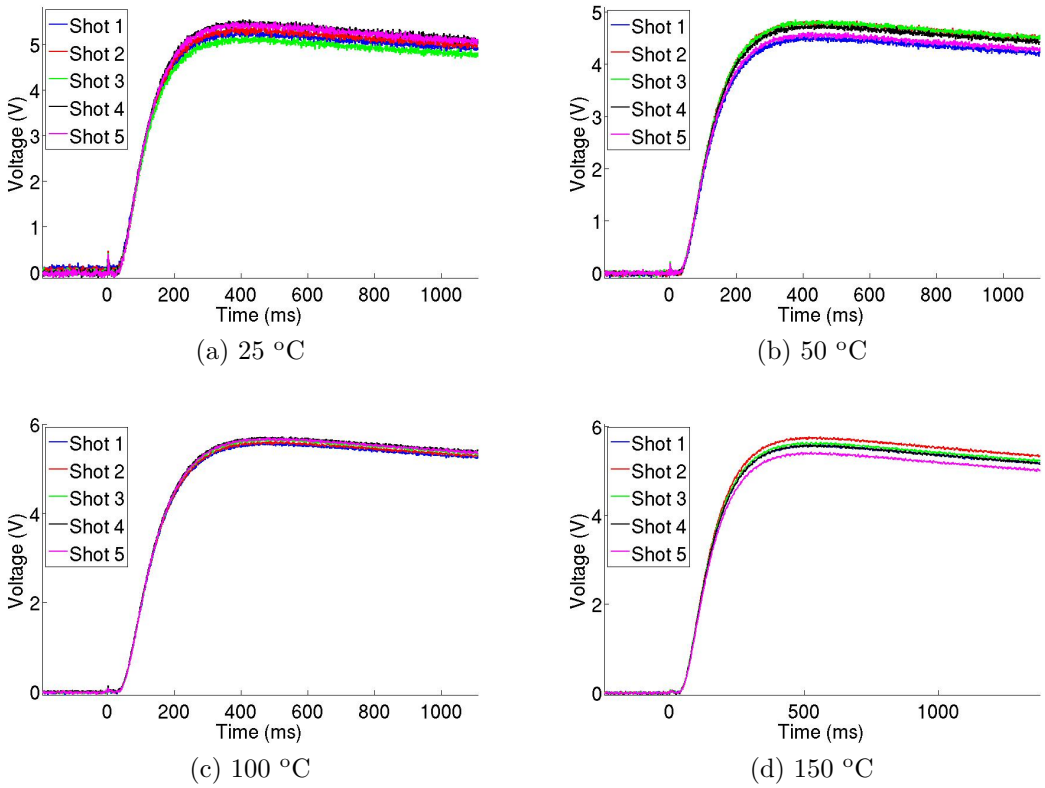

(a) 25 °C (b) 50 °C

(c) 100 °C (d) 150 °C

Figure D.1: The raw data for sample SB-1-1 at 25, 50, 100, and 150 °C are shown in (a), (b), (c), and (d), respectively.

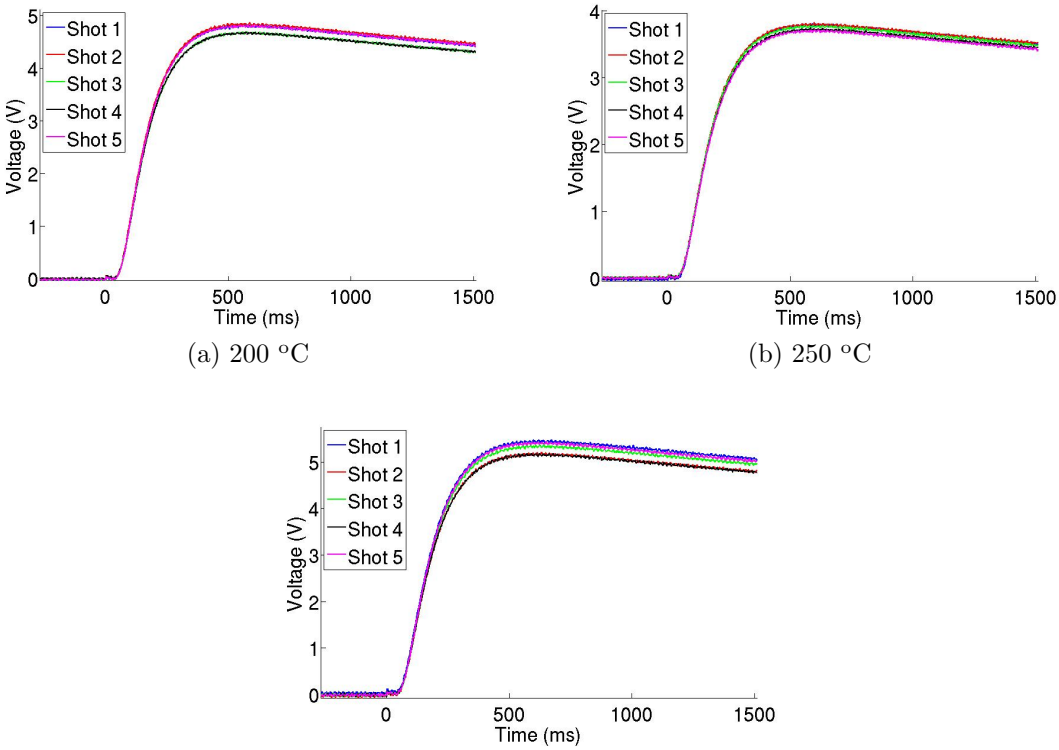

(a) 200 °C

(b) 250 °C

(c) 300 °C

Figure D.2: The raw data for sample SB-1-1 at 200, 250, and 300 °C are shown in (a), (b), and (c), respectively.

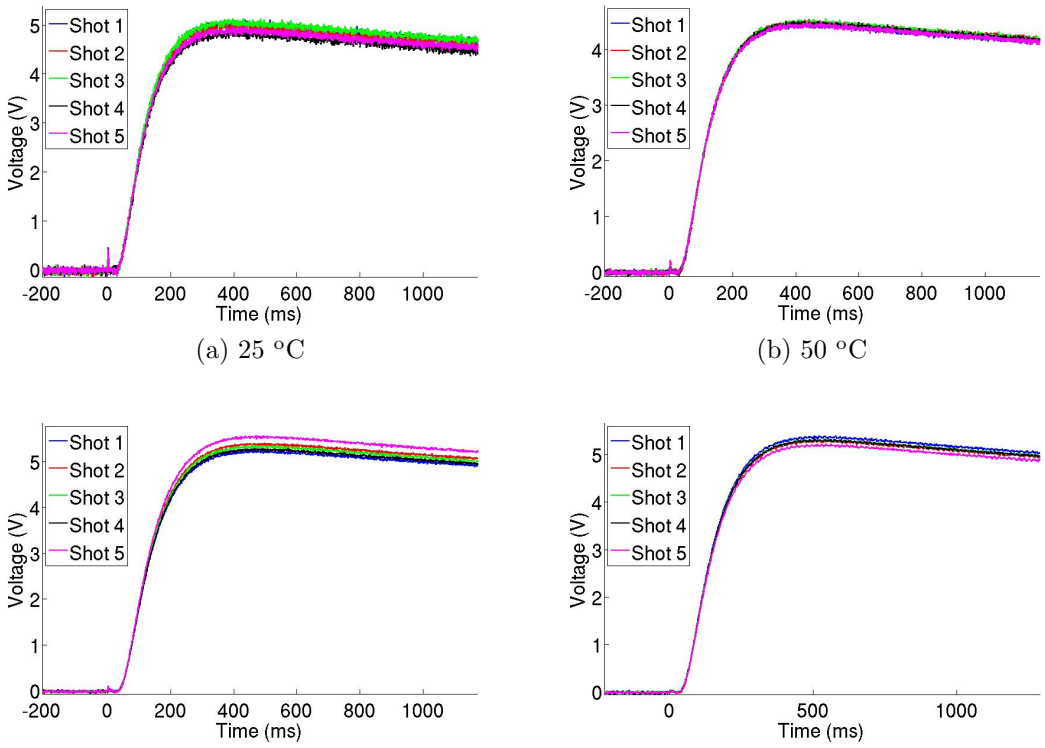

(a) 25 °C (b) 50 °C

(c) 100 °C (d) 150 °C

Figure D.3: The raw data for sample SB-1-2 at 25, 50, 100, and 150 °C are shown in (a), (b), (c), and (d), respectively.

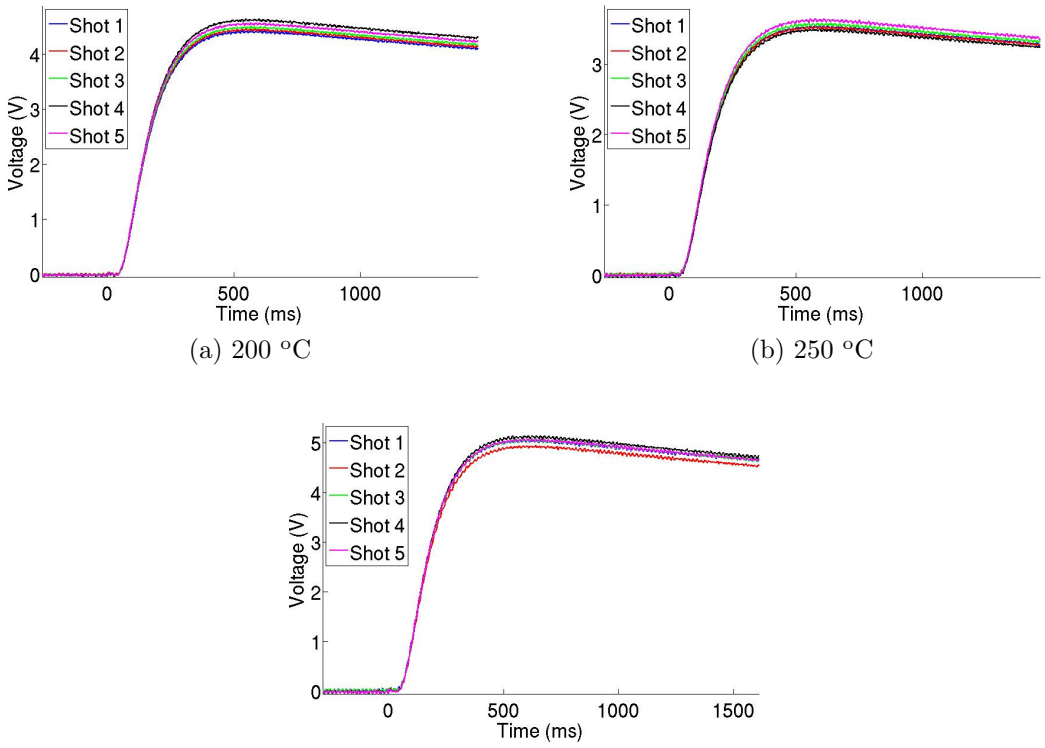

(a) 200 °C

(b) 250 °C

(c) 300 °C

Figure D.4: The raw data for sample SB-1-2 at 200, 250, and 300 °C are shown in (a), (b), and (c), respectively.

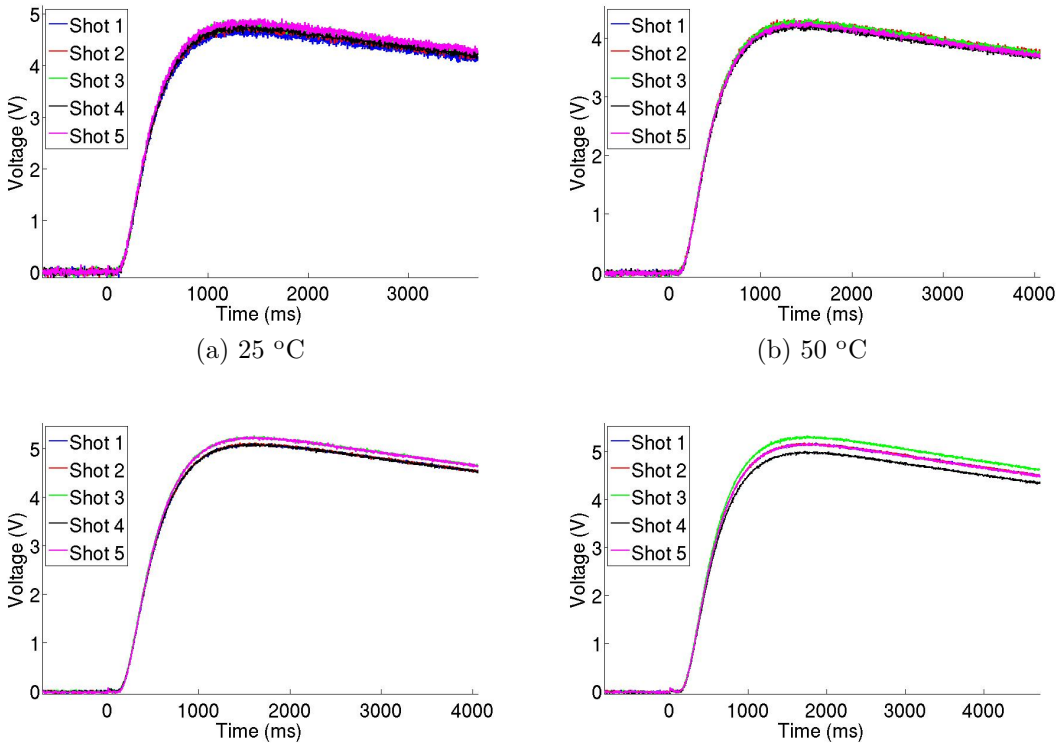

(a) 25 °C (b) 50 °C

(c) 100 °C (d) 150 °C

Figure D.5: The raw data for sample SB-2-1 at 25, 50, 100, and 150 °C are shown in (a), (b), (c), and (d), respectively.

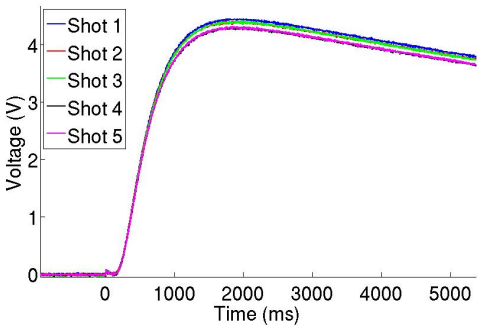

(a) 200 °C

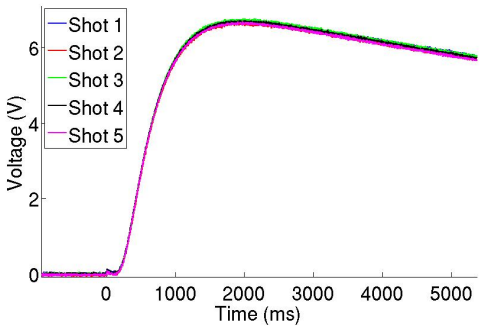

(b) 250 °C

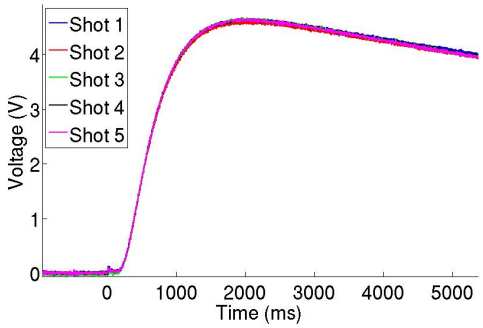

(c) 300 °C

Figure D.6: The raw data for sample SB-2-1 at 200, 250, and 300 °C are shown in (a), (b), and (c), respectively.

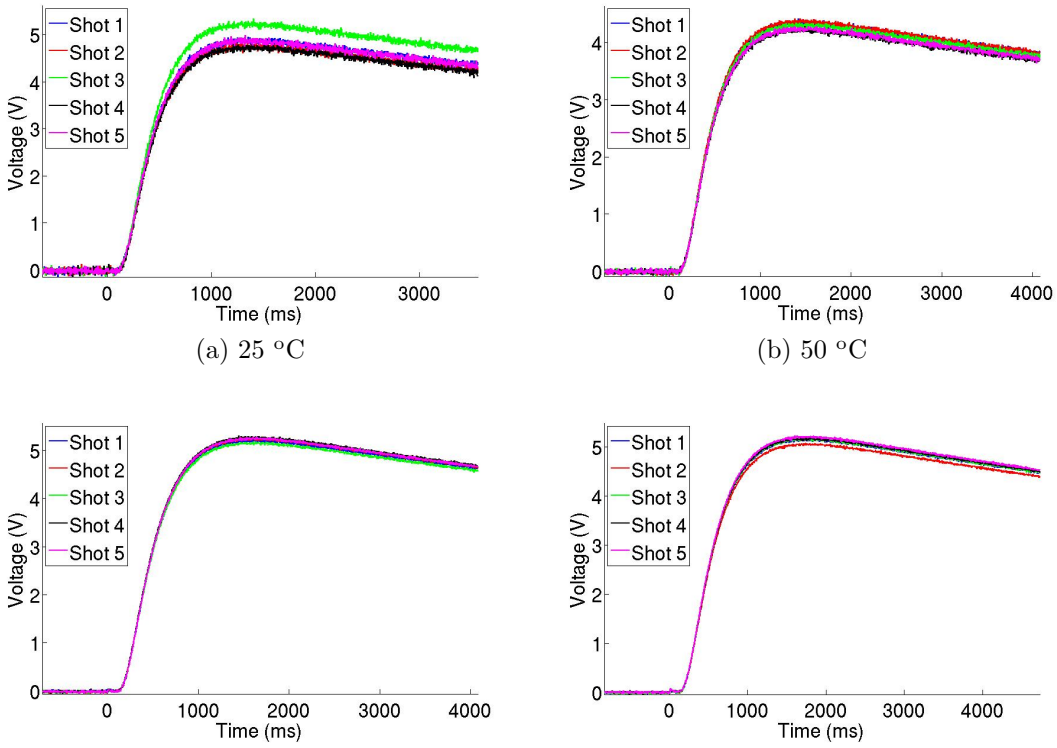

(a) 25 °C (b) 50 °C

(c) 100 °C (d) 150 °C

Figure D.7: The raw data for sample SB-2-2 at 25, 50, 100, and 150 °C are shown in (a), (b), (c), and (d), respectively.

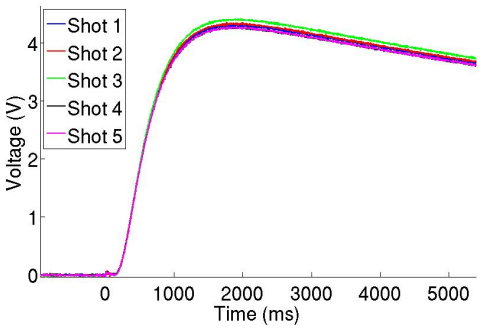

(a) 200 °C

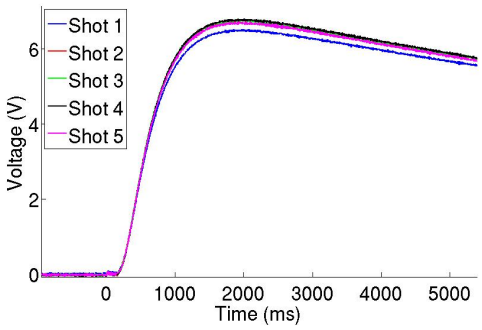

(b) 250 °C

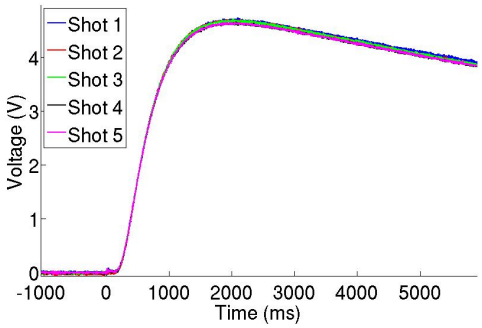

(c) 300 °C

Figure D.8: The raw data for sample SB-2-2 at 200, 250, and 300 °C are shown in (a), (b), and (c), respectively.

Appendix E

Raw Data for the C-4000 Muscovite Mica Sample

Figure E.1 and E.2 show the raw data for the C-4000 Muscovite Mica sample. In Figure E.1, subfigures (a), (b), (c), and (d) correspond to the raw data at 25, 50, 100, and 150 °C, respectively. Figure E.2, subfigures (a), (b), and (c) correspond to the raw data at 200, 250, and 300 °C, respectively.

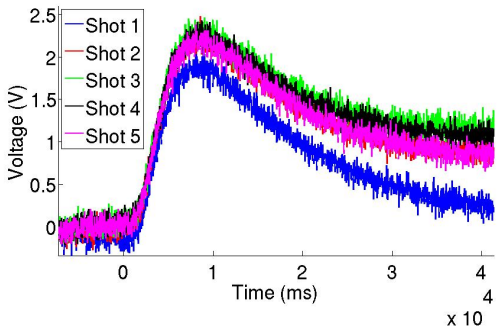

(a) 25 °C

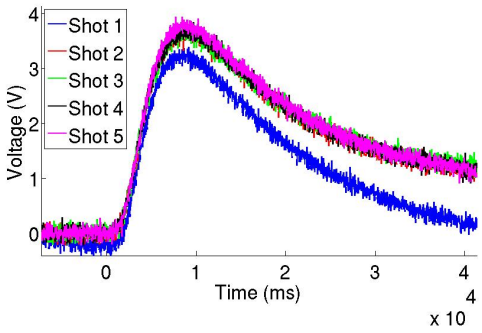

(b) 50 °C

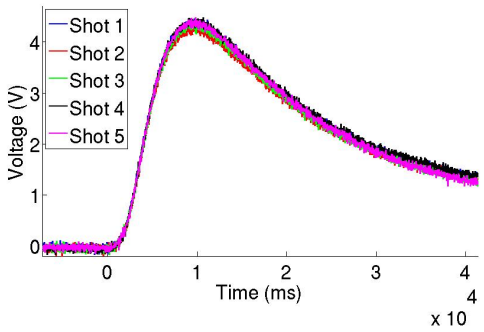

(c) 100 °C

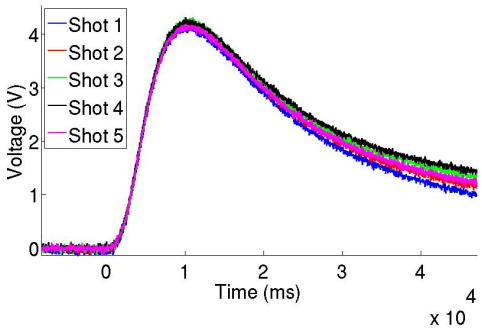

(d) 150 °C

Figure E.1: The raw data for the Mica sample at 25, 50, 100, and 150 °C are shown in (a), (b), (c), and (d), respectively.

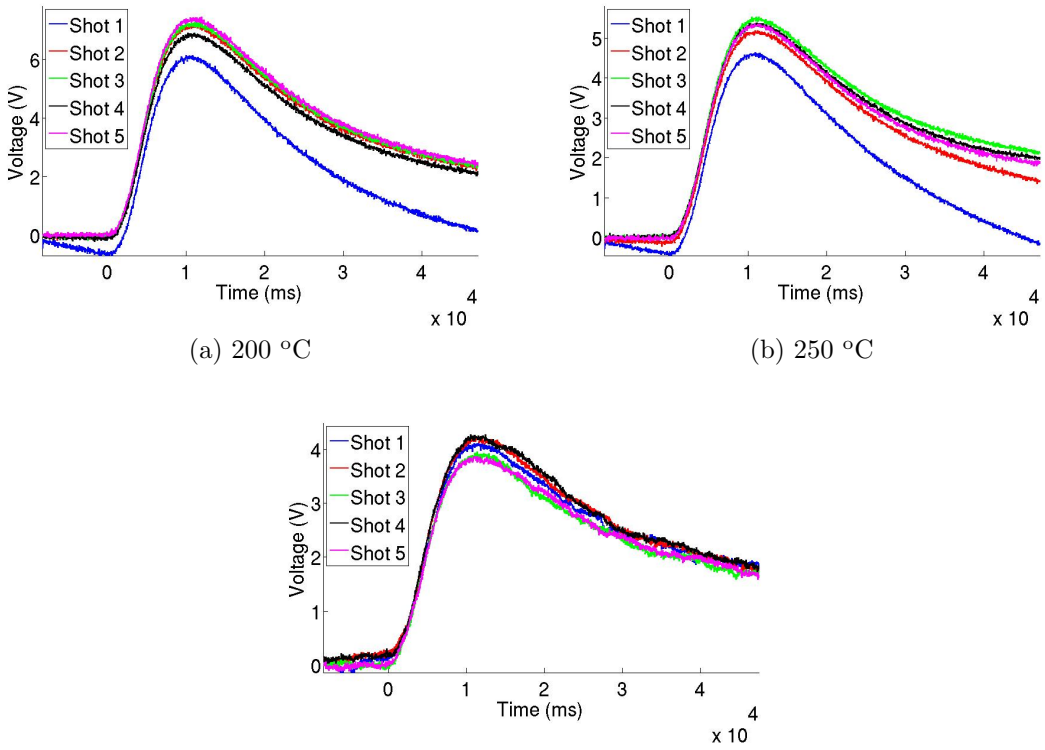

(a) 200 °C

(b) 250 °C

(c) 300 °C

Figure E.2: The raw data for the Mica sample at 200, 250, and 300 °C are shown in (a), (b), and (c), respectively.

DISTRIBUTION:

1	MS 0346	Leslie M. Phinney, Org. 1512
1	MS 0828	Anthony S. Geller, Org. 1516
1	MS 0836	William W. Erikson, Org. 1516
1	MS 0836	Jermey B. Lechman, Org. 1516
1	MS 1314	Dan Bolintineanu, Org. 1516
1	MS 1452	Nathan M. Glenn, Org. 2553
1	MS 1452	Gregory Noel, Org. 2553
1	MS 1452	Joseph D. Olles, Org. 2554
1	MS 1452	Gregg A. Radtke, Org. 2552
1	MS 1452	Tracy L. B. Zullo, Org. 2552
1	MS 1453	Jaime L. Moya, Org. 2550
1	MS 1454	Marica A. Cooper, Org. 2554
1	MS 1454	Leanna M.G. Minier, Org. 2554
1	MS 1454	Tom Pfeifle, Org. 2552
1	MS 1454	William Wente, Org. 2552
1	MS 0899	Technical Library, 9536 (electronic copy)

This page intentionally left blank.


Sandia National Laboratories